Theoretical Aspects of Metal Atom Clusters

JAROSLAV KOUTECKÝ*

Institut für Physikalische und Theoretische Chemie, Freie Universität Berlin, 1000 Berlin 33, Federal Republic Germany

PIERCARLO FANTUCCI

Dipartimento di Chimica Inorganica e Metallorganica, Centro CNR, Universita di Milano, 20133 Milano, Italy

Received January 3, 1986 (Revised Manuscript Received February 28, 1986)

Contents

I. Introduction: The Task of Quantum Chemistry in Cluster Research

It is superfluous to repeat the arguments justifying why an understanding of the electronic structure of clusters is important. Similarly, it is needless to enumerate the far-reaching consequences of this understanding for our general knowledge of some basic properties of matter as well as for practical applications (e.g., in heterogeneous catalysis and astrophysics). The necessary information can be drawn from several sources in the recent literature (cf., e.g., ref 1–13). A large and still increasing number of experimental and theoretical contributions to cluster research convincingly demonstrates that the scientific community well understands the importance of this field.

On the other hand, it is more difficult to reach a consensus about the real meaning of the interpretation of the basic properties of clusters. This state of things is due to the very nature of clusters. They represent a natural bridge between molecules on the one side and solids or liquids on the other side. Therefore, they offer a challenging field of research for both physicists and chemists. More specifically, the theory of clusters has been simultaneously developed using the concepts and methods of the solid-state theory and those of the theoretical chemistry. Although both these branches of science are naturally based on a common general background, the concepts actually used differ substantially. Consequently, we assume that a few remarks concerning the formulation of the problems and tasks in the theory of clusters will be useful.

Clusters can be defined as agglomerates of a limited number of atoms or molecules. The number of atoms or molecules in a cluster is very small in comparison with the number of atoms or molecules in a liquid or solid. The average number of nearest neighbors of an atom in a cluster does not usually correspond to its chemical valence, and it differs also from the number of nearest neighbors in the corresponding crystal. This circumstance is often formulated by physicists as a relatively large ratio between the "surface" particles and the "bulk" particles in a cluster, or, otherwise, as a large number of "dangling bonds" on the "surface of a cluster". Let us notice that the ratio is not at all small for relatively big clusters (cf., e.g., ref 14). Notions such as surface tension or surface curvature are frequently employed in classical models which are sometimes used

0009-2665/86/0786-0539$06.50/0

Jaroslav Kouteckỳ was born in Kroměříž, Czechoslovakia, in 1922. He got his RNDr degree in theoretical physics at Charles University in Prague in 1951. He worked in various industrial institutions in 1941–1945 and 1949–1952. He was scientific co-worker and later leader of the department of quantum chemistry in the Institute of Physical Chemistry, Czechoslovak Academy of Sciences, Prague, in 1953–1969. He was awarded with a State prize in 1954 for the solution of the problem of polarographic kinetic currents (together with Prof. R. Brdička) and in 1963 with a State prize for establishing research in quantum chemistry in Czechoslovakia. He was corresponding member of Czechoslovak Academy of Sciences in 1962–1971. In the year 1969 he was elected in the International Academy of Quantum Molecular Sciences. He was professor of physical chemistry at Belfer Graduate School of Science, Yeshiva University, New York, in 1970–1973. In 1973 he moved to the Free University Berlin, West Berlin. He was interested in the theory of electrode processes, in the semiempirical quantum theory of conjugated compounds, and the general properties of the solutions of Hartree–Fock equations. His recent research activities cover a broad range of the theoretical chemistry field, including purely theoretical aspects, and applications of quantum chemistry methods to electronic structure of metallic clusters, to surface phenomena, and to models for catalytic processes, as well as on molecular excited states.

Piercarlo Fantucci was born in Angera, Italy, in 1943. He graduated in chemistry from the University of Milano, Italy, in 1969 and developed strong interest in spectroscopy and bonding theory of inorganic complexes. From 1973 to 1981 he was appointed as a lecturer of inorganic chemistry at the University of Milano. At the same time he was associated with the Department of Computational Chemistry led by E. Clementi at Donegani Institute, Novara, Italy. Since 1983 he has been Associate Professor of Inorganic Chemistry at the University of Milano. For several years, his interest has mainly focused on the theoretical aspects of the electronic structure of metallic clusters and on simple cluster models for the chemisorption processes.

to rationalize certain deviations from crystal properties (e.g., the deviations of the ionziation potential of clusters from the work function).[15,16] Similarly, some methods of solid-state quantum theory are often modified in such a way that they take into account the finite dimensions of clusters. In this connection, the various versions of the spheric jellium model[17–20] as well as the local potential approaches should be mentioned (cf. 21–23). It is evident that the applicability of methods based on concepts and notions well proven in solid-state physics can start to be questionable when a cluster is very small. Moreover, the translational symmetry properties of crystals which help substantially to reveal the interesting and important features of very large systems studied by solid-state theory do not exist for relatively small clusters.

Therefore, it seems quite natural to employ the methods used in quantum chemical investigations of molecular systems. Let us emphasize that, roughly speaking, quantum chemistry has been successful in two fields: first, in the qualitative explanation of the electronic structure and properties of relatively stable molecules with well defined bonds; second, in the prediction of the behavior and properties of unusual small molecular systems which are of great importance in modern chemistry and molecular physics. The procedures used in these two research directions are quite different: The first group of problems can be treated with relatively simple theoretical methods that in principle allow for an extrapolation of the knowledge about small molecules of a given type obtained from higher level of theory to other, very often quite large, molecules of a similar kind treated at different levels of sophistication. Simple ab initio methods and various semiempirical procedures belong to this category of procedures. A reliable investigation of molecular systems with unusual fundamental properties requires more sophisticated quantum chemical approaches. The application of the more elaborate quantum mechanical methods borders very often on limits of practical feasibility if the systems under investigation are not really quite small. For this reason severe limitations exist in the size of manageable systems, if the unmodified or unadapted methods of quantum chemistry are used. The application of relatively sophisticated quantum chemical methods to small properly selected representative systems sometimes yields new insights in the form of regularities which may be generalized to obtain general rules.

These features of quantum chemical methods pose a dilemma to a would-be investigator: The use of sophisticated methods is desirable to solve the relevant problems of the electronic structure of small clusters, but their applicability seems to be limited only to aggregates that are too small.

The danger is to lose the possibility to thoroughly examine just those clusters whose size is such that they exhibit peculiar properties intermediate between those characteristic of molecules and those characteristic of solids.

The dilemma is further aggravated by the circumstance that the practically most interesting and experimentally most frequently studied clusters are composed of relatively heavy atoms with large numbers of electrons. The difficulties are particularly serious in the case of clusters built from transition-metal atoms because they not only have a large number of electrons but also a very dense spacing of energy levels. This last

property opens many possibilities of interaction of the transition-metal atoms with suitable partners. Moreover, relativistic effects are no longer negligible for a correct examination of interesting heavy atoms. This troublesome situation in the electronic theory of clusters is similar to the difficulties in the electronic theory of inorganic complexes and is perhaps even more complicated. Notice, nevertheless, that recently quite encouraging progress has been achieved just in the application of ab initio quantum chemical procedures in the chemistry of complexes.

Is there any escape from these troubles with the application of quantum molecular methods appropriate for answering relevant questions about the electronic structure of clusters? Or, on the contrary, are the approaches typical for solid-state theory more practicable here and consequently more promising so that there is no advantage in employing quantum chemical methods in cluster theory?

According to our opinion the recent literature on quantum chemical investigations of the electronic structure of small clusters clearly shows the usefulness of quantum molecular methods in cluster theory. Of course, some precautions should be taken in order to make such investigation really effective and informative. To be able to formulate the corresponding recommendations it is necessary to try first to define the goals of the electronic theory of clusters more precisely and concretely, taking into account the limitations of quantum chemical methods.

The most frequently asked question concerning clusters of metal atoms is at what cluster size the typical metallic properties, such as high electronic conductivity, start to appear? Another topic of special interest is the comparison of magnetic and spectroscopic properties of clusters with the corresponding properties of crystals. One can ask at which rate the ionization potential of clusters converge to the bulk work function or at which rate the average binding energy per atom in a cluster converges to the cohesion energy of a crystal. Is the geometric arrangement of particles in a cluster similar to that in the crystal or crystal surface or are, on the contrary, the geometric features of clusters very specific? Is it possible to obtain the most stable cluster by adding more atoms or atom groups at proper places to a smaller stable cluster or, oppositely, should the cluster undergo deep qualitative rearrangements during its growth? Is cluster stability a monotonic function of cluster size? If mass spectroscopy is used for the detection of clusters the experimentalists very often find especially high abundances for certain cluster sizes in the mass spectra. What are the reasons for the appearance of these "magic numbers"?[17,24,25] The theory of electronic structure should be in principle able to yield at least the basic starting point to answer all these questions.

The criteria by which theory judges the differences between cluster and crystal bulk properties are sometimes obvious, but in many cases the opposite is true. An example for the first case are the geometrical features of clusters. Here, the only problem is the choice of a proper theoretical method able to find the energetically favorable geometry without prejudices and a prior constraints which can result from them. This does not mean, of course, that the task of finding the cluster geometry is an easy one because the number of degrees of freedom is extremely large if it cannot be assumed a prior that the cluster has a high symmetry.

A typical example of a property for which the criterion discriminating between the bulk and the cluster behavior is not evident is the electric conductivity. The usual criterion of the metallic state in solid-state theory is a large density of states at the Fermi level. The concept of density of states is based on a one-electron approximation on the one hand and on the continuous spectrum of one-electron energy levels on the other hand. The first feature is of a questionable value for many clusters. The second feature is evidently not appropriate for finite clusters at all, and an artificial broadening of the calculated discrete one-electron energy levels of a cluster does not necessarily yield a good simulation of the density of states for a metal crystal. It is mainly necessary to realize that very often two or more states of a cluster have very similar total energies, but the spectra of one-electron levels in the main electronic configurations (cf. appendix VII.A) differ very much just in the vicinity of higher occupied and lower virtual molecular orbitals (around the "Fermi level"). In the special case, quite often occurring for stable cluster shapes, only one configuration has a very large weight in the configuration expansion of the wave function. Consequently, the one-electron energy gap between the occupied and virtual orbitals can be taken as a measure of the conductivity. This gap can, however, vary substantially for various close-lying electronic states of the same cluster geometry. Therefore, it is dangerous to draw any conclusion about the electric conductivity by making an analogy between the energy difference between the highest occupied and lowest unoccupied MO for a particular state of a cluster and the existence or nonexistence of an energy gap between the valence and conductivity band of an infinite system. Here we meet the above-mentioned dangers when usuing the concepts of solid-state theory for small systems—the clusters.

Since the criterion of the width of the energy gap near the "Fermi level" in the density of states dependence is not easily applicable for clusters, other criteria of the evolution of the metallic state with the cluster size should be considered. One can suggest the existence of few excited states with very small excitation energies as a criterion related to the "energy gap" criterion. Indeed, the small clusters very often exhibit a very rich spectrum of excited states with energies near to that of the ground state. Nevertheless, it has been noticed that many clusters can show a "biradicaloid" character[26] which can be accompanied by very small energy differences among states with different multiplicity (cf. appendix VII.A). It can therefore be argued that the existence of the nearly degenerate states of clusters is a consequence of the surface and not of the interior properties. Owing to the very nature of the "metallic" clusters the presence of excited states near to the ground state is probably due to both features: For very small clusters the influence of the "cluster surface" prevails, and for very large "metallic" clusters the conductivity in the interior of the clusters is more important. The separation of the two influences is probably impossible.

Therefore, some other criteria for the development of the metallic state should be thought of. The degree of delocalization of the one-electron density over the cluster seems to be an appropriate supplementary measure for this property. The delocalization of the chemical bonds *and* the simultaneous existence of states with low excitation energies in the same cluster allow the assumption that the electrons in the cluster are mobile.

Experimental research on clusters undergoes a stormy development with all the associated advantages and drawbacks for a parallel theoretical investigation. The theory can give valuable hints for experimental activities and important interpretations of empirical findings, but it can easily be misled by an uncertain or incorrect interpretation of experimental results. Caution is mainly recommended if enormously complicated processes or phenomena, such as relative abundances, are interpreted on the basis of a single feature or a few theoretically predicted features of clusters. In general, a direct comparison of the numerical results of the theory with an experiment is quite risky without a careful and critical consideration of the origin and nature of the quantities compared.

The main goal of investigation of electronic structure of clusters with quantum molecular methods is to unveil the manifestation of the general physical and chemical properties of atoms under the specific conditions existing in clusters. The resulting cluster properties either can be specific for a cluster of a given chemical nature and size or they can be considered as characteristic for an extremely small section of a crystal without any pronounced specificity. For example, the shapes of small clusters can either be considered to represent deformed sections of an infinite crystal lattice or they can be specific and not resemble any part of the corresponding crystal. Interatomic distances can be similar to or essentially different from crystal distances.

The quantum theory of clusters should also contribute to further development of the theory of crystal growth. Until now the superposition of various pair potentials has been used as a tool for the determination of the probable steps in the growth of very small aggregates. The two-body potentials favor more compact structures. According to the form of the potential (Lennard-Jones, Morse, Mie, etc., cf., e.g., ref 27) different growth sequences have been proposed. One fact clearly results from all these investigations: Very small compact clusters can deviate quantitatively from sections of the crystal lattice. This is mainly true for cluster geometries with a fivefold rotation axis, which cannot be continued until any infinite crystal lattice is built. The explicit consideration of the electronic structure of clusters can introduce new aspects in the determination of the stability of clusters of a given size and thus help to suggest the probable growth sequences.

The consequences of the described requirement for the methodological aspects of the small cluster theory are obvious. The methods used should not be selected on the basis of any prejudices taken over from the experience with the more usual molecular systems. They should be in principle able to describe quite reactive states with open electronic shells and therefore be able to yield states of arbitrary multiplicity. On the other hand, the tractability of the investigation of relatively large clusters should be guaranteed to some extent. These seemingly contradictory requirements on the methods useful in cluster theory can be hopefully satisfied in a time-consuming development of careful investigations. Analogies to the solution of problems encountered in the description of large organic and inorganic molecules may help, but at the same time cluster research should evidently follow its own footpaths.

As a first step, a careful invesigation of small clusters of relatively light atoms by means of quantum molecular methods (as sophisticated as possible) is advisable. One hopes that relatively simple laws or rules govern the cluster structures and that basically very complicated phenomena can be reduced to some essentials. The use of elaborate approaches should also serve to discover the necessary methodological aspects which must be respected in the simplified methods. The method thus modified can be employed without a big risk for the investigation of larger clusters if the general problems connected with its application on large systems (e.g., size consistency effect in CI, Appendix VII.A) can be properly taken into account.

A typical example is the problem of an appropriate choice of the atomic orbital basis set (extent and quality) in the so-called "ab initio" calculation (cf. appendix VII.A). Evidently, a satisfactory flexibility in the description of electron density requires the use of very extended basis sets, containing components of high angular symmetry (polarization functions).

However, advanced computational methods making use of extended basis sets are of limited applicability in the study of clusters of relatively high nuclearity. This is true, first, because of the rapidly increasing computational costs and, second, because a near linear dependence can occur, especially in the case of very compact cluster shapes.

Both difficulties can be overcome by adopting basis sets of smaller size but the basis of reduced dimensions should include at least the polarization functions which are essential for the description of the directionality of the interatomic interaction.

The degree of the possible simplifications concerning the level of sophistication of the theoretical treatment cannot be established with "a priori" considerations. It depends, in general, on the particular nature of the system under study and on the nature of physical properties to be investigated. In order to carry out these simplifications it is useful to carefully compare the results obtained with more complete as well as with simpler methods for smaller aggregates. Simultaneously, the interpretation of the achieved results should be made. The investigation of group Ia (1),[360] IIa (2), and IVa (4) clusters very nicely illustrates the usefulness of this approach.

The difficulty in treating systems with atoms having many electrons can be partially overcome by using methods in which only the valence electrons (or, in general, some subgroups of electrons) are explicitly treated; the "core" electrons are assumed to modify the potential in which the valence electrons move (effective core potential or pseudopotential procedures).[28-35] Up to the present, this approach has been unavoidable, especially for the treatment of transition-metal clusters. An investigation with pseudopotential methods must

be carried out with extreme care and, when practicable, the comparison of the pseudopotential and all-electron procedures is highly advisable (e.g., for the sp metal clusters where both approaches can be employed).

Other methods very often applied in cluster investigation are the local potential and electron density approaches[21-23] which make studies on relatively large clusters possible. Here the comparison with other methods without any assumptions about the potential in which electrons are moving is very useful, too, and can justify the application of these important approaches.

The effective core potential methods are very often combined with the local potential approach and provide a relatively simple tool for the investigation of clusters with a larger number of electrons (cf., e.g., ref 28–29, 35).

In this review theoretical studies of clusters built from group Ia (1), IIa (2), IIIa (3), and IVa (4) atoms as well as from transition-metal atoms are considered and discussed. We do not review work on a very important and interesting category of mixed clusters. We rather concentrate our attention on the analysis of consequences that the covalent and metallic bond can have upon the properties of small clusters. If the cluster is composed of two kinds of atoms, two cases can occur: Either the differences in electronegativity are so small that they only can complicate the general features determined by the covalent and metallic interactions or they completely dominate the electronic structure. In the latter case other methodological means have to be employed for the elucidation of the basic cluster properties. At any rate, a careful discussion of mixed clusters would require the introduction of additional concepts and their incorporation in the structure of the present review article. We feel that it would be better to consider the mixed clusters separately because of their evident importance for cluster research as well as their challenging connections with the modeling of impurities in solids and the chemisorption sites on the surfaces of ionic solids.

The contemporary state of art in isolating relatively unstable systems makes experimental investigation of van der Waals and molecular clusters possible. In spite of the evidently fundamental differences in the very nature of the forces stabilizing van der Waals and molecular clusters, some surprising similarities of their "abundances" (very high yields of clusters of a given size) with the "abundances" of metallic clusters have been quoted in the literature (cf., e.g., ref 12).

These analogies in behavior of metallic and van der Waals clusters (e.g., the existence of the so-called "magic numbers") certainly need to be explained, but the difficulties encountered in an appropriate theoretical treatment of van der Waals forces are enormous. Therefore, the consideration of the van der Waals and molecular clusters is beyond the scope of this review.

Clusters that have forms of a part of the crystal surface are very often used as models for chemisorption sites in the theory of chemisorption and catalysis. Sometimes the influence of the crystal bulk is taken into account, by using the "embedding" procedure. In this approach the crystal bulk is described with some kind of a simple method that allows for an approximate treatment of a large electronic system. The whole philosophy of this cluster modeling is quite different from the objectives of cluster theory. Therefore, in this review, we do not attempt to cover this interesting and very broad field although we will occasionally discuss the consequences of cluster theory investigations for the cluster modeling in the theory of chemisorption.

In general, the whole field of the theoretical studies on clusters nowadays undergoes a very intensive development. The limitations imposed on the scope of the review leave a sufficient number of fundamental theoretical problems in cluster research to be discussed in the present work.

II. Alkali Metal Clusters

A. Introduction

Alkali metal clusters are a challenging and also for many reasons a natural target of basic research. Indeed, each alkali metal atom has only one electron outside of the electron core and, consequently, is monocovalent at least according to the simple ideas of bond theory. The bond in diatomic molecules built from alkali metal atoms is quite weak, in contrast with the relatively high stability of the corresponding alkali metal solids. On the other hand, alkali metals have, of course, all characteristic metallic properties. The rise of metallic properties with the growth of clusters of metallic atoms is a very interesting problem. Because of the freely mobile electrons the alkali metals are often considered as prototypes of metals well described with the free electron methods.

Frequently it is argued that the quantum mechanical methods based on the use of localized one-electron functions (LCAO-type methods) are not appropriate tools for the description of metallic properties. Such arguments against LCAO-type procedures are no longer convincing if the localized functions are used only for the mathematical convenience to expand the one-electron functions needed in some steps of the theoretical procedure used (see appendix VII.A).

It is useful to illustrate the main problems of the electronic structure of small clusters on the example of alkali metal clusters and especially lithium clusters because their nature is relatively transparent. Numerous theoretical predictions of the optimal geometry for small alkali metal clusters and changes in cluster stability with the increase in the size of alkali metal clusters as well as some predictions of the ionization potentials can be found in the recent literature. Moreover, the variety of theoretical methods used allows some statements on the basic properties of alkali metal clusters independent on the approach employed.

B. Alkali Metal Tetramers

It is useful to start the discussion of chemical bonds in alkali metal clusters with the consideration of tetramers. Li and Na tetramers have been studied with the Hartree–Fock,[36-41] CI,[39-41] CEPA,[38] effective core potential,[42-44] X_α–SW,[45] and spin-density-functional methods[46-50] (see appendixes VII.A,B,C). The semiempirical CNDO[51] methods and the DIM approach[52-55] have been employed as well.

The tetramer built from alkali metal atoms can be considered as a dimer of biatomic molecules which should be inert closed shell moieties. One asks whether

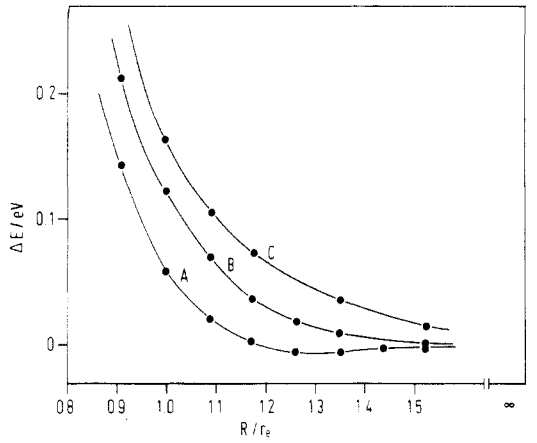

Figure 1. Energy change (ΔE) of two Li_2 (with a constant bond length r_e = 3.02 Å) as a function of their mutual distance R (see Figure 3). The approaches A–C are shown in Figure 3. The SRD–CI procedure (1 M, 1 μhartree) and the (10s) uncontracted AO basis set (see ref 56) have been used. The extrapolated values are plotted. For very large R and R's corresponding to the minima in Figure 2 the appropriate MRD–CI method has been employed to demonstrate that the (10s) basis set gives the repulsive curves.

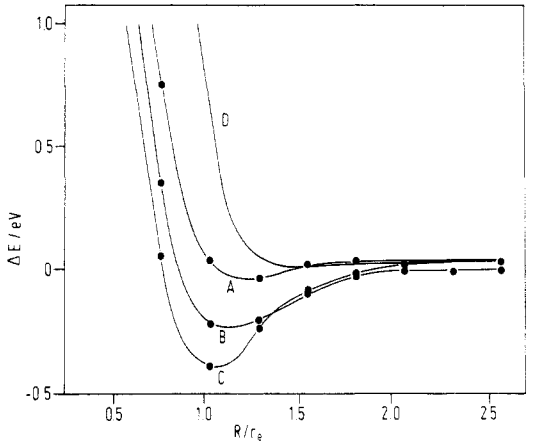

Figure 2. Energy change (ΔE) of two Li_2 (with r_e = 3.02 Å) as a function of R. The approaches A–D are shown in Figure 3. The MRD–CI procedure with an AO basis set (6s1p/2s1p) has been employed.

the tetramer is more stable than two noninteracting dimers. If the answer is positive then it is important to know whether no energy barriers exist for some approaches of two dimers. The answer to this question can give interesting general suggestions about the origin of bonds in clusters in general.

General understanding of the interaction of two Li_2 molecules can be obtained from the comparison of Figures 1 and 2. Three characteristic simple approaches, A, B, and C (Figure 3), are shown here (cf. ref 38). The data listed in Figure 1 have been obtained with the MRD–CI method (see appendix VII.A) based on ab initio SCF calculations with a basis set including ten s-type Gaussian functions but no p-type polarization function at all.[56] The quality of the AO basis set for description of atomic properties is very high and the SCF energy of the Li atom is near to the Hartree–Fock limit. Only the colinear approach exhibits a very shallow minimum for r = 3.8 Å. The other two potential curves are repulsive.

A nearly minimum AO basis set augmented with one p-type AO (6s1p/2s1p)[57] gives qualitatively completely different results: The approaches B and C yield

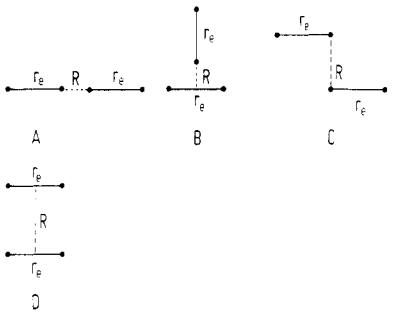

Figure 3. Approaches A, B, C and D of two dimers (see Figures 1 and 2).

clear-cut minima which are only saddle points on the complete energy hypersurface of the Li_4 ground state. Geometry optimization indicates the rhombus as the most stable geometrical structure of Li_4 (4.1) (see Chart I). Let us emphasize that only the main characteristic features of this "dimerization" are relevant here. The details depend on the AO basis set employed as well as on the quality of the configuration interaction. For example, square Li_4 (D_{4h}) has a singlet ground state with an energy near to the sum of two noninteracting Li_2 if a good quality AO basis set and a large CI are employed. The lowest triplet for this biradicaloid geometry is nearly degenerate with the singlet ground state (cf. ref 39). The nearly minimal AO basis set was chosen for the calculations illustrated in Figure 3, in order to show the dramatic role played by p-type basis functions. However, this simple AO basis set leads to the triplet ground state of D_{4h} Li_4 and to an energy of the lowest singlet state slightly higher than the energy of two noninteracting Li_2 molecules treated at the same level of approximation. On the other hand, and this is the point that we wish to stress, this "nearly minimal" AO basis set qualitatively leads to the same main result about Li_2–Li_2 interaction as more flexible basis sets, and shows that the main features (which we are interested in) are basis set independent if p functions are introduced.

To sum up, "dimerization" of Li_2 moiety is energetically clearly favorable, but it proceeds without an energy barrier only for some approaches. Further, it is evident that cluster growth is supported by the p orbitals of lithium which are empty in the electronic configurations of the Li atom. In ab initio calculations these p-type one-electron functions are usually named polarization functions. One should notice some analogies in the properties of the Pauling's metal orbitals.

A look at the composition of natural orbitals (see appendix VII.A) corresponding to the highest occupied MO's for Li_4 in the geometrical arrangements corresponding to the minima for approaches B and C as well as for rhombic Li_4 confirms the participation of p-type AO's in these NO's. The HOMO as well as the NO with the sixth largest occupation number exhibit nodal planes for the three related geometries considered (A, B, C). The p-type basis functions with large weights are located in centers lying in the nodal plane or near to it.

The striking role played by the p polarization functions in the interaction just considered is due to the bonding overlap of the p orbitals with appropriate antisymmetric linear combinations of s orbitals localized in two parts of the cluster separated by the HOMO

CHART I. Topologies of the Clusters (and Symmetry Groups)

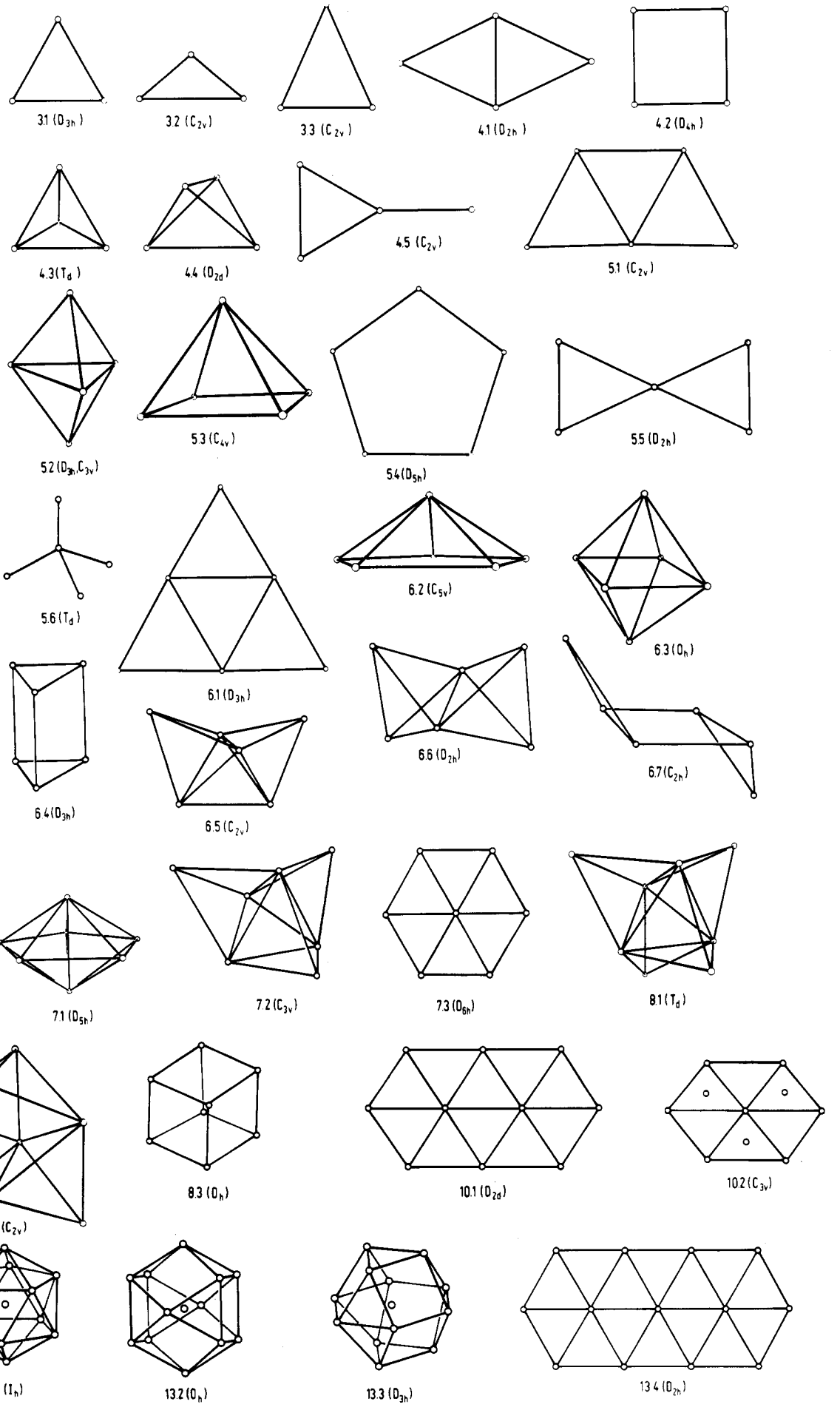

TABLE I. Some Calculated Properties of Li_4 Clusters

geometry[a]	a, Å[b]	b, Å[c]	BE/n, eV[d]	method[f]	ref
4.2 (D_{4h})	2.82		0.22	DIM	53
4.2 (D_{4h})	2.88		0.74	DIM	52
4.2 (D_{4h})	3.52		0.41	Xα-SW	45
4.3 (T_d)	3.25		0.41	Xα-SW	45
bcc (2,2)	3.50		0.06[e]	SCF, (9s4p/4p3p)	36
4.1 (D_{2h})	3.04	2.70	0.61	CEPA, (8s2p/6s2p)	38
4.1 (D_{2h})	3.05	2.60	0.76	CNDO/BW	51
4.3 (T_d)	3.01		0.17	CNDO/BW	51
4.1 (D_{2h})	3.08	2.70	0.57	MRDCI (8s2p/6s2p)	39
4.2 (D_{4h})	2.95		0.46	MRDCI (8s2p/6s2p)	39
4.3 (T_d)	3.05		0.36[e]	MRDCI (8s2p/6s2p)	39
4.1 (D_{2h})	3.07	2.70	0.68	LSD (4s3p)	46
4.1 (D_{2h})	3.08	2.75	0.62	ECP (4s2p) MRDCI	42
4.2 (D_{4h})	2.92		0.51	ECP (4s2p) MRDCI	42
4.3 (T_d)	3.05		0.41[e]	ECP (4s2p) MRDCI	42
4.3 (T_d)	2.89		0.72	DIM	55
4.2 (D_{4h})	2.77		0.78	DIM	55
4.1 (D_{2h})	3.09	2.61	0.30	ECP (4s2p)-LSD	43
4.1 (D_{2h})	2.94	2.61	0.73	UHF + CI, STO-3G	40
4.1 (D_{2h})	3.05	2.60	0.58	(7s3p/7s2p) CI-GUGA	41

[a] The symbols for cluster geometries are from Chart I; bcc (2,2) means the section from (bcc) lattice with two atoms in the first and second (100) plane. [b] a is the edge of the cluster with exception of bcc (2,2) where it means the distance between nearest neighbors. [c] b is the shorter diagonal in the rhombus. [d] BE/n is the binding energy per atom. [e] Triplet state. [f] DIM diatomic-in-molecule method. ECP = effective-core potential approximation. LSD = local spin density approximation. Other symbols are self-explanatory.

nodal plane (or NO with the sixth largest occupation number). Interestingly enough, the relatively small participation of p-type basis functions causes quite strong effects.

The Li_4 cluster in the most stable rhombic geometry has a singlet ground state. On the contrary, Li_4 with square geometry is as typical biradical with nearly degenerate lowest singlet and triplet states. According to ref 39, the most favorable geometry of a triplet is the bent square with an energy very near to the energy of two noninteracting Li_2 molecules. The unstable tetrahedron $Li_4(T_d)$ is an typical biradical with the triplet lying at an energy much lower than the most stable singlet state and slightly higher than the energy of two isolated lithium dimers.

The highest occupation orbitals in the square and tetrahedral form are only partially occupied. Especially the deformation of the planar Li_4 square to the planar Li_4 rhombus can be attributed to a stabilizing pseudo–Jahn–Teller effect. During this deformation the degenerate HOMO of the square is split into two nondegenerate orbitals of the rhombus. Of course, the molecular orbital with the nodal plane in which the shorter rhombus diagonal lies has the lower energy. Further stabilization of this lower b_{2u} orbital is due to the p polarization functions located at the centers on this shorter diagonal. The choice of the pseudo-Jahn–Teller deformation specifically into the direction of the rhombic shape (and not toward the rectangle) is due to the stabilizing effect of the p functions at the two Li atoms on the shorter diagonal.

Another interesting feature of the electronic structure of the Li_4 rhombus is the presence of two three-center bonds located within the two "acute" triangles. This circumstance can be illustrated by one-electron density difference maps (DED) in which the difference between the actual one-electron density of the cluster studied and the superposition of the one-electron densities of noninteracting atoms situated at the atomic positions in the actual cluster is plotted (Figure 4). Regions with the positive and negative values of the DED depict regions with accumulation and depletion of electron density due to the interaction in the cluster, respectively.

Once more, let us emphasize that the Li_4 tetramer does not prefer the most compact tetrahedral geometry but the much less compact rhombic form. This circumstance is due to the possibility to occupy more or less "fully" with the available valence electrons just only one-electron function (MO or NO according to the approach used) with one nodal plane. (Two valence electrons already reside in the one-electron function without nodes.) This conclusion should be qualitatively valid also for the clusters built from heavier group Ia (1) atoms.

This leads us to a quite general conclusion which is confirmed by a variety of theoretical approaches provided they contain a few important methodical ingredients. Indeed, many contributions, working with different methods essentially agree in their results concerning the electronic structure of alkali metal clusters (compare Tables I–III).

C. Electronic Structure and Geometry of Small Alkali Metal Clusters

It has been shown in section II.B that the electronic and geometric structure of alkali metal tetramers is influenced by the following factors of very general importance:

1. The cluster geometry exhibiting maximal possible compactness can be favorable for cluster stabilizing because interaction with the maximal number of neighbors can take place. As is well-known, deformed sections of the fcc (or hcp) lattice and the structure with fivefold symmetry (steps in pentagonal growth) are such very compact structures. Two-center potential calculations (Lennard-Jones, Morse, Mie potentials, etc.) favor very compact and, therefore, quite often very symmetrical geometries.[27] Quantum chemical calculations also show that clusters which are deformed three-dimensional sections of the fcc or hcp lattices have a quite large binding energy per atom (cf. e.g., ref 57). However, they do not always represent local minima on

TABLE II. Some Calculated Properties of Li_n Clusters (n = 5–9)

geometry[a]	a, Å[b]	b, Å[c]	BE/n, eV	method	ref
5.3 (C_{4v})	3.61	2.88	0.71	DIM	53
5.2 (D_{3h})	3.00	3.69	0.74	DIM	53
bcc (5,0)	3.50		0.01	SCF (4s4p/4s3p)	36
bcc (4,1)	3.50		0.16	SCF (4s4p/4s3p)	36
5.3 (C_{4v})	3.19	2.77	0.80	DIM	55
5.2 (D_{3h})	2.83	3.80	0.82	DIM	55
5.3 (C_{4v})	3.21		0.60	CNDO/BW	51
5.1 (C_{2v})	3.06	3.06	0.55	MRDCI, (6s1p/2s1p)	58
5.1 (C_{2v})	2.99	2.88	0.74	UHF–CI STO-3G	40
5.1 (C_{2v})	3.11	3.11	0.55	MRDCI	78
6.4 (D_{3h})	3.21	2.71	0.87	DIM	53
6.3 (O_h)	3.11		0.83	DIM	53
6.6 (D_{2h})	3.50		0.24	SCF (9s4p/4s2p)	76
"6.3" (D_{4h})	3.18	2.71	0.73	CEPA (8s2p/6s2p)	38
6.2 (C_{5v})	3.44		0.61	MRD–CI	76
6.1 (D_{3h})	3.12		0.60	MRD–CI	76
"bcc" (1,4,1)	3.30		1.00	CNDO/BW	82
6.1 (D_{3h})	3.11		0.59	MRD–CI (6s1p/2s1p)	78
6.2 (C_{5v})	3.13	3.09	0.60	MRD–CI (6s1p/2s1p)	78, 58
bcc (1,4,1)	3.28		0.3	UHF–STO-3G	80
6.2 (C_{5v})	3.49		0.62	MRDCI (10s1p/5s1p)	77
6.1 (D_{3h})	3.49		0.62	MRDCI (10s1p/5s1p)	77
6.3 (O_h)	3.49		0.60	MRDCI (10s1p/5s1p)	77
7.1 (D_{5h})	3.14	3.13		PP–MRDCI (6s1p/2s1p)	58
"fcc" (2,4,1)	3.10	3.10	0.61	PP–MRDCI (6s1p/2s1p)	78
"bcc" (2,1,4)	3.00	3.00	0.95	CNDO/BW	82
8.3 (O_h)	3.22	3.22	0.11	UHF (3s1p)	83, 84
bcc (6,2)	3.50	3.50	0.22	SCF (9s4p/4s2p)	36
8.3 (O_h)	2.96	2.96	0.78	Xα–SW	45
fcc (3,4,1)	3.14	3.14	0.65	MRDCI	78
bcc (3,1,4)	3.00	3.00	1.22	CNDO/BW	82
bcc (5,4)	3.50	3.50	0.30	SCF (9s4p/4s3p)	36
"bcc" (2,5,2)	3.00	3.00	0.15	UHF (4s2p/3s1p)	83, 84
"bcc" (2,5,2)	2.78	2.78	0.74	Xα–SW	45
bcc (4,1,4)	3.06	3.06	1.09	CNDO/BW	82
bcc (5,4)	3.50	3.50	0.60	MRDCI (6s2p/2s1p)	57

[a] The symbols for the geometries are from Chart I. fcc (n_1,n_2,n_3) and bcc (n_1,n_2,n_3) mean (100) sections of the fcc and bcc lattices with n_j atoms in the jth layer. "fcc" and "bcc" are the deformed sections from the corresponding lattices. "m;n" means a deformed cluster geometry from Chart I. [b] Maximal interatomic distance. [c] Minimal interatomic distance.

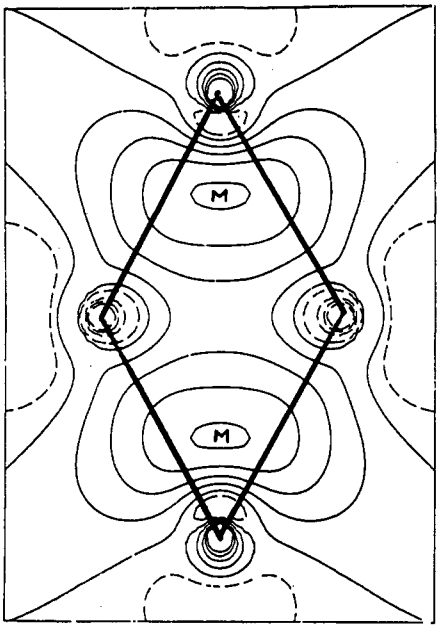

Figure 4. Difference one-electron density map of the Li_4 rhombus. The full and broken lines depict enhancement and depletion of the one-electron density in the plane of the four Li atoms, respectively. Symbols M show maxima in the difference one-electron density map. Adapted from ref 74.

the ground-state energy hypersurface. According to the general rules of binding theory not every interaction is binding as, for example, the well-known Woodward–Hoffman rules very clearly demonstrate. Clusters exhibiting fivefold symmetries[58,59] are quite stable and they sometimes indeed correspond to minima on the ground-state energy hypersurfaces.

2. The Jahn–Teller effect[60] or pseudo-Jahn–Teller effect[61] can destabilize remarkably symmetrical geometrical arrangements (cf. also ref 62). Quite compact structures of course very often exhibit high symmetry. The corresponding symmetry groups have irreducible representations of higher dimensions and consequently degenerate molecular orbitals in the one-electron approximation (and degenerate natural orbitals in many electron treatments). If the number of electrons is not sufficient to fill up the HOMO's fully then the Jahn–Teller effect or pseudo-Jahn–Teller effect destabilizes the compact symmetrical geometry. The degeneracy and—more importantly—the near-degeneracy of the relevant one-electron function is in general closely connected with the nodal features of the one-electron functions (MO's as well as NO's).

For obvious reasons the nodal structure influences the sequence of the occupancy of the MO's (or more generally, of natural orbitals) with electrons (cf. also ref 17 and 48). The details in the geometry of the system considered do not influence the shapes of the one-electron functions in a crucial manner. In addition, they are quite independent of the theoretical approach used.

TABLE III. Some Results on the Na Clusters

geometry[a]	a, Å[b]	b, Å[c]	BE/n, eV[d]	method	ref
3.2 (C_{2v})	3.02	3.75	0.43	ECP-LSD	47, 48, 50
3.2 (C_{2v})	3.18	4.08	0.34	ECP-LSD (4s,3p)	49
3.3 (C_{2v})	3.63	3.07	0.33		
3.2 (C_{2v})	3.19	4.54	0.377	ECP-LSD	44
3.3 (C_{2v})	3.73	3.05	0.380		
3.2 (C_{2v})	3.22	4.25	0.287	ECP-LSD	46
3.3 (C_{2v})	3.60	3.10	0.273		
3.2 (C_{2v})	3.23	4.82	0.288	ECP-LSD	44
3.3 (C_{2v})	3.75	3.02	0.279		
3.2 (C_{2v})			0.378	SCF + CI (11s7p1d/6s4p1d)	70
3.3 (C_{2v})			0.370		
4.1 (D_{2h})	3.28	2.91	0.61	ECP-LSD	47, 48, 50
4.1 (D_{2h})	3.53	3.10	0.44	ECP-LSD	43
4.1 (D_{2h})	3.48	3.00	0.44	ECP-MRDCI	42
4.1 (D_{2h})	3.23	3.07	0.48	ECP-LSD	46
4.1 (D_{2h})	3.48	3.15	0.47	ECP-MRDCI	39
4.1 (D_{2h})	3.51	3.02	0.34	ECP-LSD	44
"5.1"	3.33	3.2	0.64	ECP-LSD	47, 48, 50
"5.2"	3.72	3.01	0.33	ECP-LSD	44
5.3 (C_{4v})	3.28	3.07	0.73	ECP-LSD	47, 48, 50
5.2 (D_{3h})	3.28	3.23	0.723	ECP-LSD	48
5.3 (C_{4v})	3.37	4.27	0.36	ECP-LSD	44
7.1 (D_{5h})	3.70	3.69	0.37	ECP-LSD	58
7.1 (D_{5h})	3.23	3.23	0.82	ECP-LSD	48
"fcc" (2,2,2,2)	3.81	3.12	0.86	ECP-LSD	47, 48
"13.2"	3.39	3.28	0.86	ECP-LSD	47, 48

[a] The symbols for cluster geometries are from Chart I. "$m.n$" means a deformed cluster geometry from Chart I. "fcc" (2,2,2,2) means the deformed section from the fcc lattice with two atoms in the first, second, third, and fourth layer. [b] a refers to the length of the two equal triangle sides in (3.2) and (3.3), the length of the side in 4.1 (D_{2h}), and the maximal interatomic distances in "5.1", "5.2", 5.2 (D_{3h}), 5.3 (C_{4v}), 7.1 (D_{5h}), "fcc" (2,2,2,2), and "13.2". [c] b refers to the third side in the isosceles triangle, the shorter diagonal in the rhombus 4.1 (D_{2h}), and the maximal interatomic distances in "5.1", "5.2", 5.2 (D_{3h}), 5.3 (C_{4v}), 7.1 (D_{5h}), "fcc" (2,2,2,2), and "13.2".

Evidently, the valence MO with lowest energy (or the NO with the highest natural orbital occupation number (NOON)) has no nodes. Further, one-electron functions exist with one not closed nodal surface. The MO's (or NO's) exhibiting two not closed nodal surfaces have even higher energy (or smaller NOON). Also one-electron functions with one closed nodal surface can exist for larger clusters. This kind of one-electron functions with a "closed" nodal surface exist if distinction between the inner and outer shell centers of the cluster is possible. The analogy with the s, p, and d orbitals of the quantum mechanical problem of an electron in a spherical central field is obvious. In addition, the number of independent degenerate or nearly degenerate one-electron functions with the same nodal character for an arbitrary three-dimensional structure with one relevant AO on each center is similar to the number of corresponding degenerate AO's in the problem of an electron in a spherical field: only one for the s-type and three for the p-type.

A two dimensional system is characterized by one-electron functions of very similar appearance but the number of linearly independent functions is quite different. For example, only two p-type functions exist. The number of valence electrons (and consequently the number of centers) in a cluster for which the Jahn–Teller or pseudo-Jahn–Teller effect arises completely differs for two-dimensional clusters and three-dimensional ones.

It is necessary to emphasize that the near degeneracy and consequently an approximate symmetry are of great importance for cluster stability. In this context it is possible to speak about the "topology" of the cluster as a relevant factor influencing its electronic structure.

The number of "bonds" or "lines" in the "graph" of a cluster which are crossed by the nodal planes of a MO (or NO) approximately determines the position of the MO (or NO) eigenvalue in the corresponding eigenvalue spectrum. It is, therefore, not necessary to limit the above considerations to very symmetrical cluster forms only.

A more general conjecture which can be considered as a generalization of the consequences of the pseudo-Jahn–Teller or Jahn–Teller effect seems to be valid. The existence of the partly occupied MO's with nearly degenerate eigenvalues is not favorable for the energy stability of the cluster geometry investigated. A parallel conjecture is possible to draw for the NO's which are typical for biradicaloid geometries.[26] The biradicaloids with an even number of electrons exhibit some natural orbital occupation numbers (NOON's) appreciably differing from values zero or two. This characteristic feature of biradicaloids can be easily understood when a natural orbital occupation number near two is interpreted as a manifestation of spin pairing: Indeed, the diagonal matrix element of the operator $\hat{A}$ for the given NO is multiplied by the corresponding NOON in the expression for an expectation value of an arbitrary one-electron property A in a many-electron state. If the values of NOON's are either equal to zero or two, the ideal spin pairing evidently is present. Cluster geometries with NOON's approximately equal to zero or two are more stable than clusters with NOON's with opposite properties. Likewise, the NOON's of stable clusters with an odd number of electrons should not deviate too much from the values two, one, and zero.[26] In addition, it can be expected that for particularly stable forms of clusters the energy difference between the ground state and the first excited state with higher multiplicity will not be too small. Oppositely, less stable cluster geometries can have a few states with energies near to that of the ground state.

TABLE IV. Some Preliminary Results of the MRD-CI Investigation of the Small Li Clusters (Ref 75)

		SCF		CI									
n^a	geometry^b	a, Å^c	b, Å^c	a, Å^d	b, Å^d	BE/n, eV^e	IP$_v$, eV^f	IP, eV^g	$\Delta\sigma^h$	$\sigma_p{}^i$	$N_{min}{}^j$	$N_{max}{}^j$	N^k
2		2.83		2.79		0.38	5.12	5.0	0.0	0.056–0.087	1	1	1.0
3	3.1	4.06	2.96	3.99	2.97	0.35	4.17	3.98	0.05	0.11–0.20	1	2	1.3
4	4.1 (D_{2h})	3.21		3.16		0.54	4.57	4.51	0.16	0.11–0.3	2	3	2.5
5	"5.1"	3.19	3.14	3.12	3.08	0.56	4.40	4.09	0.07	0.11–0.31	2 (3)	4	2.8
6	"6.1"	3.23	3.16	3.19	3.11	0.63	4.76	4.18	0.09	0.1–0.28	2	4	3.0
	6.2 (C_{3v})	3.39	2.99	3.33	2.94	0.63		4.19	0.044	0.14–0.44	3	5	3.3
7	7.1 (D_{5h})	3.22	3.16	3.17	3.16	0.67	3.79	3.70	0.02	0.2–0.34	4	6	4.6
	7.2	3.21	3.03	3.21	2.73	0.65	3.98		0.07	0.12–0.38	3 (5)	6	4.2
8	8.1 (T_d)	3.23	3.09	3.12	3.09	0.71	4.45	4.45	0.08	0.11–0.35	3	6	4.5

[a] The number of Li atoms in the cluster Li_n. [b] Cluster geometries are from Chart I. The symbols in quotation marks mean the deformed geometries from the Chart I. [c] a and b are the maximal and minimal interatomic distances in the geometry obtained with the SCF energy minimization, respectively. [d] a and b are the maximal and minimal interatomic distances obtained with the scaling of the SCF optimal geometry to obtain the minimal MRD-CI energy. [e] BE/n is the binding energy per atom. The BE/n after the scaling is only in the third decimal place lower than BE/n calculated from the SCF optimal energy. [f] IP$_v$ the vertical ionization potential. [g] IP$_a$ the adiabatic ionization potential for the calculated optimal cation geometry. [h] $\Delta\sigma$ the average deviation from the neutrality. [i] σ_p the miminal and maximal participation of the p AO's in the custer. [j] N_{min} and N_{max} are the minimal and maximal numbers of nearest neighbors in the optimal neutral Li cluster. The numbers in parentheses correspond to a more liberal definition of a nearest neighbor. [k] Average number of nearest neighbors for the cluster considered.

3. The p-type polarization functions can strongly stabilize some cluster geometries as has been shown in the section II.B on the example of two interacting Li_2 molecules. These basis functions, which are without a practical importance for the ab initio description of the electronic configuration of Li atoms, play a nonnegligible role when deformations of the electron clouds around the Li atoms in a many-atom system are to be properly described. The importance of this "polarization" effect is well-known for example in the simplest possible case of H_2 molecule. This kind of polarization is present also in Li clusters and, more generally, in alkali metal clusters.

Moreover, the stabilizing effect of the "polarization" basis functions mainly appears in the composition of the one-electron functions with nodal planes. The additional binding is due to the participation of the polarization functions localized on the centers lying in the nodal plane or at least very near to it. The nodal plane of the p-type MO's (and NO's) goes through the center of a cluster where the atoms generally have a larger number of nearest neighbors (higher efective coordination numbers). Indeed, the atoms in a Li cluster which have higher coordination numbers also exhibit higher participation of the p-type polarization functions. This effect is shown in Table IV.

Due to the Jahn–Teller effect nearly all theoretical investigations have found that trimers of Li, Na, and K have the form of an "obtuse" isosceles triangle (3.2) (Chart I) and not the "ideal" shape of an equilateral triangle (3.1).[40,41,43,44,46,48-55,63-70] The energy hypersurfaces have very shallow minima and the barrier between three equivalent energy minima are so smal that individual "isosceles" triangular geometries should not be directly distinguishable because of a small zero-level vibration energy. The nuances of the shallow features of energy hypersurfaces depend upon the computational details, of course. The majority of theoretical studies claim additional small minima (3.3) as well. Dietz,[71] on the contrary, has found with the X_α–SW method the absolute minimum for the acute triangular form of K_3 (cf. also the results on Li_3 in ref 72,73).

As already discussed in section II.B, the Jahn–Teller effect destabilizes the compact tetrahedral form (4.3) of the Li_4 and Na_4 clusters, and the pseudo-Jahn–Teller effect causes further deformation of the square shape (4.2) (D_{4h}) to the rhombus geometry (4.1) for these clusters.[39,74] Since the shorter lengths of the diagonal in the rhombic Li_4, Na_4, and K_4 are nearly equal to the sides of the rhombus these clusters can be considered as deformed sections of the (111) plane in the fcc or hcp lattice.

In spite of methodological differences, all theoretical investigations employing quantum mechanical methods agree upon the general "topology" of the alkali metal tetramers and moreover, yield a similar bond length and the angle of the rhombus (compare Table I). This is true with the only exception of older studies and papers in which the proper rhombic geometry was not considered at all and therefore was not compared with other possible forms of tetramers. Also the cations of the alkali metal tetramers have a rhombic shape but with a slightly different rhombus angle and side[43,44,48] or a "T-shape" (4.5) (C_{2v}).[75]

The SCF energy optimization[75] of the Li_5 cluster as well as the energy minimum search with the Hellmann–Feynman forces in the framework of self-consistent pseudopotential local spin-density calculations for Na_5[48] predicts that the slightly deformed part of the (111) fcc lattice with five atoms (5.1) is a minimum on the singlet ground-state energy surface. CI corrections do not qualitatively change this result, which agrees with earlier predictions based on some plausible arguments without a systematic energy optimization. Quantum chemical theory favors the less compact planar form of the pentamer, as it did in the case of the tetramer.

According to the self-consistent LSD pseudopotential investigation,[48] Na_5^+ should have a (5.5) (D_{2h}) planar form, quite different from the optimal (5.1) (C_{2v}) planar geometry of Na_5. In an analogous fashion, the SCF ab initio optimization search[75] gives the same topology (5.5) (D_{2h}) as the most stable Li_5^+ has. Both studies agree in the prediction that the alkali metal pentamer cations and the neutral pentamers should differ fundamentally in their optimal geometrical structure.

The results[58,75,76] for Li_6, Li_6^+, Na_6, and Na_6^+ are again very similar. The ab initio SCF optimization predicts the (6.2) (C_{5v}) pentagonal pyramid and a deformed planar section of the (111) fcc lattice plane with the (6.1) (D_{3h}) symmetry to be the most stable forms of Li_6 with comparable energies[75] (cf. also ref 70 and 77). The (6.5)

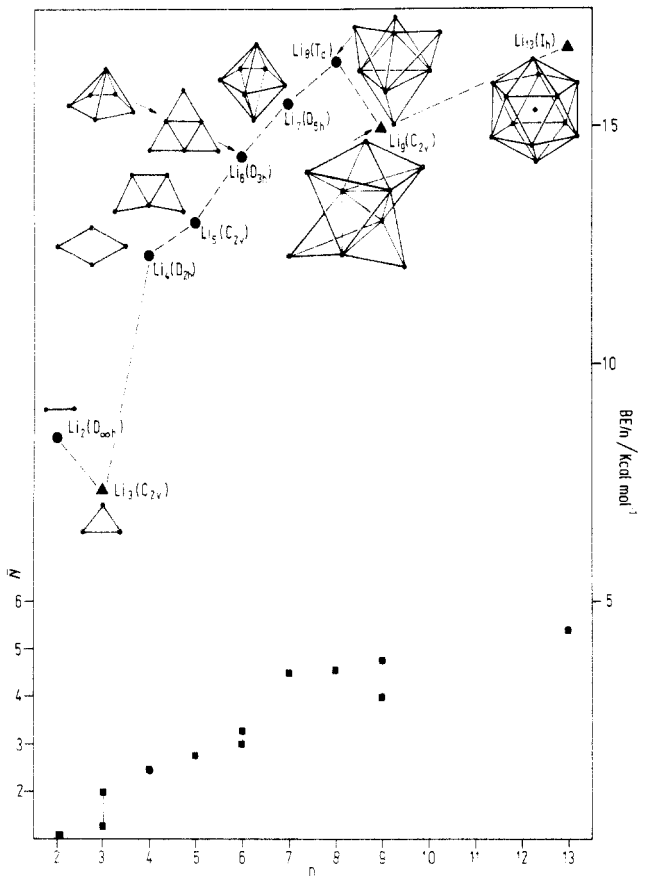

Figure 5. Dependence of the MRD–CI binding energy per atom (BE/n) on the number, n, of atoms in Li clusters. The graphs of the most stable clusters are schematically shown. Points labeled with ▲ are preliminary results. The average numbers of nearest neighbors (N) for the optimal clusters are also shown as points ■ at the bottom of the Figure 1.

(C_{2v}) "tripyramid" which is very often considered as a logical step between M_4 (T_d) and M_7 (D_{5h}) has a higher energy than C_{5h} and planar D_{3h} Li_6 clusters.[77] Martins, Buttet, and Car[48] have obtained similar forms as the most favorable Na cluster shapes. In the case of the hexamer the cations can have very specific and unexpected forms: Indeed, self-consistent SCF calculations for Li_6^+ yield a minimum for the form (6.6) (D_{2h}) which is again analogous to the minimum for Na_6^+ obtained with the self-consistent pseudopotential local spin-density procedure.[48,74] Notice that the Li_6^+ cluster, which is planar section of the (111) plane in the Li fcc lattice, and the form of Li_6^+ with the fivefold symmetry have similar but a little higher energies.

Less stable geometries of A and B Li_6 (Figure 6) show the crossing between the lowest singlet and triplet with a deformation of the angle from 90° (A) to 60° (B).[78] Topological arguments (Pariser–Parr–Pople model with complete CI) show that the topology B has a typical biradical character.[79] Notice the danger that a seemingly acceptable cluster model for a chemisorption site on a metal surface exhibits unusual chemical properties. These biradicaloid properties (high reactivity) can lead to an artificial overestimate of the chemisorption energy which a section of a crystal surface chosen in another way will not show.

The pentagonal bipyramid (7.1) (D_{5h}) is the optimal geometry for Li_7[75,78] as well as for Na_7.[48] The SCF energy optimization yields, of course, the C_{3v} structure (7.2) as slightly more favorable than D_{5h} Li_7.[75] This (7.2)

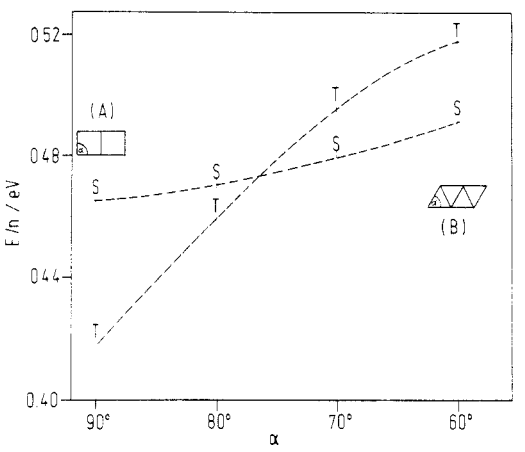

Figure 6. MRD–CI binding energy per atom (BE/n) for the lowest singlet (S) and the lowest triplet (T) as functions of the angle α in the Li_6 during the deformation from the geometry A to the geometry B. Reproduced with permission from ref. 78. Copyright 1983 VCH Verlagsgesellschaft mbH.

(C_{3v}) geometry can be looked upon as three pyramids built on the three faces of the central tetrahedron. The CI procedure inverts the energy sequence in favor of the bipyramid Li_7 (D_{5h}). The pentagonal bipyramid is well-known as a possible step in the pentagonal growth and it has been predicted earlier as a very stable form of Li_7.[37,58]

Pentagonal bipyramid is also found to be a very stable geometry for both Li_7^+[75] and Na_7^+.[48] Both investigations found that the distance between the two apical vertices of the bipyramid is very similar but slightly smaller than the distance between atoms on the periphery of the central pentagon.

The results of ref 48 and 75 differ in the case of octamers: The Hartree–Fock optimization yields an energy minimum for a highly symmetrical T_d form of Li_8 (8.1), whereas the Hellmann–Feynman minimum energy search with the local spin-density method obtains a different form (8.2) (C_{2v}) as the most stable geometry of Na_8; the latter can be considered to represent a deformed three-dimensional section of a fcc lattice.

Likewise, the icosahedron cluster (13.1) (I_h) was found to be a very stable form of Li_{13} with the ab initio MRD–CI method,[59] but according to the local spin-density procedure a deformed cubo-octahedron (13.2) (O_h) corresponds to an energy minimum for Na_{13}.[48] The ab initio SCF–MRD–CI investigation for Li_{13} should be considered preliminary because no systematic search of minima on the energy hypersurface has been tried.

Generally, it is obvious that different investigations working with different methods nearly always reach analogous results for the general optimal cluster forms of alkali metals. Some exceptions naturally occur (e.g., ref 44).

It is worth mentioning that the ground states of clusters in their optimal geometry seem to be always singlets for clusters with an even number of electrons and doublets for clusters with an odd number of electrons. The only exception is the ground state of Li_{13} (I_h),[59] which ought to be a sextuplet. Already this exception in the spin behavior of the ground state needs a careful checking. The circumstance that the ground states of lithium clusters in their optimal geometries have the lowest possible multiplicity is by no means obvious. The tendency of clusters to exhibit biradi-

caloid properties, which has been mentioned for lithium tetramers, is of a quite general character. For unstable geometries a few states have energies very similar to the ground state, and the ground state can in principle exhibit a higher multiplicity.

Table IV shows a quite remarkable property of the predicted interatomic distances in Li clusters. Namely, they are not too far from the experimental value 5.86 au in the fcc crystal lattice. The SCF optimization yields an interatomic distance in average about 2% longer than the CI procedure.

Especially interesting are the data for the pentagonal bipyramidal Li_7 (D_{5h}) and Li_8 (T_d).[75] CI gives bipyramid edge lengths equal to 5.80 and 5.87 au. According to the SCF optimization the lengths of the bonds between the Li atoms at the vertices of the inner tetrahedron are 5.83 au long, and the distances between the atoms in the outer and inner tetrahedra in Li_8 (T_d) are much longer (6.11 au). The CI procedure causes these distances to diminish to the value 5.87 au. The reliability of these predictions should not be overestimated. Nevertheless, the small interval in which the predicted interatomic distance lie is very interesting. In Li_8 (T_d) two types of centers exits which differ in the nominal number of nearest neighbors according to the simple "graph" (8.1) (T_d) of the cluster (cf. Chart I). Nevertheless, the distances between two vertices of the inner tetrahedron and between one vertex of the inner tetrahedron and one vertex of the outer tetrahedron differ only slightly. This is even more surprising because the shapes of the energy hypersurface are very shallow and consequently the theoretical predictions quite difficult.

The binding energy of a cluster per atom, BE/n, is defined as

$$\mathrm{BE}/n = -(E_n - nE_1)/n$$

where E_n is the ground-state energy of the cluster with n atoms and E_1 is the energy of the isolated atom. The dependence of BE/n on the number n of atoms in cluster illustrates the change of cluster stability with cluster growth. Figure 5 shows this dependence for energy-optimized small lithium clusters Li_n (n = 1–8).[75] The tentative values for Li_9 and Li_{13} have also been added. The average number of nearest neighbors for the optimal cluster geometry is shown in Figure 7 as well. Evidently, the definition of nearest neighbors in a cluster with energy-optimized geometry is somewhat arbitrary. Nevertheless, especially in the case of optimum cluster forms, the identification of the nearest neighbor in a cluster is not difficult. As mentioned above, their distance is quite similar indeed to the interatomic distance in the fcc lithium crystal lattice.

The characteristic quantity BE/n increases monotonically with n for $3 < n < 8$. The trimer shows a slightly lower value of BE/n than the dimer. The Li_9 cluster has lower BE/n than Li_8 (T_d), which seems to be especially stable. A preliminary investigation of Li_{10} gives again a small increase of the quantity BE/n from n = 9 to n = 10.[75]

The inequality BE/(n + 1) < BE/n signals a high stability for Li_n. According to this criterion the Li dimer and octamer should be quite stable clusters. The CI size effect error which generally causes an underestimation of the stability of larger systems can only work against the predicted increase of the quantity BE/n with n. Consequently, the real increase of cluster stability with cluster size can be only larger than predicted by limited CI calculations. Notice that Knight et al.[17a] have drawn the same conclusions from their spherical jellium model of clusters. The arguments of these authors are based on the symmetry properties and degeneracies of the solutions of the one-electron spherical quantum mechanical problem (jellium model). A more general consideration on the nodal properties of one-electron functions (MO's as well as NO's) and their consequences for cluster stability has been developed in the beginning of this section. It is possible to see that clusters substantially change the general type of their geometrical structure when their size grows: from planar forms to geometries with fivefold symmetry and to condensed tetrahedral shapes. Thus, Jahn–Teller and pseudo-Jahn–Teller effects are avoided, and moreover an optimal electron density distribution is achieved.

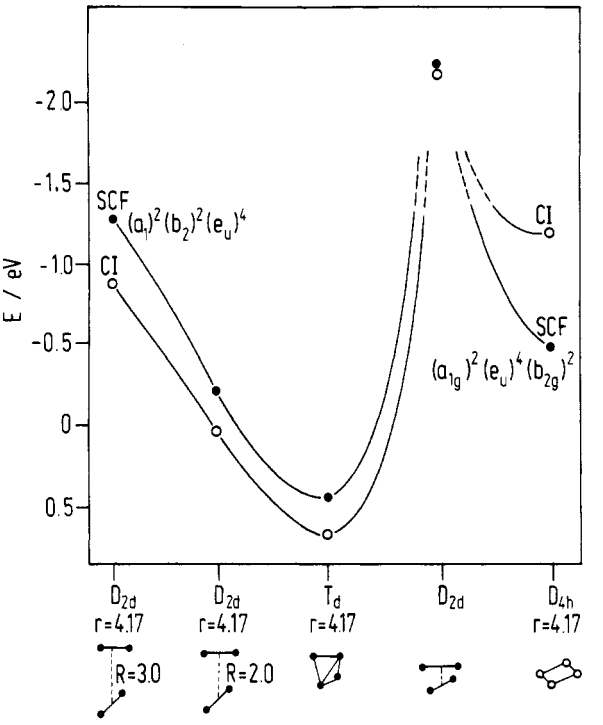

Figure 7. Change of the energy E of two Be_2 moieties with the distance R during their approach depicted at the bottom of the figure. Reproduced with permission from ref 118. Copyright 1982 Elsevier.

The generalized valence bond (GVB) approach[17b] leads to two predictions concerning optimal cluster structures which are somewhat parallel to the general results of the MO-type methods:[24] first, the very small *planar* alkali metal clusters and, second, three-dimensional clusters having a geometry with a large number of tetrahedral subunits (OPTET, optimal tetrahedral clusters) should exhibit high stability. In details, GVB[17b] and investigations using SCF geometry optimization[75] agree upon the high stability of (4.1) Li_4 and (8.1) Li_8 clusters. For the optimal structure of Li_6 GVB yields a trigonal hexagon (6.1),[17b] and SCF geometry optimization followed by MRD–CI yields almost the same energies for (6.1) and (6.2) geometries.[24]

Ab initio calculations[75] show several other general features (cf. Table IV): Mulliken global atomic populations are large on Li centers with small number of nearest neighbors. Consequently, cluster surfaces are in general negatively charged. This charge separation

is not significant and decreases further when correlation effects are taken into account. It is easy to understand why the methods which do not consider self-consistency at all seriously overestimate the charge separation in clusters. Especially interesting in this context is the pentagonal pyramid Li_6 (6.2) and pentagonal bipyramid Li_7 (7.1), which exhibit very small effective charges due to small differences in the number of nearest neighbors for individual centers in these cluster geometries. On the other hand, a direct connection between the stability of a cluster and the amount of charge separation does not exist.

Another remarkable property is the population of p-type basis functions (AO's, approximately speaking). The centers with large effective coordination numbers (large number of nearest neighbors) in general also exhibit a large population of p-type orbitals σ_p. These centers are, of course, just in the nodal planes going through the interior of a cluster, or at least, they are situated near thesenodal planes. The importance of the participation of those p-type basis functions has been already explained.

The average number of nearest neighbors, $\bar{N}$, in a cluster can be considered a measure of the compactness of a cluster. In Table IV are shown the average numbers of nearest neighbors for optimized geometries of cluster of a given size. This quantity also increases with the cluster size, but it is once more necessary to remember that cluster compactness is not the only relevant factor. This circumstance, which has been already discussed above, is again illustrated by the example of Li_7 and Li_8. Li_7 has the same average number of nearest neighbors as Li_8. Nevertheless, a lithium octamer has an outstanding stability which is larger than the stability of Li_7.

Lithium crystallizes in close-packed lattices at very low temperatures. Therefore, the sections of the Li or Na bcc lattices have been investigated as models for the chemisorption sites on the (100) and (110) bcc lattice planes. It has been shown that these clusters exhibit also increasing binding energy per atom with increasing nuclearity (at least until $n = 8$[57]), but they have higher energies than the "fcc-type", pentagonal, and "condensed tetrahedral" clusters. It has not yet been investigated if deformed "bcc-type" clusters represent local energy minima.

On the other hand, the unrestricted Hartree–Fock calculations with the STO-3G AO basis carried out by Rao et al.[80] for octahedrons, which are sections of bcc and fcc lattices, suggest that the bcc lattice of alkali metals is energetically favored over the fcc one. However, the reliability of this prediction should be checked since the generalization has been made by using the result obtained for only one cluster form, which is moreover not the most stable Li_6 geometry. On this occasion, the importance of the proper choice of the cluster form for the purpose of the problem under investigation should be mentioned once more. The CNDO/BW study[81,82] of bcc clusters Li_5–Li_{35} indicates quite rapid convergence of the "lattice constant" of the investigated clusters to the experimentally determined lattice constant of Li metal.

Marshall et al.[83,84] have compared the results obtained from the RHF, UHF, general valence bond (GVB), and X_α methods for Li_8(8.3) (O_h) and Li_9 bcc (4,1,4) with the aim to judge the reliability of these methods for Li cluster studies. Their results indicate that Li_9 bcc (4,1,4) is unstable according to RHF and GVB but stable according to UHF and X_α procedures. The $X\alpha$–SW method[45] yields a binding energy per atom five times higher than that from UHF approximation.

A procedure which improves the convergence of the truncated CI expansion employing transformation of virtual orbitals[58] allows for investigations of lithium clusters even larger than Li_{13}. With this procedure the question might be answered whether the "magic number" 20[17a] can really be justified like the "magic numbers" 2 and 8.

D. Some Experimental Results Relevant to the Theory of Group Ia (1)[360] Clusters

The relative instability of clusters and mainly the difficulties connected with the preparation of clusters with well-defined nuclearity are serious obstacles to the determination of cluster properties. On the other hand, theory can be potentially very helpful in guiding the interpretation of experimental data.

The intensities of the peaks in the mass spectra of the cluster beams show quite noticeable features (cf., e.g., ref 16, 17, 25, 85–91). They depend on the details of the experimental arrangements and on the conditions of beam production and cluster detection under which the experimental is performed. In particular, the heights of the peaks depend upon the backing inert gas used. Some experiments give clear "magic numbers" of specially high abundances. The mass spectroscopic peaks are very high for clusters with $n = 7,8$ alkali metal atoms (Na or K) and around $n = 18$–20. Peaks for an even number of alkali metal atoms seem to be higher than neighboring peaks for clusters with odd number of atoms.

A simple interpretation of these experimental data is somewhat daring. Notice that the mass spectroscopic peaks detect ionized clusters. The stability of neutral and cationic clusters can be quite different, and, in addition, fragmentation processes can in principle take place after the ionization. A careful investigation of the influence of different ways of cluster preparation on abundances and other properties is necessary. The preparation of clusters starting directly from ionic species and the comparison of results obtained with different techniques can be very helpful to elucidate the factors that determine the abundances.

Another experimentally studied property is the ionization potential. Naturally, its magnitude is a very important quantity for the proper understanding of abundances, too. The ionization potentials found experimentally generally show a decrease with increasing cluster size. A rough proportionality of ionization potential to R^{-1} (where R is the "radius" of the cluster) agrees quite well with the model of the conducting droplet.[15,16,86] More detailed observation of the magnitudes of the ionization potentials reveals quite large deviations from the just described "classical" behavior. The somewhat arbitrary definition of the "radius" of a very small cluster cannot be the only reason for these deviations. The electronic structure of an alkali metal cluster clearly plays an important role. For example, it is noticeable that ionization potentials of clusters with an odd number of atoms are relatively low and that the

photoionization potentials of Na clusters for n = 4, 6, and 8 have very similar values.[86] The theoretical predictions[75] roughly agree with these experimental findings (cf. Table IV).

The other experimental technique which gives highly interesting information on clusters with an odd number of electrons is ESR spectroscopy.[92-95] With this experimental method the probable distribution and some other properties of the unpaired electrons can be found. The ESR investigations of Li_3,[94] Na_3,[93] and K_3[92] is in agreement with the expectation that not all centers in the alkali metal trimers are equivalent. The energy barriers among three possible isosceles triangles are very low, as they are supposed to be. The Na and K heptamers exhibit ESR properties which can be plausibly interpreted as consistent with a pentagonal (7.1) (D_{5h}) bipyramid geometry. Thermochemical studies on the dissociation energy of alkali metal clusters are also very useful[24,96,97] especially if they could be in the future combined with other experimental evidence. Wu[97] has concluded from the thermochemical analysis that Li_4 should not have the tetrahedral shape (4.3) (T_d).

Experimental determination of the polarizability of small metal clusters[98] is another field that is relevant for cluster theory. Calculations[18] assuming a spherical symmetry of the metal particle show some specific quantum effects and yield a general trend similar to the experimental dependence of the polarizability of the Na and K clusters upon the number of atoms in the cluster.

Other spectroscopic methods[99-100] (Raman, infrared, ultraviolet, etc.) can in general decisively support the effort to clear up the problem of the geometric and electronic structure of clusters. For this purpose, of course, further progress in the experimental methods for the preparation and isolation of well-defined clusters is a necessary precondition.

E. Conclusions: What Can We Learn From Group Ia (1) Clusters?

After we have described the results of quantum mechanical investigation of alkali metal clusters in some detail, the question can be asked whether this problem is worth investing a large computational effort at all. It is true that the theoretical investigation of transition-metal clusters is of major interest to the large experimental activity in this field and many open questions which remain to be answered. It was already mentioned that theoretical description of transition-metal atoms and transition-metal diatomics represent a very difficult task. A description of specific cluster properties is certainly affected by difficulties due to the complicated nature of transition-metal atoms and due to the need to employ less than transparent theoretical methods. Consequently, general knowledge gained on s–p metal clusters is a good starting point for a thorough and detailed investigation of the specific properties of small transition-metal clusters.

Some results of quantum chemical investigations of alkali metal clusters indeed demonstrate that this effort pays off. For example, one of the interesting points is certainly the relative stability of noncompact planar cluster geometries which is purely due to the quantum mechanical effects. The competition with more compact structures already starts for the alkali metal hexamers and completely prevails for larger clusters.

An "aufbau" algorithm for the "growth sequences" starting with a given "seed structure" does not seem to be valid for the most stable clusters. For example, the Li_4 (4.3) (T_d), Li_5 (5.2) (D_{3h}, C_{3v}), and Li_6 "tripyramid" (6.5) (C_{2v}) do not correspond to the absolute minima on the respective energy hypersurface. Heptamers prefer the shape of a pentagonal bipyramid but the octamer has a T_d symmetry. Both geometries follow the Boerdijk's principle of a high degree of tetrahedrality (cf. ref 27), but the pentagonal bipyramid of Li_7 is not a subgraph of the graph which can be assigned to Li_8 (8.1) (T_d). A rearrangement of the atoms must take place if Li_8 should be created by addition of one Li atom to Li_7 (7.1) (D_{5h}). On the other hand, the dimerization of two Li_4 rhombs with a slight deformation yields the geometry of Li_8 (T_d).[75] As a generalization it is possible to state that a single "growth sequence" in the cluster stability cannot be followed during cluster growth and major rearrangements are likely to occur. The kinetics and dynamics of cluster growth are certainly quite complicated matters because few possible channels of the cluster enlargement can be imagined. Evidently, deep rearrangements can be expected also as a consequence of ionization. Interesting hints about the "abundances" can be obtained when the quantity BE/n is carefully discussed. The simultaneous critical consideration of the electronic and geometric structure of the neutral as well as the positively charged clusters together with the possible channels of cluster growth (and fragmentation) can have a key role in solving the problem not only of the "abundances" but also of the magnetic properties of clusters. Information about energy changes with the geometric rearrangement and the form of energy hypersurfaces can also help to understand the spectroscopic properties of clusters which in the future will certainly play an important role in cluster research.

The predominant importance of the electronic effects is evident, and, therefore, very different detailed features of group IIa (2), IIIa (3), and IVa (4) clusters are to be expected.

The cluster shape as well as other cluster properties mainly depend upon the number of valence electrons available to occupy the one-electron levels. The MO (and NO) spectrum is crucially determined by the type of the actual cluster geometry.

The jellium-type models as well as the theories that do not consider the quantum theoretical aspects of the electronic structures of clusters are necessarily one-sided, and they are not able to predict some important properties of clusters.

All these aspects found to be important for the group Ia (1) and other s–p metal clusters must be considered also in the studies on transition-metal clusters for which additional specific features should be expected.

III. Alkaline-Earth Metal Clusters

A. Introduction

Individual group IIa (2) atoms posses a closed-shell electronic structure $(ns)^2$ and are consequently quite inert without any participation of the np or nd orbitals. Indeed, the Be_2 molecule is so unstable that it is not known in the gas phase. To the contrary, crystals of alkaline-earth metals are very stable and exhibit a

binding energy per atom larger than that of alkali metal solids. Therefore, the problem is similar but even more challenging for the theorist than the problem of stability of alkali metal crystals. This is probably one of the reasons why so many investigations of the Be_2 molecule (e.g., ref 101) and of Be_4 clusters have been carried out.

The published work on alkaline-earth metal clusters can be divided into two categories. The majority of papers treat group IIa clusters as models for chemisorption on the surface of hcp or fcc crystals of group IIa (2) metals (e.g., ref 102–107). For this purpose, a fixed geometry is assumed and attention is paid mainly to the estimate of the energy of interaction between a group IIa (2) cluster and a chosen atom or small molecule. For this reason the general tendency in these contributions is to study clusters as large as possible hoping to mimic a chemisorption site on the surface of a solid accurately.[102,104,106] Sometimes interesting results on these naked clusters can be deduced from this kind of investigation, too.

Papers studying the properties of group IIa (2) clusters as such form the second category.[106–117] These contributions are unfortunately less numerous than the publications of the first category. The relatively intensive investigation of Be_4 clusters is an exception.

Theoretical investigation found no or very weak bonding in Be_2 even when electronic correlation has been properly taken into account (e.g., ref 101 and 119). On the other hand, Be tetramer can mobilize p-type atomic orbitals (p-type basis functions) and use them for hybridization; this property allows relatively strong chemical binding in the Be tetramer.[107,109,115]

The capability of ns and np AO's to hybridize depends, of course, on two conditions: The promotion energy should not be prohibitively large and simultaneously the overlap of ns and np AO's should not be too small. Generally speaking, if these two conditions are fulfilled, the binding is due to the p-type polarization functions. This behavior of Be clusters is not surprising because in inorganic compounds beryllium has the coordination number two and under some conditions even four. This property is explained by the abolition of the spin pairing and by the hybridization of 2s and 2p orbitals. In the electronic structure of group IIa (2) clusters the polarization functions take over another task in addition to the one they have in the group Ia (1) clusters: They permit hybridization in the proper sense of the word. It is evident that in the electronic structure of group Ia (1) and IIa (2) clusters only the degree of participation by p-type polarization functions is different. A substantially larger participation of the p-type one-electron functions in the wavefunctions causes some directionality of the bonds in Be clusters. If the above-mentioned conditions are not satisfied, the p-type polarization functions cannot hybridize efficiently enough. For example, the inclusion of the p-type polarization functions in the AO basis set does not account for the stability of Mg_4 and Ca_4 due to the lack of hybridization capability between 3s and 3p AO's and between 4s and 4p AO's, respectively.

The qualitative explanation of significantly different properties of group Ia (1) and IIa (2) clusters by using the same theoretical concepts is a quite satisfactory achievement of the application of chemical bond theory and especially of quantum chemistry. The understanding of the nature of chemical bond in alkaline-earth metal clusters also helps to elucidate the essential features of binding in group IIa (2) solids.

B. The Beryllium Tetramer

As in the case of alkali metal clusters, it is very instructive to analyze the bonding in the tetramer of the simplest alkaline-earth metal cluster, Be_4.

All theoretical investigations carried out with various methods yield Be_4 to be a stable cluster in contrast to weakly bonded Be_2 and Be_3.[109,113,120–124] The symmetric and compact tetrahedron is predicted to be the most stable geometry of Be_4.[103,109,110,112,115]

The reason for this behavior of Be_4, which completely differs from that of Li_4, is mainly due to the full occupancy of the three degenerate t_2[109,118] MO's (or NO's) with the available electrons in Be_4. No Jahn–Teller or pseudo-Jahn–Teller effect can cause the deformation of the most compact and symmetrical geometry of the tetramer. The necessary condition for the formal coordination number three is naturally the hybridization. The promotion energy from the 2s to the 2p AO is compensated by the formation of three bonds per atom. Moreover, the a_1 and t_2 symmetry orbitals built from the appropriate p-type polarization functions in the AO basis set of Be exhibit an arrangement very favorable for chemical bonding. Consequently, the participation of the p AO's in t_2 but also in a_1 MO's (and NO's) is very large as Mulliken population analysis clearly demonstrates.

The comparison of the approach of two Be_2 moieties in the mutual orientation depicted in Figure 7 with the analogous approach of two Li_2 (Figure 4 in ref 38) shows the difference between the nature of interaction in the two tetramers Be_4 and Li_4. With the approach of the two Be_2 moieties the energy of the state with leading valence configuration $(a_{1g})^2(b_{2u})^2(e_u)^4$ decreases and reaches a relatively deep minimum precisely for the tetrahedral arrangement (Figure 7). A further approach causes an increase in energy which goes over a maximum before a local minimum for the planar square configuration is reached. The behavior of the valence MO energies during this approach is quite instructive (Figure 8). A very striking feature is the strong increase of the participation of the p-type AO's with the approach to the tetrahedral geometry.[118] The contribution of the p-orbitals to the a_1 MO shown in Figure 8 is indicative for the importance of hybridization. The similar role of the p orbitals for the composition of the t_2 MO's has been emphasized by Whiteside et al.[109]

Figure 9, which describes the energy change with the simultaneous decrease of all interatomic distances in Be_n (n = 4, 5) for a fixed general shape convincingly shows that the intervention of the p AO's alone overcomes the repulsive character of the interaction among the closed shell Be atoms. Only for such distances for which the hybridization is switched on the attractive interaction takes place. Consequently, the dependence of the ground-state energy upon interatomic distance exhibits a clear minimum. The analogous behavior of the ground-state energy with the decrease of the interatomic distances (with the general "topology" of the cluster kept fixed) has been found for the Be pentamers which differ in their assumed symmetries trigonal (D_{3h}) bipyramid, square pyramid (C_{4v}), and planar C_{2v} ar-

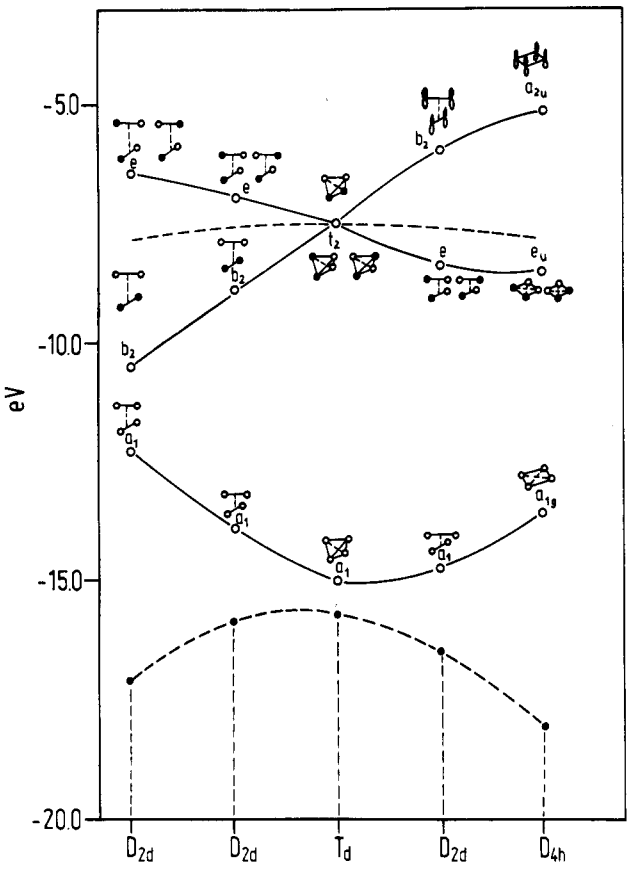

Figure 8. Orbital energy curves for the occupied MO's of Be_4 during their approach of two Be_2 moieties shown at the bottom of the Figure 7. The participation of the p-type AO's is given with a broken line at the bottom as well. Adapted from ref 118.

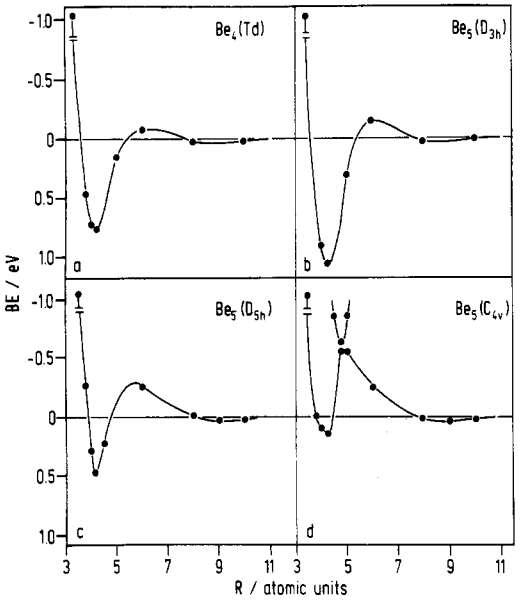

Figure 9. Binding energies (BE) of (a) Be_4 (4.3, T_d), (b) Be_5 (5.2, D_{3h}), (c) Be_5 (5.4, D_{5h}), and (d) Be_5 (5.3, C_{4v}) clusters as functions of the interatomic distances R among all centers in the clusters. Adapted from ref 118.

rangement (cf. ref 117 and Figure 9b–d). Here, too, the decrease in the interatomic distances (with the general cluster shape fixed) leads to an energy maximum before an energy minimum belonging to stable structure is reached.

The important problem of the electronic structure and stability of Be_4 has been studied with the all-electron Hartree–Fock as well as pseudopotential SCF procedure.[118] Various kinds of the configuration interaction procedures[118] and the Møller–Plesset perturbation method[108] have been used for the evaluation of the effects of electron correlation corrections. The coupled electron pair approximation (CEPA)[111] has been employed for the description of the correlation effects in Be_4 as well. The choice of the AO basis set ranges from a nearly minimal up to a large one. The results are not qualitatively different if the AO basis set is reasonably chosen. The quantitative differences must be expected because the nature of the bonds in Be clusters is based on hybridization: If p-type polarization functions are better described[112,118] or if d-type functions[109,111,112] are included in the AO basis set, the computed binding energy can be substantially increased and also the energy sequences of the states for some Be clusters can be changed. On the other hand, the character of the bonds in clusters is essentially well described employing relatively simple basis sets.

An indirect proof that the hybridization between s and p orbitals plays a fundamental role in chemical bonding in alkaline-earth metal clusters is the fact that the Mg_4 and Ca_4 clusters are unstable toward atomization unless d polarization functions are included in the AO basis set and unless correlation effects are appropriately respected simultaneously.[112,114-116] 3s and 3p as well as 4s and 4p AO's exhibit too large differences in AO energies, and moreover their spatial scales are too different for Mg and Ca. Thus, in contrast to Be_4 the stability of the Mg_4 and Ca_4 cannot be attributed to the hybridization of the p and s orbitals alone.

C. Electronic Structure and Geometry of Small Group IIa (2) Clusters

As already mentioned papers dealing with the electronic structure and geometry of the most stable naked group IIa (2) clusters X_n ($n > 4$) are less numerous than publications treating the same problems for group Ia (1) clusters. A systematic investigation of the electronic structure and geometry of clusters as a function of their size and geometry is lacking.

It is well established that the binding energy per atom (BE/n) increases with the growing number of Be atoms in the cluster (cf. Figure 10).[78,108,118,123] At least, BE/n for the Be_{13} cluster which is a section of the hcp lattice with the D_{3h} symmetry as well as for Be_{13} as a cuboctahedron (O_h), which is approximately a section of the fcc lattice, is much larger than the BE/n for smaller Be_n clusters with n = 4–7 and 10, which can be considered as a section of the hcp lattice. The relatively high stability of the Be_{13} cluster found by using a method that combines the effective potential and the MRD–CI treatments[118] has been confirmed in recent work of Bauschlicher et al.[108] The examination of the binding energy per atom as a function of the cluster size is not yet systematic enough even for the clusters which can be considered as sections of the hcp lattice, but the indications that the stability increases seem to be quite convincing. It is necessary to emphasize, however, that no systematic attempts have been made until now to optimize the energy of clusters of a given size.

A generalization of the conclusions that result from the investigation of a given type of Be clusters only and the assumption that trends in stability of clusters do not strongly depend on geometrical details should be

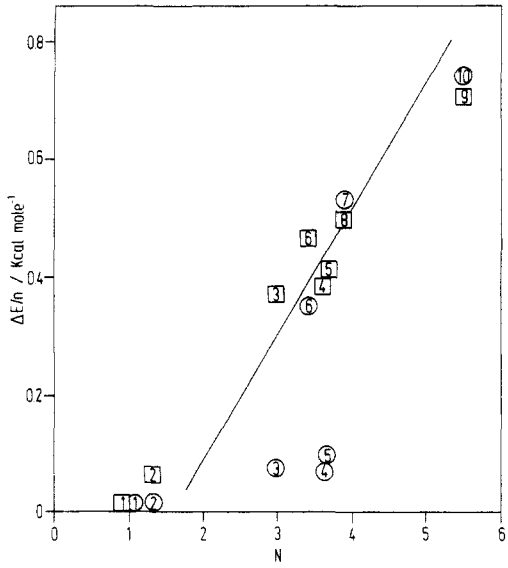

Figure 10. Binding energy per atom (BE/n) as a function of the average numbers of nearest neighbors (N) in the Be clusters. The circles and squares are the MRD-CI results for the AO bases (4s4p/2s1p) and (4s4p/4s2p), respectively. The numbers in the circles and squares label the Be clusters: 1, Be_2 ($D_{\infty h}$); 2, Be_3 ($D_{\infty h}$); 3, Be_4 (4.3, T_d); 4, Be_5 (5.2, D_{3h}); 5, Be_6 (6.6, D_{2h}); 6, Be_7 (7.3, D_{6h}); 7, Be_{10} (10.1, D_{2h}); 8, Be_{10} (10.2, C_{3v}); 9. Be_{13} (13.4, D_{2d}); 10, Be_{13} (13.3, D_{3h}). Adapted from ref 78.

taken with caution. The admittedly very limited information on Be clusters does not show until now any indications of the existence of "magic numbers" smaller than 13. Be_4 with eight valence electrons is a very stable cluster indeed, but a not fully optimized Be_5 is a still more stable system.

The theoretically predicted quite high stability of relatively large planar sections of the hcp lattice[118] (Be_7, Be_{10}, and Be_{13}, Figure 10) is a surprising fact which can be attributed to the strong hybridization effect. The applicability of a spherical jellium-type model for the Be clusters is therefore questionable. The different geometry properties of Be and Li clusters can be explained as due to two factors: The different number of valence electrons causes a different occupation of MO's (or NO's), and, therefore, the destabilization effects can be avoided for Be systems. Further the s–p hybridization influences the directionality of the bonds; the latter can be the deep reason why the jellium model is not suitable for the group IIa (2) metal clusters. Probably due to the directionality factor no decrease in cluster stability was found up to now when nuclearity increases from 4 (eight electrons) to 5 (ten electrons).

The Mulliken population analysis shows a very large participation of the p AO's for Be clusters: For Be_7, Be_{10}, and Be_{13} the p population is approximately twice larger than the s population. The dramatic change of the s and p populations with the decrease of the interatomic distances R can be seen on the example of the planar Be_7 (D_{6h}) cluster:[118] In the $^1A_{1g}$ state for interatomic distances equal to 9.0 au the MRD-CI method gave 1.92 for the s population and 0.08 for the p population while for R = 4.15 au the s population is 0.85 and the p population is 1.15 in the $^3B_{1g}$ ground state.

The existence of a few electronic states with very similar energies and the crossings and avoided crossings which occur among them when the cluster geometry is changed are typical features of Be clusters. An opening of the originally closed shells of the Be atoms during their mutual interaction can be responsible for this behavior. The existence of states with similar energy values and/or different multiplicities does not make a theoretical investigation of the Be clusters easy at all. The task to correctly determine the electronic configuration of the ground state is not trivial, and the chances that an excited state will result from the calculations are quite large.

Different values of correlation energy for different states very often lead to a reversed order of states in the SCF and CI treatments. As a general rule, the assignment of the ground state and the determination of its multiplicity are a delicate problem which can strongly depend on computational details of the method employed. The differences between the energies of the singlets and triplets of small Be clusters that are sections of hcp lattice are very small and sometimes the effective potential treatment with a small basis set yields triplet ground states (Be_7 (7.3) D_{6h}; Be_{13} (13.3) D_{3h}).[118] Bauschlicher and Peterson[108] obtained a singlet ground state or the compact Be_{13} D_{3d} section of the hcp lattice with a triplet ζ AO basis set. The differences in the results of ref 108 and 118 are probably due to different assumptions concerning the extent of the participation by the p basis functions. On the other hand, according to the work of Bauschlicher and Peterson,[108] the (13.3) D_{3h} geometry of Be_{13} is characterized by a lower energy than the D_{3d} one, although the (13.3) D_{3h} cluster is a part of the fcc and the D_{3d} cluster is a section of the hcp lattice.

The theoretically predicted high stability of Be_2^-, Be_3^-, and Be_4^- cluster anions toward electron detachment is an other interesting property of Be clusters.[122]

The magnesium and calcium clusters larger than tetramers have not been carefully studied because even a qualitatively appropriate description of the bonds in Mg_4 and Ca_4 requires the inclusion of the d polarization functions in the AO basis set.

D. Conclusions

The binding energies of Be clusters are relatively large so that a general statement about the increasing stability of Be clusters with increasing cluster size is reliable enough. The main qualitative features of clusters seem to be rather independent of usually important methodological ingredients like the detailed choice of the AO basis or the details of the electron correlation treatment.

The theoretically predicted geometrical properties of the alkaline-earth metal clusters are fundamentally different both from those of group Ia (1) and of group IIIa (3) and IVa (4) clusters as will be shown in section IV. These cluster forms can be in general well understood by applying the basic rules formulated in section II: The participation of the polarization functions and the occupation of the one-electron functions with the available electrons determine the cluster form.

On the other hand, it seems that quantitative results for the Be and even more for the Mg and Ca clusters depend more strongly on the computational details than in case of the group Ia (1) clusters (compare Tables II and V, and Figures 4 and 10).

It is very satisfactory that the strongly increasing stability of the Be clusters with the cluster size is still

TABLE V. Some Calculated Properties of Group IIa (2) Tetramers with T_d Symmetry

element	a, Å[a]	BE/n, eV	method	ref
Be	2.12	0.33	SCF (6s3p/2s1p)	110
	2.09	0.44	SCF (9s4p1d/4s2p1d)	
Be	2.11	0.37	CEPA (9s4p/5s2p)	111
Be	2.17	0.45	SCF-CI (9s4p/4s2p)	112
	2.07	0.70	SCF-CI (TZP + 2d)	
Be	2.02	0.65	ECP-LSD	113
Be	2.00	0.92	STO-3G Pople	114
	2.11	0.27	STO-3G Clementi	
	2.07	0.50	6-31G*	
Be	2.21	0.38	ECP-MRD-CI (4s4p/4s2p)	118
Be	2.10	0.48	SCF (5s2p)	116
Mg	3.19	0.13	SCF-CI (12s9p/6s4p) + 1d	117
Mg	3.39	0.11	ECP-MRD-CI (4s2p1d)	115
Mg	4.1	*b*	SCF (6s4p)	116
Mg	3.33	0.26	CEPA (18s8p1d/5s3p1d)	117
Ca	4.23	0.05	ECP-LSD	113
Ca	4.19	0.20	SCF-CI (12s8p/6s4p) + 1d	112
Ca	4.29	0.15	ECP-MRD-CI (4s2p1d)	115

[a] a is the edge of the tetrahedron 4.3 (T_d). [b] Only a very shallow minimum of the energy dependences on the edge length was obtained.

evident in the case of high nuclearities. The trend is not even masked by the existence of the CI size consistency error which in general strongly affects a reliable estimate of the binding energy of a many-electron cluster.

To sum up, the investigation of the Be_n clusters with $n > 4$ is a field in which more systematical theoretical work would be highly desirable. Primarily the comparison with the properties of the group Ia (1) clusters can bring interesting insights into the theory of clusters.

IV. Group IIIa (3) and IVa (4) Clusters

A. Introduction

The investigations of group IIIa (3) and IVa (4) clusters have been less systematic than the studies of group Ia (1) and IIa (2) clusters.

Aluminum clusters are an exception because of the evident importance of aluminum metal. Recently some attention has been paid to silicon and carbon clusters. Because the electronic structures of the clusters formed by these elements have not been studied as intensively as the electronic structures of group Ia (1) and IIa (2) clusters only a very limited number of regularities and rules can be formulated here.

Small carbon clusters have been investigated by spectroscopic methods,[145-147] which show that C_3 and C_4 are linear. Experimental work on Si clusters is unfortunately quite scarce.[148-149] Experimental data on the atomization energies of germanium clusters are available in the literature[150-152] and can be compared with the theoretical predictions (see Figure 14).

The evident participation of p-type basis functions certainly has a decisive importance for the electronic structure of these clusters; this is mainly true for nonmetallic elements (like groups IVa (4), VA (5), and VIa (6)), of course. On the other hand, it is necessary to realize that the formation of the real hybrid orbitals with a larger p orbital component (such as sp^2 and sp^3) costs an amount of promotion energy which must be balanced by the formation of a sufficient number of directed chemical bonds. The hybridization between s and p orbitals is, however, a necessary condition for less compact structures, such as the diamond crystal lattices. The average coordination number is, of course, small even for relatively large clusters. Therefore, it is possible to assume that carbon and silicon clusters will not have the forms of sections of the diamond crystal lattice. More compact geometrical structures of small clusters of these elements can be expected, unless of course, effects (e.g., nodal structure of MO's and NO's) similar to those occurring in the case of Li and Be clusters bring about a preference for planar cluster geometries.

For reasons mentioned earlier for group IIa (2) elements, hybridization between 2s and 2p orbitals is easier than the hybridization between 3s and 3p or 4s and 4p orbitals. Therefore, a partly different behavior can be expected for clusters of the elements from the first and second or third row of the periodic table.

The partial occupancy of the p AO's in the atoms of groups IIIa (3) and IVa (4) permits a chain form for small clusters. Therefore, also this type of noncompact shapes should be considered an important possibility for the geometry of these clusters.

In principle, the same basic laws can be employed also for the qualitative understanding of the structures of the group IIIa (3), IVa (4), Va (5), and VIa (6), clusters if the appropriate characteristic number of valence electrons is taken into account.

B. Group IIIa (3) and IVa (4) Tetramers

The main features of the bonds in the clusters of the elements from groups IIIa (13) and IVa (4) can be shown on examples of B_4, Al_4, C_4, Si_4, and Ge_4. Tetramers have, in principle, the choice between one-, two-, and three-dimensional geometries and indeed, many investigations speak in favor of the linear C_4 as the most favorable geometry of the carbon[149] tetramer; its energy is only slightly lower than that of the rhombic form.[143,144] The rhombus is again, as for group Ia (1) clusters, the optimal geometry of B_4, Al_4, and Ge_4.[108]

Pseudopotential MRD-CI calculations with a valence basis set of double ζ quality show two characteristic features of planar Al_4:[108] The potential energy curve for the deformation of the square to the rhombus shape is very flat and the lowest singlet and lowest triplet are nearly degenerate. Hybridization between the 3s and 3p atomic orbitals is quite difficult, and molecular orbitals built from the 3s AO's therefore have clearly lower

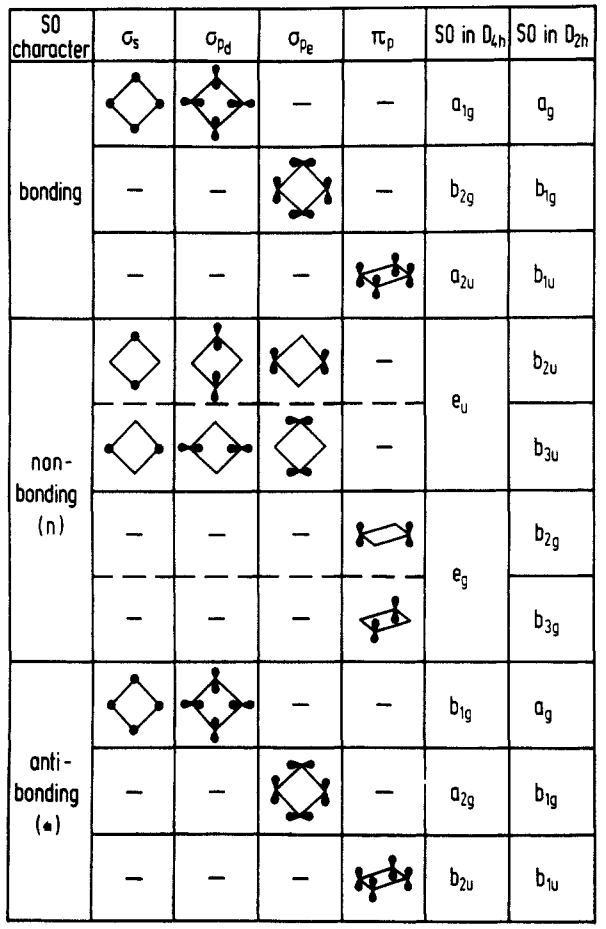

Figure 11. Schematic description of symmetry orbitals (SO) built from the s and p AO's for the planar tetramers with D_{4h} and D_{2h} symmetries. Reproduced with permission from ref 123. Copyright 1935 Elsevier.

MO energies than the MO's with the high participation of the 3p AO's. The stability of the Al_4 cluster thus depends mainly on the one-electron functions with high participation of the 3p-type AO's. The 4 electrons remaining after the occupation of 4 "s-type" MO's, must be distributed among the 12 "p-type" MO's. The linear shape for B_4 and Al_4 seems to have higher energy than the two-dimensional arrangements. The tetrahedron is again destabilized because of the Jahn–Teller effect.

Figure 11 shows the types of symmetry orbitals for the square (D_{4h}) and rhombic (D_{2h}) geometries. The σ_{pd}, σ_{pe}, and π_p symmetry orbitals have similar MO energies in Al_4. The $^3B_{1u}$ ground state of Al_4 (D_{2h}) has in its leading configuration a doubly occupied σ_{pe} MO and a singly occupied σ_{po} and π_p combination of p-type atomic orbitals. The rhombic tetramers of Al_4 with the internal angle α near to 90° are biradicaloids with nearly degenerate singlet and triplet states. With the change of the internal rhombus angle the energy varies very little. On the other hand, the binding energy per atom is quite high, and it is significantly increased when d-type polarization functions are included in the AO basis set.

Since the 2s and 2p atomic orbitals can hybridize more easily than the 3s and 3p AO's, some mixing between σ_{pd} and σ_s symmetry orbitals of B_4 can take place. The favorable geometry of the B_4 clusters is again a rhombus, with sides equal to 1.59 Å. According to MRD–CI calculations the singlet ground state of this cluster belongs to the A_g representation of the D_{2h} symmetry group. B_4 exhibits BE/n equal to 2.42 and

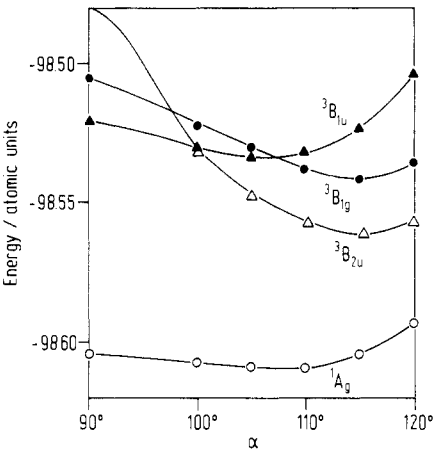

Figure 12. Energies of the ^1A_g, $^3B_{2u}$, $^3B_{1g}$, and $^3B_{1u}$ states of the planar B_4 as functions of the internal angle α during the deformation B_4 (D_{4h})–B_4 (D_{2h}). The B–B bond length is fixed (1.39 Å). The MRD–CI results with a double ζ AO basis set. Reproduced with permission from ref 123. Copyright 1985 Elsevier.

2.18 eV without and with the d-type polarization functions included in the AO basis set, respectively. The leading configuration in the ^1A_g wave function shows a doubly occupied combination of the symmetry orbitals σ_{pd} and σ_s and a doubly occupied π-electron p-type MO. The states $^3B_{1u}$ and $^3B_{1g}$, which are important for Al_4, have for the boron tetramer energies about 2 eV higher than the ground state (cf. Figure 12).

Roughly speaking, the 16 valence electrons of a group IVa (4) tetramer can be distributed among the valence molecular orbitals according to two different criteria: If no pronounced hybridization can take place, then the four orbitals originating from the ns AO's will be first filled up. The next six electrons occupy the three p-type symmetry orbitals without nodal planes. The remaining two electrons should be distributed among MO's with a single nodal plane. Consequently, the linear tetramer is a biradicaloid which can have a triplet ground state. The situation is quite similar for the D_{4h} tetramer since after the occupation of three binding MO's (σ_{pd}, σ_{pe}, and π_p) the remaining two electrons should be put on the degenerate e_u MO's (σ_{pe}, cf. Figure 11). A deformation of a square form to a rhombus can cause the splitting of the e_u energy levels and a stabilization of the group IVa (4) cluster (Figure 13). The resulting energy of the ground state depends certainly on many other factors, but the above-mentioned considerations show that the rhombic form can be advantageous also for group IVa (4) tetramers. The d-type polarization functions will evidently only favor the tendency to take a two-dimensional form. In this way one can roughly understand the preference of Si_4 and Ge_4 for the rhombic geometries.

Hybridization stabilizes the linear form of a C_4 tetramer. All theoretical calculations predict the linear forms of C_4 to be more stable than the other possible shapes. The inclusion of d polarization functions lowers the energy of the C_4 rhombus very much so that the rhombic and linear C_4 clusters have comparable energies. Nevertheless, the linear geometry has probably in fact the minimal energy among the carbon tetramer cluster forms.

In spite of the differences in the number of valence electrons the reasons for a relatively large stability of the rhombic geometry of the group IIIa (3) and IVa (4)

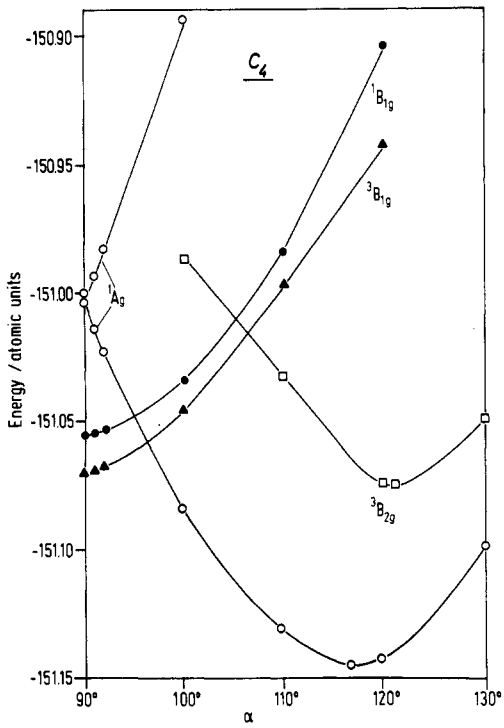

Figure 13. Energy of the states ^1A_g, $^3B_{3g}$, $^3B_{1g}$, and $^1B_{1g}$ of a planar C_4 cluster as a function of the internal angle α during the deformation C_4 (D_{4h})–C_4 (D_{2h}). MRD–CI results with 4.31 G AO basis set are shown. Reproduced with permission from ref 123. Copyright 1985 Elsevier.

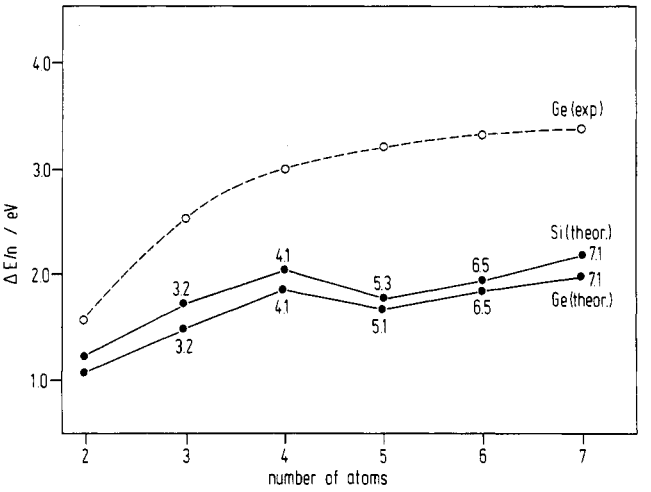

Figure 14. Binding energy per atom (BE/n) of Si and Ge clusters as a function of the number of atoms n in cluster. The interatomic distances are fixed to the value 1.49 Å. The theoretical values (theor.) are results of effective core potential (ECP) MRD–CI calculations of the geometries of Si and Ge clusters described with the labels from Chart I. The experimental values (exp.) are taken from the ref 150 and 151. Adapted from ref 144.

tetramers are very similar to those that cause the rhombus to be the optimal form of group Ia (1) tetramers: Since entirely different one-electron functions exhibit similar degeneracies for group Ia (1) and IVa (4) tetramers and since the same number of valence electrons is available to occupy the nearly nonbonding MO's of these tetramers similar tendencies for optimal cluster geometries can exist for small group IVa (4) and Ia (1) clusters. On the other hand, some new features of the more complicated electronic structure of the larger group IIIa (3) and IVa (4) clusters with larger number of valence electrons should be expected.

C. Electronic Structure and Geometry of Small Group IVa (4) Clusters

The ability of theoretical predictions of geometric properties of small group IVa (4) clusters will be illustrated in this section on the example of a work in which the effective potential (pseudopotential) procedure combined with the MRD-CI method has been applied to a series of geometries for silicon and germanium clusters with a number of atoms ranging from three to seven. No systematic energy optimization has been attempted, but the selection of the investigated cluster topologies makes it possible to compare the linear geometries, very compact arrangements, sections of a diamond crystal, and finally the geometries which have been found to be very stable for group Ia (1) clusters. The above-mentioned similarities in the properties of group Ia (1) and IVa (4) tetramers have served here in particular as a useful guide in the selection of the cluster topologies studied.

The SCF states of Si_3 and Ge_3 are triplets, but the configuration interaction favors the singlets so strongly that the singlet states have lower energies for these trimers than the triplets. The energies of Si_3 and Ge_3 do not change too much with the variation of the angle between the two bonds, and, moreover, the crossing between states with different multiplicities can occur. Therefore, it is very difficult to predict the optimal geometries of Si_3 and Ge_3 with a good reliability since the small energy differences for different angles and different states depend quite strongly on the details of the computational method applied.

As described in section IV.B, the theory predicts the rhombus to be the most stable form of Si_4 and Ge_4. These Si_4 and Ge_4 clusters exhibit ^1A_g ground states with quite large binding energies (BE/n = 1.73 eV and BE/n = 2.6 eV, respectively). The tetrahedron shape is very unfavorable for silicon and germanium tetramers. In contrast to C_4, the chain is also not the optimal form for these two tetramers.

The difference in the binding energies for the pentamers studied are relatively small with the exception of clearly unfavorable T_d and D_{4h} forms. Mainly the computed stabilities of the square pyramid (5.3) (C_{4v}) and trigonal bipyramid (5.2) forms of Si_5 and Ge_5 are very similar. The optimal geometry found for Si_6 and Ge_6 is the (6.5) (C_{2v}) form (cf. Chart I), which is a very compact tripyramid, but other shapes have only a little smaller computed binding energies, so that again, a more detailed prediction of the optimal shapes of Si_6 and Ge_6 is very difficult.

The geometry of a pentagonal bipyramid (7.1) (D_{5h}) is quite favorable for Si_7 and Ge_7. The MRD–CI calculations estimate the binding energy per atom to be more than 75% higher than the BE/n of the corresponding dimers (compare Figure 14).

It is necessary to emphasize that the description of the electronic structure of systems with such a large number of electrons is inaccurate, mainly because of the limited basis sets, the non-size-consistent CI treatment, and, in the case of Ge_4, the neglect of relativistic effects. Nevertheless, it is satisfactory that a trend of an increasing cohesive energy with increasing size of group IVa (4) clusters is well reproduced by these calculations. This property of small germanium clusters has been also found experimentally.[150,151] Numerical disagreements

are not surprising because of the already mentioned methodological deficiencies and the choice of cluster geometries based on qualitative considerations only.

D. Conclusions

The consideration of the forms of one-electron functions is again quite informative for clusters built from the atoms of groups IIIa (3) and IVa (4).

The analysis of the occupied molecular orbitals built mainly from the s AO's in leading configurations in the wave functions of Si and Ge clusters is very simple: The sequence of orbital energies is mainly determined by the number and character of nodal planes. A parallel consideration of the MO's (or NO's with larger occupation numbers) in which the p AO's prevail is much more difficult and less transparent. It is only possible to state that the similarity between the optimal geometries for the alkali metal and group IVa (4) tetramers cannot yet be generalized for the shapes of clusters with higher nuclearities in a straightfoward manner. The methodological complications connected with the large number of electrons make the detailed predictions very difficult. It is very hard to think of parallel features between the jellium droplet model and MO–LCAO approaches for group IIIa (3) and IVa (4) clusters, as it is possible for group Ia (1) clusters. It would be particularly interesting to attempt such a rationalization at least for aluminum clusters since the metallic character of aluminum should justify the use of the jellium model for Al clusters according to the usually accepted ideas of solid-state theorists.

Some general features relevant to the electronic and geometric structure for group Ia (1) and IIa (2) clusters can be found also for group IIIa (3) and IVa (4) clusters. The compactness of the cluster is not the only important factor determining the best cluster geometry. Less compact structures are also favorable. The lower cluster compactness is not caused by directed valences due to the s–p hybridization but is caused by the pseudo-Jahn–Teller effect or related factors that destabilize the more compact arrangements.

The very limited and unsystematic investigation of group IIIa (3), IVa (4), and Va (5) clusters should be completed by appropriate studies. These important clusters offer a challenging field within reach of the theoretical methods of quantum chemistry at least for the first row of the periodic table.

V. Transition-Metal Clusters

A. Introduction and Methodological Problems. Transition-Metal Diatomics

A recent review[153] of the experimental data and theoretical results concerning transition-metal (TM) clusters led to the conclusion that such systems, especially those of high nuclearity, remain largely unexplored. One of the reasons is the paucity of the experimental data which does not challenge the interest of the theorists. According to our opinion, however, the main reason for the persistent lack of unified interpretation and understanding of the electronic properties of small transition-metal clusters and particles is certainly represented by the enormous difficulties met in studying molecular systems containing a large number of electrons and heavy atoms when using very sophisticated quantum mechanical methods. This is proved by the fact that only few diatomics of the transition metals have been studied by employing rigorous theoretical methods and that even for such relatively simple systems, the results cannot in general be considered completely satisfactory. There are several examples for the lack of satisfactory accuracy in theoretical predictions compared to available experimental data and for the inability of theory to make unambiguous predictions of values of physical quantities not yet experimentally determined.

The seriousness of the methodological and computational problems encountered in the theoretical investigations of the metal–metal bond can be easily understood considering the case of transition-metal diatomics.

In the following discussion, three metal dimers will be considered in detail, namely, Sc_2, Cr_2, and Cu_2, while only short comments will be given for other TM diatomics. The reader may refer to the review of Weltner[153] for a more complete tabulation and discussion of the available experimental and theoretical results.

The choice of these three examples is justified by the fact that the metal–metal bond in the three species is dominated by quite different electronic mechanisms, as simple qualitatively considerations may suggest. The Sc, Cr, and Cu atoms have just one d electron, a half-filled d shell and a complete d shell, respectively. Sc and Cu have low-spin ground states, $^2D(3d^14s^2)$ and $^2S(3d^{10}4s^1)$, respectively, while the Cr atom has the highest multiplicity, $^7S(3d^54s^1)$. In addition, along the transition series, the d orbitals are more and more contracted. Therefore, the 3d–3d interaction is expected to be much more important in Sc_2 and in Cr_2 than in Cu_2. In fact, this latter diatomic has been considered as an alkali-like molecule, at least in a qualitative manner, due to the assumption that the Cu–Cu bond is dominated by the overlap interaction between diffuse 4s orbitals, while the contracted 3d shell scarcely contributes to bond formation.

For all three diatomics, Sc_2, Cr_2, and Cu_2, some properties of the ground state such as the bond length (r_e), the dissociation energy (D_e), and the harmonic vibrational frequency (ω_e) have been experimentally determined with satisfactory accuracy. Thus, the predictive capability of any theoretical approach can be easily checked.

The Sc_2 molecule has been studied with different Hartree–Fock (HF),[154-160] discrete-variational HF–Xα[161] (DV–X$_\alpha$), and density functional (DF) methods[162] (see appendix VII.B). The states which correlate with the two Sc atoms in their ground state, $^2D(3d^14s^2)$, are $^3\Sigma_g^-$, $^1\Sigma_g^+$, and $^3\Sigma_u^+$. The most accurate calculations[155,157,159] performed with an extended basis set and MC and CI treatments led to the conclusion that the three states are all characterized by a long Sc–Sc distance (>4 Å) and a very low vibrational frequency and dissociation energy, in disagreement with the experimental values $D_e = 1.13 \pm 0.2$ eV and $\omega_e = 238.9$ cm^{-1}.[164] The $^3\Sigma_g^-$, $^1\Sigma_g^+$, and $^3\Sigma_u^+$ molecular states are thus characteristic of a van der Waals molecule, and none of them can be the true ground state. EPR investigations[163] suggested that the ground state of Sc_2 is a quintuplet which, however, cannot correlate with the $^2D + {}^2D$ dissociation limit. Further theoretical investigations[160] showed that the

lowest energy state is the $^5\Sigma_u^-$. The leading configuration $(4s\sigma_g)^2(4s\sigma_u)^1(3d\sigma_g)^1(3d\pi)^2$ has three of the four unpaired electrons in MO's mainly composed by d orbitals and correlates with a dissociation limit $^2D(3d^14s^2)$ + $^4F(3d^24s^1)$, which is nearly degenerated with the dissociation limit ^2D + $^4F(3d^14s^14p^1)$. The computed molecular constants for the $^5\Sigma_u^-$ state, at r_e = 2.789 Å, are D_e = 0.44 eV and ω_e = 184 cm^{-1}. The vibrational frequency is in good agreement with the experimental value, while the calculated D_e deviates from the experimental value by 60%.

Earlier calculations carried out with a DF method[162] gave the values r_e = 2.699 Å, D_e = 1.80 eV, and ω_e = 200 cm^{-1} for the same state. The quite large (~40%) overestimation of the dissociation energy has been attributed to the limitations of the local approximation adopted when defining the exchange-correlation functional.

The main conclusion which can be drawn from the theoretical studies of the electronic structure of the Sc_2 molecule is that the ground state does not correlate with the ground state of the separated atoms. This means that during the formation of the Sc–Sc bond the metal atoms undergo an s–d electron excitation and a spin reorganization.

The problems connected with the electron spin reorganization which occurs during the formation of the metal–metal bond are of special importance in describing the bond in the Cr_2 molecule. This molecule is characterized by a short equilibrium distance (1.68 Å),[165-168] a high dissociation energy (1.6 eV),[169] and vibrational frequency (452 cm^{-1}).[166-168] All the experimental data yield consistently $^1\Sigma_g^+$ as the ground state which stems from coupling all the six unpaired electrons originally present on each Cr atom, giving rise to a hexuple bond. However, this qualitative description is far from being satisfactory. In fact, a single closed-shell Slater determinant cannot property describe the dissociation into two Cr atoms in their ground state and the HF solution has an energy much higher than the dissociation limit (see for instance ref 170). The inclusion of f and g functions in the basis set greatly improves the HF results but the computed value of the total energy at the minimum point (r_e = 1.454) lies about 19 eV above the dissociation limit.[170] Still, in this case the effect of f and g functions hardly has a physical meaning since it cannot be assumed that functions with a high angular quantum number have a large bonding capability. The importance of the f and g functions is clearly a spurious effect of the inadequacy of the HF solution which generates Cr atoms in a very high energy state in which interaction with f and g atomic states can occur.

An alternative representation of the bond in Cr_2 is that of an antiferromagnetic molecule in which the unpaired electrons remains localized on each metallic center but with opposite spin. This, however, would imply the existence of local magnetic moments, a fact contradicting some experimental evidence.[166,167] UHF and GVB calculations[171,172] performed on the Cr_2 antiferromagnetic molecule provided a D_e value of 0.35 eV only, much lower that the experimental one, and a very long Cr–Cr distance (3.1 Å).

Attempts to overcome the inadequacy of the one-electron picture of the Cr_2 bond by means of CAS–SCF and extended CI calculations[173] did not quite solve the difficulties. As expected the total energy is significantly lowered, but the potential energy curve is still unbound with respect to the dissociation limit ^7S + ^7S. The same is true for CI calculations using partially localized MO's.[174] First DF calculations on Cr_2 failed to predict the true ground-state symmetry.[162] More recent results obtained from the density functional theory, which adopts different local approximations for the exchange-correlation energy, are claimed to be largely superior to the HF–CI ones.[175] For instance, calculations performed allowing a symmetry broken solution ($C_{\infty v}$ instead of $D_{\infty h}$) gave the values 1.68 Å and 441 cm^{-1} for r_e and ω_e, respectively, which agree with the experimental data. On the other hand, D_e is estimated to be about 2.6 eV, a value considerably larger (55%) than the experimental one. From the results of these DF calculations, the conclusion has been drawn that the Cr–Cr potential energy curve is not that of a hexuply bonded molecule. As the Cr–Cr bond is slightly stretched the binding interaction suddenly decreases and the molecule behaves like an antiferromagnetic one with large local magnetic moments and large anharmonicity in vibration; a hexuply bonded molecule would be characterized by a much higher vibrational frequency with a small anharmonic correction. In spite of the success of the DF methods in predicting a stable Cr_2 molecule and in accounting for some experimental data, the large overestimate of D_e poses some questions about the reliability of the local density approximation for the exchange-corelation functional. On the other hand, all the reported computations on Cr_2 performed within the HF–CI scheme prove that such an approach is inadequate to describe the Cr–Cr bond.

Recently, Goodgame and Goddard[172b] offered a very plausible explanation of such a drawback. In the framework of the GVB theory, the ionic contributions (involving doubly occupied atomic-like orbitals) are affected by a correlation error much higher than the covalent structures (involving singly occupied orbitals). In order to introduce a proper correction, a simple scheme was derived[172b] to modify (in a semiempirical manner) the one-center self-Coulomb repulsion integrals J_{ii}. When such modified integrals are used in the purely theoretical GVB procedure, the experimental values of the atomic electron affinity are exactly reproduced and the correct behavior of covalent and ionic wave function for molecular systems is obtained for every internuclear separation.

The modified GVB procedure (MGVB[172b]) applied to the Cr_2 diatomic (as well as to the Mo_2 one) gave results very satisfactory for both the r_e and D_e quantities (1.61 Å and 1.86 eV, respectively). Moreover, the MGVB investigation of the Cr–Cr potential curve revealed the existence of a second minimum at r_e = 3.06 Å, bound by only 0.3 eV. At a large distance the Cr–Cr bond is essentially due to s–s interaction, while the five d unpaired electrons on each chromium atom are antiferromagnetically coupled. Notice that the DF study[175] was unable to identify the existence of the minimum occuring at large Cr–Cr distance.

The Cu_2 molecule will be our third example: it is the simplest TM diatomic and has been used as a benchmark in developing a theory of the metal–metal bond. The theoretical study of Cu_2 is not complicated by the

presence of unpaired electrons giving rise to a manifold of states of different spin multiplicity, as was the case for the Sc_2 molecule.

The ground state of Cu_2 is $^1\Sigma_g^+$, which dissociates correctly into two ^2S Cu atoms. Furthermore, the full d shell of the Cu atom does not create the problem of spin coupling like Cr_2 does. Because of this character the Cu_2 molecule is the easiest transition-metal diatomic. Nevertheless, theoretical studies of Cu_2 have dramatically shown that its quantitative description is a formidable task.

Hartree–Fock "all-electron" calculations[176-186] gave for the Cu–Cu distance values ranging from 2.25 to 2.43 Å, which depend on the size of the basis set, and a dissociation energy of only about 25% of the experimental one.[187] The largest basis set adopted, including up to f polarization functions, predicted r_e and D_e values differing by 0.2 Å and 1.5 eV, respectively, from the experimental values of 2.22 Å and 2.05 eV.[187]

The disagreement between theoretical and experimental results is certainly due to the lack of electron correlation. Attempts to correct this inadequacy have been made by employing CI[176,182,183,186] or MC–SCF[178,181,183] computational schemes. The need to include at least the 22 valence d and s electrons into the correlation treatment clearly shows the important role played by the completely filled 3d shell in stabilizing the Cu–Cu bond. Consequently, it appears that the picture of the copper dimer as an alkali-like molecule is very crude. Accurate CI calculations led to an overestimate of r_e of about 0.12–0.14 Å and to a dissociation energy not better than 75% of the experimental one. This persistent disagreement may have two main reasons. The first is the size-inconsistency of a CI procedure which includes singly and doubly excited configurations (SD–CI) only or an incomplete estimate of the contributions of highly excited configurations. The second reason is to be sought in the neglect of the relativistic corrections in standard HF–CI calculations. These corrections are notably large even in the case of the Cu atom and may certainly affect the description of the Cu–Cu bond. The qualitative features of the relativistic effects can be summarized as follows. In the relativistic representation, the 4s orbital of the Cu atom undergoes a contraction which can cause a shortening of the Cu–Cu bond and a larger 4s–3d correlation energy which, again, may considerably increase the computed dissociation energy. These effects are well documented by the work of Pelissier[188,189] in which atomic orbitals obtained in the framework of the relativistic effective core potential (RECP) method were utilized in the CI including 22 electrons leading to the corrections of −0.05 Å and of about 0.5 eV for r_e and D_e, respectively, with respect to the corresponding nonrelativistic results.

The need for relativistic corrections is further demonstrated by very recent calculations on Cu_2[180,184-186] carried out according to the following computational prescriptions. The basis set is very flexible and includes up to two or three sets of f polarization functions (the effect of the g functions has also been checked).[185] The correlation treatment is size-consistent, that is the effect of the "unlinked clusters" is taken into account[184] by means either of the CEPA (see appendix VII.A) or of the newly proposed CPF[185] method. Finally, relativistic corrections are computed in first-order approximation using the Cowan–Griffin[190] operator. These very sophisticated theoretical treatments[180,184,185] gave nearly equivalent results: r_e = 2.33 Å and D_e = 1.80–1.85 eV. The improvements of the results due to the relativistic corrections are very convincing and it can be assumed that the small remaining deviations from the experimental values are only due to an incomplete evaluation of the correlation effects and due to the approximations adopted in computing the relativistic corrections.

Calculations performed within the framework of the DF theory using different local approximations[162,191,192] for the Cu_2 molecule gave results in agreement with the experiment: $2.17 < r_e < 2.28$ Å and $268 < \omega_e < 280$ cm^{-1}, while, as in other cases, the binding energy is overestimated: $2.22 < D_e < 2.65$ eV. It is important to note that the DF theory is able to describe a correct Cu–Cu bond distance without considering the relativistic effects which, in the context of the HF–CI methods, seem to play a dominant role.

The theoretical and computational difficulties commented on in the cases of Sc_2, Cr_2, and Cu_2, are encountered also in studying all other transition-metal dimers.

The aim of the following discussion is to stress this important aspect connected with the present status of the quantum chemical theories and computational developments and, at the same time, to comment on a very particular feature of the transition metal–metal bond that is on the degree of participation of the d electrons in forming stable TM aggregates.

The case of the diatomics Ti_2 and V_2 is interesting in order to show that for the first elements of the transition series the d–d interaction plays an important role in the formation of the metal–metal bond. Little is known experimentally about the molecular parameters of Ti_2[156,193,194] and theoretical calculations[158,162] did not reach a complete agreement about the symmetry of the ground state. Both the high ($^7\Sigma_u^+$) and low spin ($^1\Sigma_g^+$) ground state have been proposed but the most refined CAS–SCF CI calculations[195] seem to suggest a singlet ground state in which the two Ti atoms are bound by a triple bond mainly involving the 3d orbitals.

Recent calculations[161] based on the DV–Xα method have been performed with the aim to compute the ionization potential and the electronic transition energies for the titanium dimer. The theoretically estimated values are in acceptable agreement with experiment, and the Ti–Ti bond length in the $^1\Sigma_g^+$ ground state has been found to be 1.96 Å.

The ground state of V_2 is known to be $^3\Sigma_g^-$[196] and it does not correlate with V atoms in their ground state. Two ground-state atoms interact in a repulsive manner, while two excited atoms V $^6D(3d^4 4s^1)$ can form a strong bond (r_e = 1.76 A, ω_e = 537 cm^{-1}, and D_e = 1.85 eV[196]) which can be described by the SCF configuration $(4s\sigma_g)^2(3d\sigma_g)^2(3d\pi_u)^4(3d\delta)^2$, with a formal bond order as high as five. Also in this case the large stability of the dimer is due to the important participation of the 3d electrons in the metal–metal bond. CAS–SCF CI calculations[173] showed that the HF configuration has a weight of only about 70% in the final wave function and that at least one set of f function is needed in order to compute a stable V_2 molecule. The best estimate of D_e is 0.33 eV, while r_e and ω_e values are in good agreement

with the experiment. Improved results for D_e were obtained in a CI study[174] using partially localized orbitals expanded in a basis of 6s5p4d2f Slater orbitals. In this study it was shown that a D_e value of 1.45 eV can be obtained by a CI treatment including the 3p intrashell and 3p–3d intershell correlation.

Local spin-density calculations of Salahub and Baykara[197] gave results in optimum agreement with the experimental data as far as r_e and ω_e are concerned (1.75 Å and 594 cm^{-1}, respetively) while D_e was largely overestimated. Moreover, this theoretical investigation further confirmed that the symmetry of the ground state is $^3\Sigma_g^-$.

As described above, the Sc_2, Ti_2, V_2, and Cr_2 diatomics are characterized by a large contribution of the d electrons to the metal–metal bond. This contribution suddenly becomes of little importance in the case of the Mn_2 molecule and in the diatomics of metals which have more than half-filled d shell. In fact, the five d unpaired electrons of the Mn atoms are involved in Mn_2 in a very weak antiferromagnetic coupling only ($J = 9 \pm 3$ cm^{-1}).[198,199] HF calculations of Nesbet[200] indicate that the antiferromagnetic $^1\Sigma_g^+$ ground state of Mn_2 is characterized by $D_e = 0.79$ eV and $r_e = 2.88$ Å, while the DF method[162] proposes a high spin state. The two theoretical methods, however, agree on indicating Mn_2 as a van der Waals molecule, a fact confirmed by experimental evidence.[198,199] The high stability of the $3d^54s^2$ configuration with respect to the excited one $3d^64s^1$ prevents the Mn atoms from forming a strong s–s bond. The antiferromagnetic character of Mn_2 is confirmed also by recent LD calculations.[197]

On the basis of HF–CI[201] and Xα–SW[202] calculations, the iron dimer is found to have a $^7\Delta_u$ ground state. The formation of Fe_2 can be qualitatively described assuming that the iron atoms undergo the excitation $3d^64s^2 \rightarrow 3d^74s^1$. Three unpaired electrons remain strongly localized in the d orbitals at each center and no antiferromagnetic coupling occurs because of the very small d–d interaction. Therefore, the iron dimer has a single s–s bond. The HF–CI study[201] confirmed this general feature of the Fe–Fe interaction but was not able to predict the stability of a Fe_2 molecule with respect to the ground state atoms due to the limitations in the basis set and in CI treatment. On the other hand, the DF method, as applied by Harris and Jones[162] gave a ground-state symmetry in agreement with the HF–CI study but estimated a binding energy four times larger than the experimental one.[210] The theoretical analysis of the Fe–Fe bond is very complicated by the existence of many low-lying states. Shim and Gingerich[201] showed that 112 states, all arising from the interaction $3d^74s^1 + 3d^74s^1$, lie within an energy range as small as 0.5 eV.

The same qualitative description of the bond is valid also for Co_2 and Ni_2. The ground state of the dimers correlates with the metal atoms in a $3d^{n+1}4s^1$ configuration. In the case of Co_2, HF–CI calculations[203] showed that the molecular states arising from the excited atomic state $^4F(3d^84s^1)$ lie at lower energy: 84 states are computed within an energy interval of only 0.42 eV for a Co–Co distance of 2.5 Å. On the basis of the geometry optimization carried out at CI level[203] it was concluded that $^5\Sigma_g^+$ should be the ground state, even if several other singlets, triplets, and quintuplets lie close to the ground state within an interval of 0.04 eV. Notice that the ordering of so closely spaced states can be easily changed by some technical computational details and by inclusion of the spin–orbit coupling perturbation. In any case, the Co–Co bond has been interpreted as essentially due to the s–s interaction, but, once more, the limitations of the theoretical approach prevented the computation of a stable species.

The nickel atoms in their ground state $^3F(3d^84s^2)$ can only form a weakly bound van der Waals molecule[205] while 30 states[206a] arising from the interaction of two Ni $^3D(3d^94s^1)$ atoms are strongly bound and lie within an energy interval of 0.5 eV. Singlet and triplet $\delta\delta$ combinations of the two d holes lead to the states $^1\Sigma_g^+$, $^1\Sigma_u^-$, $^3\Sigma_u^-$, $^1\Gamma_g$, and $^3\Gamma_u$ but only the $^1\Gamma_g$ and $^3\Gamma_u$ states seem to be consistent with the most refined experimental work.[207] The prediction for $D_e = 1.4$–1.9 eV and $r_e = 2.0$–2.3 Å obtained from CI calculations are in qualitative agreement with the experimental values $D_e = 2.07 \pm 0.01$ eV and $r_e = 2.20$ Å.[207]

Quantum mechanical calculations have been reported for diatomics of the second and third transition metals (see Table 1 in ref 153) and from their analysis the conclusion can easily be drawn that the predictive capability of the theory is even lower than in the case of the first transition series. This is not surprising when considering that the relativistic effects in the case of heavier metal atoms have to be taken carefully into account for a quantitative determination of the energetics of the metal–metal interactions. Only few attempts to incorporate such effects in the effective core potentials (relativistic ECP, RECP) have been done and corresponding calculations on Pd_2, Pt_2,[208,209] Ag_2,[34,210] and Au_2[30,211] have been reported.

The transition-metal dimers have been considered in this section only to underline some conceptual and computational problems which originate from the particular nature of the transition elements. The most representative and recent results from theoretical studies on first transition-metal dimers are summarized in Table VI.

The transition metals are characterized by a spectrum of low-lying excited states and even the atomic numerical Hartree–Fock calculations are very often unable to describe the energy splitting between the ground state and the first excited states. This is not only due to the fact that HF calculations do not include any electron correlation but also to the fact that the correlation energy is far from being constant for states corresponding to atomic configurations with different occupancy of the d, s, and p shells. This is easy to understand if one considers that the intrashell correlation energy is much larger for d than for s (and p) shells. As a consequence, different states obtained by intershell excitations are characterized by a change in correlation energy (the so-called "differential correlation energy") which is roughly proportional to the relative variation in the occupation number of the different shells. The correct description of such an effect requires the use of very flexible basis sets in order to account properly for both the radial and angular correlation energy and excitations of high order need to be included in the CI treatment (see for instance ref 184–186). The differential correlation energy seems to be an important constituent of the metal–metal interaction energy especially for the cases in which the metal–metal bond

TABLE VI. Experimental and Theoretical Results on Dimers of the First Transition Metals

method (ref)	r_e, Å	ω_e, cm^{-1}	D_e, eV	ground-state symmetry
		Sc_2		
exp				
(164a)			1.1 (2)	
(156, 164b)		238.9		$^5\Sigma$
(163)				
DF (162)	3.25	235	1.00	$^3\Sigma_g^+$
MCSCF (157)	2.57		1.12	$^5\Sigma_u^-$
HF (158)	3.05	210		$^1\Sigma_g^+$
ECP-MCSCF (155)	5		0.2	$^1\Sigma_g^+$
CASSCF-CI (159)	3.7		0.8	$^5\Delta_u$
	4.2		0.06	$^3\Sigma_g^-$, $^1\Sigma_g^+$, $^3\Sigma_u^-$
CASSCF-CI (160)	2.79	184	0.44	$^5\Sigma_u^-$
DV-Xα (161)	2.21			
		Ti_2		
exp				
(194b,c)			1.3 (1)	
(156, 193, 194)		407.9		
DF (162)	2.52	220	2.30	$^7\Sigma_u^+$
HF (158)	1.87	580		$^1\Sigma_g^+$
DV-Xα (161)	1.96			$^1\Sigma_g^+$
CASSCF-CI (173)	1.87	580		$^1\Sigma_g^+$
		V_2		
exp				
(194b,c)			2.5 (2)	
(196)	1.76	538	1.85	$^3\Sigma_g^-$
DF (162)	2.65	230		$^1\Sigma_g^+$
HF (158)	1.96	420		$^1\Sigma_g^+$
CASSCF-CI (159b)	1.77	594	0.33	$^3\Sigma_g^-$
MCSCF-CI (174)	1.79	557	1.45	$^3\Sigma_g^-$
DF (197)	1.75	594	3.85	$^3\Sigma_g^-$
		Cr_2		
exp				
(169)			1.6 (3)	
(165–167)	1.68	452		$^1\Sigma_g^+$
DF (162)	3.66	55	0.20	$^{13}\Sigma_g^+$
MCSCF (157)	1.90		1.48	$^1\Sigma_g^+$
HF (158)	1.56	750		$^1\Sigma_g^+$
GVB (171, 172a)	3.06	110	0.35	$^1\Sigma_g^+$
HF-f functions (170)	1.45	1181	unbound by 19.1 eV	
MCSCF-CI (174)	1.7		unbound	
CASSCF-CI	1.7		unbound	
DF (175)[a]	1.68–1.70	435–443	2.0–2.8	$^1\Sigma_g^+$
MGVB (172b)	1.61		1.86	$^1\Sigma_g^+$
		Mn_2		
exp				
(198)			0.3 (3)	
(199)	3.4			$^1\Sigma_g^+$ (antiferromagnetic)
(164b)		124.6		
DF (162)	2.7		1.25	$^{11}\Pi_u$, $^{11}\Sigma_u^+$
HF (158)	1.52	680		$^1\Sigma_g^+$
HF (200)	2.88		0.79	(antiferromagnetic) $^1\Sigma_g^+$
DF (197)	2.52	144	0.86	(antiferromagnetic) $^1\Sigma_g^+$
		Fe_2		
exp				
(201)			0.8 (2)	
(194a, 202d)		300.3		
(202b)	1.87			
(202c)	2.02			
DF (162)	2.1	390	3.45	$^7\Delta_u$
HF (158)	1.58	660		$^1\Sigma_g^+$
HF-CI (201)	2.40	204		$^7\Delta_u$
		Co_2		
exp (203)			1.0 (3)	
DF (162)	2.07	360	3.35	$^5\Delta_g$
HF (158)	2.64	200		$^1\Sigma_g^+$
HF-CI (203)	2.4	240		$^5\Sigma_g^+$
		Ni_2		
exp (207)	2.200 (7)	381	2.07 (1)	$^1\Gamma_g$ or $^3\Gamma_u$
ECP-MCSCF (206b)	2.49			$^3\Sigma_u^+$
ECP-GVB-CI (206d)	2.04	344	2.9	$^3\Sigma_g^-$
DF (162)	2.18	320	2.70	$^3\Sigma_g^-$
HF-CI (206a)	2.20	289	1.42	$^1\Sigma_g^+$

TABLE VI (Continued)

method (ref)	r_e, Å	ω_e, cm^{-1}	D_e, eV	ground-state symmetry
ECP-GVB-CI (206c)	2.26		1.89	$^3\Sigma_u^+$
ECP-MCSCF-CI (205)	2.33	211	1.43	$^3\Sigma_u^+$
HF (158)	2.28	240	3.42	$^1\Sigma_g^+$
		Cu_2[b]		
exp (187)	2.22	266	2.05	$^1\Sigma_g^+$
HF (158)	2.32	210		
DF (162)	2.27	280	2.30	
MRD-CI (176)	2.33		1.67	
HF (177, 179)	2.41	235	0.68	
GVB (180)	2.48	162	0.83	
GVB-relativitic (180)	2.42	176	0.90	
CASSCF-CI (181)	2.32		1.61	
HF-CI (182)	2.76	134		
CASSCF-CI (183)	2.35	227	1.99	
CEPA (184)	2.27	242	1.69	
CEPA-relativistic (184)	2.23	263	1.80	
HF-CI (CPF) relativistic	2.24		1.84	
MP4 (SDTQ) (186)	2.23	283	2.20	
ECP-CI (189)	2.31	272	1.48	
ECP-CI relativistic (188)	2.25	274	2.00	
DV-Xα (191)	2.26	268	2.21	
DF (192)	2.17	330	2.65	
ECP-DF-SIC (336b)	2.222		2.049	
ECP (DF for correlation) (358)	2.26	262	1.95	
ECP-CI (357b)	2.14	269	1.54	

[a] Different results within the quoted ranges have been obtained by using exchange and correlation functional of different forms. [b] All the reported calculations on Cu_2 have been carried out for the ground state $^1\Sigma_g^+$.

formation requires the "preparation" of the atoms in their excited states. As shown above, such effects occur for almost all TM diatomics.

In addition, one has to consider that the changes in radial expansion of the different shells accompanying the electronic excitations are coupled with changes in relativistic deformation of the orbitals which again can affect the intershell and intrashell correlation energy. Furthermore, the assumption that the valence shells of transition elements are the nd, $(n + 1)$s, and $(n + 1)$p shells only seems to be doubtful at least in some cases. For instance, the correlation effects involving np and nd electrons are far from negligible,[174] but taking them into account in the case of polyatomic systems raises the computational difficulties over any practical limit.

From the above analysis, it is easy to draw the conclusion that a quantitative description of the bonding interaction between transition-metal atoms requires the use of very flexible basis sets. The computations must be carried out according to advanced schemes to be able to give a good correlation energy at least for the valence electrons but also to account for the main features of the relativistic effects.

The application of this type of sophisticated theoretical methods to transition-metal clusters of higher nuclearity is presently very difficult although some recent developments are highly promising.

Presently, the only way is the use of approximate quantum mechanical methods which are especially designed and adapted for the particularly difficult task of studying the electronic structure of the TM clusters.

Among the possible simplifications of the theoretical and computational methods worth mentioning are the ECP methods and the density functional (DF) methods which use the local density approximation (LD) for evaluating the exchange-correlation terms (see appendix VII.B,C). The ECP methods combined with HF SCF procedure or with one of the LD methods seem especially suitable as a routine computational tool for a qualitative study of the electronic structure of TM clusters. However, the use of ECP methods within the HF formalism removes the computational problems only partially because the evaluation of the correlation energy for the valence electrons requires the same computational effort as the all-electron calculations, if the CI treatment is carried out according to the frozen core approximation. On the contrary, the LD methods can, in principle, overcome such difficulties by means of the density functionals proposed for the exchange-correlation energy. However, an "a priori" evaluation of the accuracy of such procedures in usually difficult due to the approximate nature of such functionals. Finally, for both HF and LD methods the problem of computing at least the leading relativistic corrections remains completely open, and a literature search reveals that very little work has been done in this direction.

Despite all the described difficulties the theoretical calculations performed on relatively large transition-metal clusters using approximate methods are useful, provided that the limitations of the methods are well documented and their effects on the predictive power of the corresponding calculations are critically discussed. If these conditions are fulfilled, even the approximate calculations are very welcome and can largely contribute to the formulation of useful concepts and general rules concerning the particular features of the electronic structure of the TM clusters.

Before reviewing the theoretical studies on TM clusters reported in the literature, it is useful to mention some specific problems concerning the electronic structure which should be elucidated by the theoretical investigations. The principal question is to what extent the d orbitals participate in the formation of the metal–metal bond. In other words, do the d electrons remain strongly localized around the atomic centers or are they to some extent delocalized in the bond region? This is a basic point to which several other questions are closely connected.

First, if the d orbitals are substantially involved, the metal–metal bond exhibits a directional character which is not present in a bond dominated by the interaction between spherical s orbitals. Obviously, the directionality of the metal–metal interaction should influence the optimum energy shape of the cluster. Furthermore, if the d electrons undergo a delocalization into the bond region, the corresponding one-electron energy of the cluster orbitals can be significantly different from the "pure" atomic value. As a consequence, the energy width of the "band-like" group of the d cluster-orbitals may become broad, and strong overlapping can occur with the corresponding "s band". The overlap of the s and d bands influences also the cohesion energy of a transition metal. This aspect is of fundamental importance for the enegetics of the ionization processes of the clusters as well as for the corresponding electronic relaxation processes.

Finally, the TM clusters composed by atoms with an incomplete d shell may be characterized by the existence of different spin states corresponding to different degrees of coupling of the d unpaired electrons. An effective coupling of the electron spins is expected to parallel the extent of the d–d interaction. In turn, this interaction may strongly depend upon the metal–metal distance in different aggregates of the same element and upon the characteristic radial expansion of the d orbitals along a transition series. All these effects can cause a variety of magnetic behavior which certainly represents a characteristic feature of the TM clusters.

B. First Row Transition-Metal Clusters

1. Scandium Clusters

The simplest TM cluster, Sc_3, has been isolated in rare gas matrix, and its ESR spectrum has been fully interpreted[212] assuming a doublet ground state of D_{3h} symmetry. This has been also confirmed by a resonance Raman study in argon matrix.[213] Knight et al.[212] proposed that the unpaired electron is localized in a totally symmetric MO with large d character, following the suggestion based on simple EHT calculations of D_{3h} trinuclear metal clusters.[214] On the contrary, according to the proposal of Anderson[215] the sequence of the MO levels associated with the 4s and 3d orbitals is $a_1'a_1'a_2''e$, leading to a $^2E'$ state which is Jahn–Teller unstable.

No other more rigorous calculations have been reported and the two quoted proposals based on simple qualitative arguments seem insufficient to assign the ground-state symmetry of the Sc_3 cluster in a definite way. In addition, the lack of information about the Sc–Sc bond distance and the molecular stability further complicate this task. Another point to be mentioned is that the doublet ground state of Sc_3 cannot correlate with the system $Sc_2(^5\Sigma)$ + $Sc^2D(3d^14s^2)$. Either it correlates with $Sc_2(^5\Sigma)$ + $Sc^4F(3d^24s^1)$ or with three interacting scandium atoms in their ^2D ground states. This fact which is relevant for establishing the degree of stability of Sc_3 with respect to the dissociation limit Sc_2 + Sc should be further investigated by theoretical methods with quantitative predictive power.

A mass spectroscopy investigation[216] could identify the cluster ion Sc_4^+ which shows high reactivity toward oxygen, hydrocarbons, alcohols, and organic sulfides. In order to explain the relatively high stability it was assumed that Sc_4^+ has a tetrahedral compact structure but the proposal has not been supported by other experimental or theoretical evidence.

The Sc_{13} cluster has been considered responsible for unique hyperfine structure of the ESR spectrum recorded in gas matrix.[212] The high stability of such a 39-valence electron species was attributed to a very compact structure, like the icosahedral one (13.1). On the basis of qualitative arguments this structure should be characterized by an electronic configuration of the type $(a_g)^2(t_{1u})^6(h_g{}^{10})(t_{2u})^6(g_u)^8a_g{}^1$ corresponding to a ^2A_g ground state. It should be noted that Xα–SW calculation of Sc_{13} with hcp structure (13.3) confirmed that the cluster should have a doublet ground state.[217] However, the lowest energy conformation of the Sc_{13} cluster is still uncertain because it is to be expected that the isosahedral (13.1), truncated hexagonal bipyramidal (13.3) or cubo-octahedral (13.2) structures are of similar stability.

2. Titanium Clusters

MO calculations using Anderson's Hamiltonian have been carried out[215] on a series of Ti_n clusters (n = 3–6), with the aim of identifying the most stable conformations. The compact forms, equilateral triangle (3.1), tetrahedron (4.3), trigonal bipyramid (5.2)8 and octahedron (6.3) are characterized by the highest BE/n values equal to 0.89, 1.03, 1.14, and 1.19 eV, respectively, while the computed Ti–Ti equilibrium distances (3.1–3.2 Å) do not seem to be highly dependent upon the cluster size and are larger than that of the bulk metal (2.92 Å).

ECP–CI calculations, performed by using a valence basis set fulfilling the requirement of orthogonality with the core orbitals,[218,219] have been carried out on Ti_3 (D_{3h}) (3.1) and Ti_4 (T_d) (4.3) clusters[220] assuming a fixed Ti–Ti distance equal to the bulk value 2.95 Å. The computed BE/n values (0.58 and 1.19 eV for Ti_3 and Ti_4, respectively) show a much more pronounced dependence on the cluster size than the BE/n values resulting from Anderson's calculations.[215] According to the ECP method[220] the metal–metal bond in titanium clusters may be interpreted as essentially due to the interaction between atoms in the $3d^34s^1$ excited configuration. Three electrons per atom remain uncoupled and, in addition, one MO in Ti_3 and two MO's in Ti_4 mainly composed of 4s orbitals are singly occupied. Therefore, the ground-state configuration should correspond to states with total spin equal to 5 and 7, for Ti_3 and Ti_4, respectively.

3. Vanadium Clusters

A V_{15} cluster of (100) bcc structure (1,4,5,4,1) with lattice parameter equal to 2.63 Å has been studied by means of Xα–SW calculations by Salahub and Messmer[221] with the aim to investigate the magnetic properties of such a relatively large metal aggregate. The SCF iterations were carried out allowing free occupancy of spin-up and spin-down MO's, leading to a self-consistent configuration with just one unpaired electron. This result has been considered an indication that a 15-atom vanadium cluster (an odd electron system) which prefers the maximal coupling of electron spins is representative of the nonmagnetic behavior of the bulk vanadium metal. However, the same authors

pointed out that the magnetic properties of a finite size cluster are highly dependent on the assumed shape and volume of the cluster itself. This was proved by the fact that large variations in atomic net spin densities are computed for the V_{15} cluster when the bcc lattice parameter is increased by a factor of 1.4.

4. Chromium Clusters

The Anderson model calculations[215] carried out for the series of clusters Cr_n (n = 3–6) indicated that the most stable forms are the equilateral triangle (3.1), "diamond shape", pentagon (5.6), and trigonal prism (6.4) with a BE/n value of 1.30, 1.35, 1.48, and 1.77 eV, respectively. Other forms of Cr_4 of T_d and D_{4h} symmetry are only slightly higher in energy (~0.12 eV) than the "diamond"-like structure.

No other theoretical or experimental investigations have been reported for Cr clusters of low nuclearity so that the problem of the growth mechanism and the relative stability of different structures of the chromium clusters remains open and needs further studies based on more quantitative calculations.

A calculation similar to that carried out for the V_{15} species has been performed also for the Cr_{15} cluster.[221] The (100) bcc (1,4,5,4,1) structure contains one central metal atom surrounded by eight first and six second nearest neighbors. From the spin polarized calculation, a magnetic moment as large as −0.7, 4.1, and −3.4 μ_b/atom, was obtained for each set of symmetry equivalent atoms, respectively. The alternation of the values of the atomic spin density for the different coordination shells have been considered an indication of the antiferromagnetic behavior of the Cr_{15} cluster, similar to that observed in the bulk metal. However, in the latter case the magnetic moment is considerably smaller (0.7 μ_B/atom) than that computed for the cluster atoms. It must be emphasized that the spin-ordering phenomenon found by Salahub and Messmer[221] in the Cr_{15} cluster was not due to any particular symmetry constraint imposed on the wave function but was obtained as a result of the SCF procedure. In this sense, it seems to be a peculiar characteristic of the cluster itself.

5. Manganese Clusters

A manganese cluster whose ESR spectra data are consistent with a total spin equal to 25/2 has been studied in different rare gas matrices by Baumann et al.[199] The cluster is most likely Mn_5 for which a planar pentagonal structure (5.4) has been proposed. However, from the only available ESR data other conformations which include two sets of magnetically nonequivalent Mn atoms (trigonal bipyramid (5.2) or square pyramid (5.3)) cannot be excluded.

No other studies have been reported on manganese clusters which certainly are the last extensively investigated species of the first-row transition metals.

6. Iron Clusters

The smallest iron cluster Fe_3 has been studied[202] with the Xα–SW method. A geometry optimization showed that the equilateral triangle, with an iron–iron distance of 2.0 Å, is the most stable form. The larger stability of the ferromagnetic form of the iron trimer with respect to the nonmagnetic form has been attributed to the enhanced participation by the d electrons in the metal–metal bond. A computed ionization energy value for Fe_3 equal to 6.3 eV obtained with the "transition-state" method[22,222] and adopting relaxed orbitals for the cation species fits the experimental value determined by laser photoionization technique[202,223] remarkably well.

The series of iron clusters Fe_4 (tetrahedral), Fe_9, and Fe_{15}, both in a bcc arrangement, has been investigated by the Xα–SW method[224] (see also ref 221). The standard bulk nearest neighbor spacing of 2.49 Å was used for all the clusters. The spin polarization SCF calculation converges to a ground-state configuration with 10 unpaired electrons for Fe_4 and 12 for Fe_9 and Fe_{15}. This corresponds to an average net spin density per atom equal to 2.5, 2.9, and 2.7, respectively. According to the authors' opinion[224] the magnetic properties of the largest 15-atom cluster well mimic those of the bulk iron. In fact, band structure calculations[225,226] predicted a magnetic moment of 2.30 μ_B/atom while the corresponding experimental value is 2.12 μ_B/atom.[227]

The qualitative similarities of the one-electron energy spectrum among the clusters and between the clusters and the bulk metal have been pointed out.[224] The d band width is computed to be 1.6, 2.4, and 2.9 eV (for spin up) and 2.3, 2.8, and 4.3 eV (for spin down), for Fe_4, Fe_9, and Fe_{15}, respectively. The values derived from band-structure calculations[226] are 5.1 and 6.4 eV, for spin up and spin down, respectively. Better agreement with the bulk values is obtained if the d band width of Fe_{15} is computed as $\epsilon(7t_{2g}) - \epsilon(1e_g) = 4.5$ eV for spin up and as $\epsilon(6e_g) - \epsilon(1e_g) = 4.5$ eV for spin down. However, the highest spin up level $7t_{2g}$ is not a pure d MO but a highly hybridized dsp orbital. Therefore, the clear definition of the top of the d band and the consequent estimation of its width is matter of discussion.

LD calculations have been reported on the series of iron clusters Fe_7, Fe_9, and Fe_{15}.[228] This is an important contribution because it allows a comparison of results obtained with the Xα–SW method and a LD method making no use of muffin-tin potential and taking into account correlation effects. The Fe_7 species is assumed to have an octahedral shape and is characterized by a ferromagnetic electronic ground state. An average magnetic moment per atom of 3.7 and 3.0 μ_B has been computed for a Fe–Fe distance equal to 2.86 and 2.12 Å, respectively. Both values of the magnetic moment are larger that the bulk value of 2.12 μ_B/atom and seem to stem from the "exposed" atoms in the octahedral structure. The Fe_9 cluster was studied in the same bcc structure which was assumed in the Xα–SW study of Yang et al.[224] The computed magnetic moment of 2.89 μ_B/atom perfectly agrees with the Xα–SW result,[224] and the ionization energy computed by employing the transition-state method (5.2 eV) agrees well with the photoionization data.[202,223] The largest cluster considered, Fe_{15} (bcc structure), is characterized by a magnetic moment of 2.93 μ_B/atom, while the corresponding Xα–SW value[224] is 2.67 μ_B/atom.

The analysis of the density of states (DOS) per atom for the series of iron clusters allowed to conclude that the shape of the DOS curves does not greatly depend on the particular boundary conditions imposed on the system. The DOS curve of Fe_{15} is similar to that of the bulk iron: the computed d band width is 4.4 (3.3) eV

and should be compared with the bulk value of 7.7 (7.2) eV for the cluster and 8.20 (8.03) eV for the bulk iron. A similarity between a 15-atom cluster and the bulk metal is suggested, since a narrow d band that overlaps with a broad s band has been obtained for the cluster, a feature which is common to all transition metals. On the other hand, a still remarkable difference between the magnetic properties of the largest bcc iron cluster and those of the bulk metal was pointed out.[228] Moreover, significant differences have been found for the spin-density distribution on central and peripheral atoms in the Fe_{15} cluster with respect to Xα–SW results.[224]

In order to check whether the similarity between cluster and bulk energy-level distribution holds also in the case of a different cluster geometry, the DF method used in ref 228 was also applied to a Fe_{13} cluster[224] in a fcc arrangement with a nearest-neighbor distance equal to the bulk value. The bandwidths for Fe_{13} are intermediate between those of Fe_9 and Fe_{15},[228] but the magnetic moment is lower than that of both Fe_9 and Fe_{15} clusters. The central metal atom is characterized by large negative spin density (−1.7), as was found also in the case of Fe_{15}.[228] In the bulk metals there is a tendency for spin down electrons to accumulate on the boundaries of the atomic cell. In the relatively small clusters the reverse seems to occur: the inner atoms are dominated by a large spin-down density.

All these considerations suggest that the magnetic behavior of small metal clusters is controlled by electron and spin distribution mechanisms which are substantially different from those in the bulk metal. Clusters much larger than those studied in the previous papers[221,224,228,229] should probably be considered in order to mimic the bulk magnetic properties in a better manner. It is important to note that the evaluation of such properties may also be strongly influenced by technical details of the computational scheme and in particular by the assumed form of the exchange-correlation potential of the density functional approach, as the comparison between the DF and Xα–SW results has shown.

In the above discussed studies a fixed cluster geometry is always assumed, and only in one case was the effect of the variation of the Fe–Fe distance on the magnetic properties examined. No Xα–SW or DF calculations have been carried out with the aim of studying the cluster stability problem, and its relation to the cluster shape and size. Such an investigation has been carried out by Anderson[215] in the case of small iron clusters. The equilateral triangle (3.1), "diamond shape" (5.6), square pyramid (5.3), and triangular prism (6.4) are the most stable forms for Fe_3, Fe_4, Fe_5, and Fe_6, respectively, characterized by BE/n values of 0.82, 0.99, 1.13, and 1.27 eV, respectively. The computed iron–iron distances do not increase considerably (2.6–2.7 Å) with the cluster size and are larger than the optimum Xα–SW value computed for Fe_3[273] and the experimental bulk value.

7. Nickel Clusters

Theoretical studies of Ni_3, carried out with semiempirical[215,230] and ab initio methods[205] predicted the linear structure to be most stable. Anderson[215] noted that the linear form, bound by 1.47 eV (R_{Ni-Ni} = 2.25 Å) with respect to the dissociation in Ni_2 + Ni, can be easily transformed in the equilateral triangle form characterized by R_{Ni-Ni} = 2.4 Å and by a stability of 1.28 eV. Both the linear form in a state Δ_u of unknown multiplicity and the triangular form ($^2E'$) should be Renner–Teller[231] or Jahn–Teller[60-62] unstable.

An ECP study of Basch et al.[205] confirmed that the linear form is more stable by 0.17 eV than the triangular one. The ground-state HF MO's for both the $D_{\infty h}$ and D_{3h} symmetries can be partially localized leading to a description in which each of the three nickel atoms has an electron distribution very close to $3d^94s^1$ and three holes are localized in the 3d-type MO's. In the D_{3h} symmetry the d holes are associated with MO's spanning the same irreducible representations as the 4s orbitals (e and a_1) while in the linear geometry the unpaired electrons occupy δ-type MO's.

The semiempirical CNDO calculations of Blyholder[232] led to the opposite conclusion: the equilateral triangular (3.1) form is found to be more stable than the linear one by about 1.2 eV.

The experimental study so far carried out on Ni_3[233,234] could not establish ground-state symmetry. The resonance Raman spectrum[234] of Ni_3 recorded in solid argon matrix was interpreted as due to a C_{2v} molecule, with an apex angle falling into the range 90–100°. From the vibrational analysis an atomization energy as large as 1.7 eV was estimated. The large deviation from linearity may result from the Renner–Teller[231] effect which should split the Δ_u state into an A_2 or B_2 doublet states. However, one cannot exclude that the cluster–matrix interaction may contribute to the stabilization of a distorted conformation. Therefore, from theoretical and experimental results the conclusion can be drawn that in gas phase the Ni_3 species is probably a fluxional molecule.

Nickel clusters of low nuclearity ($n < 6$) have been investigated by semiempirical calculations.[215,232] The study using Anderson's model Hamiltonian proposed the square (4.2), pentagon (5.4), and hexagon (6.1) to be the most stable structures for Ni_4, Ni_5, and Ni_6, with BE/n values of 1.15, 1.32, and 1.33 eV, respectively. The BE/n values obtained from CNDO calculations[232] are 2.2, 2.9, and 4.6 eV for linear Ni_4 (the only investigated form of the tetramer), planar Ni_5, and Ni_6 ((100) and (111) sections), respectively. Therefore, both quoted semiempirical calculations indicate that the planar structures are more stable than the three-dimensional ones.

ECP calculations[205] yielded similar stabilities for the linear and the square forms of Ni_4 (~0.58 eV/atom) both of which are more stable than the tetrahedron (0.32 eV/atom). In the case of Ni_5 and Ni_6 the square pyramid (5.2) and the octahedron (6.3) are characterized by BE/n values of 0.71 and 0.72 eV, respectively.

As in the case of Ni_3, Basch et al.[205] showed that these Ni clusters originate from the interaction of nickel atoms in the $3d^94s^1$ configuration. The metal–metal bond is mainly due to the 4s electrons and the corresponding MO's can be described by a simple Hückel model (including overlap), while the 3d–3d interaction between nearest neighbor atoms is very small. The ground-state configuration of Ni_n clusters corresponds to n holes strongly localized in d-type MO's. This particular feature which has been investigated by these authors

only is not an artifact of the single-determinant representation, since the closed-shell configuration of Ni_6 has an energy much higher than the open-shell one, even when the closed-shell wave function is improved by means of a 36-terms MC–SCF calculation.

In the case of Ni_6[205] the DOS diagram obtained by ECP one-electron energies appear to be quite different from a typical Xα–SW DOS diagram for a small metal cluster. Actually, the ECP results do not confirm the existence of a narrow d band superimposed on a broad (s + p) band since the first band appears to be well separated from the second one and lying at lower energy.

The agreement between curves obtained from the ECP DOS and the Xα–SW DOS is reached if closed-shell HF ECP eigenvalues are employed.

The general problem concerning the relative ionization energies of 4s vs. 3d electrons in nickel clusters has been considered in detail by Newton[235] in the case of the tetramer in square configuration. The values obtained from restricted ECP–HF calculations using relaxed orbitals for the ionic species show quite a large separation (about 1.2 eV) between s and d ionization energies. But when additional electronic relaxation of the cation is introduced by allowing for a symmetry-broken character of the final wave function the s and d ionization energies become essentially degenerate, thus confirming the overlap of the d and s bands found by the Xα–SW method. This means that the HF energies (Koopmans' theorem) cannot be taken as a measure of the ionization energies of state strongly localized and characterized by a large relaxation energy. On the contrary, the one-electron energies of the Xα–SW method are claimed not to be greatly altered when the electronic relaxation of the final states is allowed.[236-238]

The electronic structure of higher nuclearity Ni clusters has only been examined with Xα–SW or DF methods.[236,238-241]

In a Xα–SW study[236] the Ni_8 and Ni_{13} clusters were assumed to be in cubic and cubo-octahedral arrangements, respectively, with a fixed Ni–Ni nearest-neighbor distance of 2.49 Å. For both clusters a magnetic moment of 0.25 and 0.46 μ_B/atom was computed. The latter value is smaller than that of the ferromagnetic crystalline nickel (0.57 μ_B/atom). But an increase of the computed magnetic moment upon going from an 8- to a 13-atom cluster has been considered[236] to be in agreement with the experimental findings that such a quantity increases in a continuous way with the dimension of the metal particles.[243] However, as mentioned in the case of the iron clusters, the predictions of the magnetic properties of the clusters obtained from the Xα–SW method can be altered by using a more accurate potential for the exchange-correlation functional. Indeed, adopting Janak–William's[244] potential in the framework of SW method, Salahub and Raatz[245] obtained a magnetic moment of 0.69 μ_B/atom (which is higher than the bulk value) for a Ni_{13} cluster in a cubo-octahedral configuration. In the case of the Ni_{14} cluster, a fcc section (9,4,1), the magnetic moment decreases to 0.57 μ_B/atom, which is coincidentally very close to the bulk value. In the same study[245] it was pointed out that the distribution of the magnetic moments associated with the individual atoms is very heterogeneous: the atoms with the highest number of nearest neighbors have the smallest net spin density, and this increases considerably as the atoms become more and more exposed.

As for other clusters, Messmer et al.[236,238] showed the similarity between the Xα–SW DOS curves and those obtained from a band structure calculation on bulk nickel.[246] This point was used to show that the EHT method is not suitable for the description of the electronic structure of transition-metal clusters because the EHT spectrum of the one-electron energies does not fit[247-250] the Xα–SW one. It is certainly true that the results of the semiempirical methods, like EHT, depend strongly on the chosen set of parameters. However, the criticism of Messmer et al.[235,238] was based upon the assumption that the Xα–SW description of the density of states is free from any approximation. The following consideration will show that this is not always the case.

In fact, other calculations on large Ni_n clusters, Ni_{13} and Ni_{19}, have been carried out by employing the DF (local density approximation) method and adopting a very flexible set of 14s, 9p, and 5d uncontracted Gaussian functions.[229] As mentioned in the case of iron clusters two important methodological differences distinguish this computational approach from the Xα–SW method: the correlation effects are included through the use of an approximate potential and no muffin-tin approximation is adopted. For the two Ni clusters a fixed central-atom–first-neighbor distance of 2.49 Å was assumed. The d band width was computed to be 4.3 eV for Ni_{13} and 4.8 eV for Ni_{19}; that is about twice larger than the bandwidths obtained from the Xα–SW method.[236,238,251] With an integrated density of states per atom (a procedure which avoids the arbitrary broadening of the discrete energy spectrum) a remarkable similarity between Ni_{19} and the bulk metal was shown both for the sum of different spins and for spin up and spin down separately. The excess of spin up per atom was computed to be 1.14 and 0.80 for Ni_{13} and for Ni_{19}, respectively, which are larger than that computed for the bulk metal (0.57 μ_B/atom).[252]

8. Copper Clusters

Copper clusters are the most widely experimentally studied transition-metal aggregates. ESR investigations have been reported for Cu_3 and Cu_5.[253,254] For the copper trimer a mass spectrometric measurement of the atomization enthalpy[255] and resonance Raman studies in rare-gas matrix[256] have been carried out. In addition, the Cu_3 species has been the object of an extraordinarily accurate study[257] which is the first reported gas-phase spectroscopic investigation of a bare transition-metal cluster. This work opens a very promising way of obtaining accurate date for TM clusters in a situation in which the cluster itself is not perturbed by interactions (sometimes very important) with a support or a gas matrix. Quantities like ionization potential and ground-state–excited-state transition energy were determined for Cu_3, together with the extent of the geometric distortions induced by the Jahn–Teller effect. The UV–vis absorption spectra were recorded in xenon matrix for copper clusters containing up to five atoms,[233,258] while ionization energies have been measured for Cu_n species (n = 29)[259] by using a supersonic beam expansion technique which produces very cold clusters

(a few K for translational, rotational, and vibrational degrees of freedom).

The theoretical chemistry literature is very rich in examples of studies carried out for copper clusters. This is probably due to the fact that the completely filled d shell of the copper atom does not give rise to difficulties represented by a manifold of states of different spin multiplicity. As a consequence, the field of the copper clusters is much more investigated than clusters of other TM's, and the situation is completely analogous to that of the copper dimer which has been also more extensively studied than other TM diatomics.

The smallest cluster Cu_3 has been identified by ESR spectroscopy in adamantane matrix at 77 K[253] and the ground state, $^2B_2$ (C_{2v}), was found to be consistent with the spectral data. About 61% of the unpaired electron is localized in 4s copper orbitals and mainly at the terminal copper atoms, while at the central atom the spin density is negative because of spin polarization effects.

Former CNDO calculations of Baetzold[260] indicated that the linear and trigonal forms (R_{Cu-Cu} = 3.2 Å) have almost identical stability (BE/n = 1.91 eV). On the contrary, Anderson's model calculations[261] predicted that the linear form should have the lowest energy (BE/n = 0.86 eV and R_{Cu-Cu} = 2.34 Å). The Cu_3 cluster is stable with respect to the dissociation in Cu_2 + Cu but its binding energy per atom is lower than that of Cu_2.

Several nonempirical theoretical studies have been reported on Cu_3.[177,179,262-271] Del Conde et al.[268] carried out restricted HF calculations using a double ζ basis for the isosceles triangle from in the $^2A_1$ ground state. This is characterized by values of the Cu–Cu bond lengths equal to 2.47 and 2.73 Å and a stability of 1.12 and 0.45 eV with respect to three copper atoms and the dissociation limit Cu_2 + Cu, respectively. The computed stability is much smaller than the experimental value of 2.93 eV,[255] and this is certainly caused by the lack of electron correlation. In the same paper, the analysis of the additive and nonadditive energy contributions has been carried out. As for other cases examined[36,268] the authors found that the nonadditive terms contribute to the cluster instability, being repulsive both for linear and triangular form.

Other HF calculations[262,263] gave an indication that the bent structure of the Cu_3 clusters with the apex angle equal to 120° and the equilateral triangle are only 0.13 and 0.14 eV higher in energy than the linear form. A change in Cu–Cu distance as small as 0.06 Å was computed for the deformation from $D_{\infty h}$ to D_{3h} symmetry.

The Cu_3 energy surface was subjected to a detailed analysis by Miyoshi et al.[179,270] with HF "all-electron" method. Three electronic states have been considered. The first $(18a_1')^2(11e')^1$, $^2E'$, corresponds to the ground state for the D_{3h} symmetry, and the other two are the states that originate from the Jahn–Teller distortion $D_{3h} \rightarrow C_{2v}$: $(18a_1)^2(19a_1)^1$, $^2A_1$, and $(18a_1)^2(14b_1)^1$, $^2B_1$. The lowest energy conformation is the obtuse isosceles triangle (BE/n = 0.34 eV) which is nearly degenerate with the acute one. Both latter forms are slightly more stable than the more symmetric D_{3h} and the linear one by about 0.11 and 0.14 eV, respectively. Thus the ordering in stability of the $D_{\infty h}$, C_{2v}, and D_{3h} forms is reversed with respect to that proposed by Bachmann.[262,263] However, it must be noted that all the above reported HF calculations are likely to be affected by basis set superposition error (BSSE) (cf. appendix VIIA) due to the limited size of the basis set adopted in the molecular calculations. The BSSE leads to binding energy overestimate which increases with the compactness of the molecular system. In the specific case of the Cu_3 cluster, the BSSE is expected to be larger for triangular forms than for the linear one. After correction for BSSE, the stability of the latter may be slightly higher than that of the D_{3h} form. According to the corrections estimated by Miyoshi et al.,[179] the right sequence of the total energies for Cu_3 should be $E_{obtuse} \sim E_{acute} < E_{linear} < E_{equilateral}$.

All the above quoted calculations do not include any correlation effects which, as already discussed in the case of the copper dimer, play an essential role in stabilizing the Cu–Cu bond. Moreover, it is important to consider such effects in order to establish in an unambigous way the order in stability of different geometric forms characterized by similar total energy. With this aim, a correlated HF wave function for Cu_3 has been computed[266] by employing the ECP–SCF procedure (almost completely free from BSSE), followed by SD–CI. The contribution of higher excitations are taken into account via perturbative procedure. The obtuse triangle (3.2) ($^2B_2$), the acute triangle ($^2A_1$) (3.3), and the linear form ($^2\Sigma_u^+$) were found to be very close in energy. The best estimate of the stability of the Cu_3 cluster is 0.50 eV, which is substantially lower than the experimental value, despite the quite large correction induced by the correlation effects (~0.38 eV). The linear form is found to correspond to a real local minimum, a rather surprising fact in comparison with Na_3,[70] where the linear form is a saddle point on the surface.

Flad et al.[264,265] studied Cu_3 using an ECP scheme in which the 3d shell of the copper atom is included in the core. The effect of core polarization is taken into account by means of a suitable operator built into the effective Hamiltonian. The valence correlation effects are computed by employing a DF scheme which includes a self-interaction correction (see appendix VII.B). The geometries of the linear, acute, and obtuse triangular forms have been optimized and the resulting stabilities with respect to three copper atoms have been found equal to 2.58, 2.63, and 2.68 eV, respectively. When Cu_2 + Cu is considered as the dissociation limit, the stability values decrease to 0.70, 0.75, and 0.80 eV, respectively, thus confirming the findings of other HF-type calculations. The computed molecular stabilities are in good agreement with the experimental values. The ionization energy computed for both the vertical and adiabatic process (values in parenthesis) are 7.23 (5.66), 5.80 (5.71), and 6.03 (5.77) eV for linear, acute, and obtuse triangle, respectively. Only the adiabatic values are in agreement with the experimental data.[257] The results of other nonempirical or empirical calculations are reported in Table VII. Remarkable are the results of the DIM calculations[269] which qualitatively agree with those of more rigorous methods. However, the DIM approach concluded that the linear form is more stable than the acute or obtuse triangle forms by 0.33 eV, a result which is not confirmed by the HF calculations but only by a semiempirical study

TABLE VII. Some Results on Cu Clusters

geometry	r_1, Å[a]	r_2, Å[a]	r_3, Å[a]	BE/n, eV	IP, eV	method	ref
3.1 (D_{3h})	2.55	2.55	2.55	1.06		DV-Xα	272
3. ($D_{\infty h}$)	2.35	2.35	4.70	0.86	5.66	ECP-CI	264
3.3 (C_{2v})	2.29	2.53	2.53	0.88	5.71	ECP-CI	264
3.2 (C_{2v})	2.84	2.34	2.34	0.89	5.75	ECP-CI	264
3.1 (D_{3h})[b]	2.42	2.42	2.42	1.55		ECP-CI	264
3.3 (C_{2v})	2.48	2.86	2.86	0.50		ECP-CI	266
3.2 (C_{2v})	3.35	2.56	2.56	0.52		ECP-CI	266
3. ($D_{\infty h}$)	2.55	2.55	2.55	0.51		ECP-CI	266
3. ($D_{\infty h}$)	2.53	2.53	2.53	0.29		SCF	270
3.2 (C_{2v})	3.13	2.50	2.50	0.34	4.39	SCF	270
3.3 (C_{2v})	2.44	2.80	2.80	0.34	4.27	SCF	270
3.1 (D_{3h})	2.59	2.59	2.59	0.30		SCF	270
3. ($D_{\infty h}$)	2.35	2.35	2.35	0.43	5.4	SCF	262, 263
3.1 (D_{3h})	2.41	2.41	2.41	0.36		SCF	262, 263
3.3 (C_{2v})	2.43	2.90	2.90	0.40		SCF	262, 263
3. ($D_{\infty h}$)	2.34	2.34	2.34	0.86		EH	261
4.1 (D_{2h})	2.45	2.51		0.60		ECP-CI	266
4.5 (C_{2v})	2.52	3.02		0.59		ECP-CI	266
4. ($D_{\infty h}$)	2.40[c]			0.55	5.4	SCF	262
4.2 (D_{4h})	2.43			0.52	5.2	SCF	262
4.3 (T_d)	2.40[c]			0.44		SCF	262
4.4 (D_{2d})	2.40[c]			0.52		SCF	262
4.3 (T_d)	2.56[c]			1.18		DV-Xα	272
4.3 (T_d)	2.43			1.21		LSD	191
4.2 (D_{4h})	2.56[c]			0.38		LSD	177
4.3 (T_d)	2.35			1.26		LSD	191
4.1 (D_{2h})	2.31	2.47		1.14	6.47	ECP-CI	264
4.5 (C_{2v})	2.29	2.30	2.30	1.08	6.20	ECP-CI	264
4. ($D_{\infty h}$)	2.26			1.20		DIM	269
4.2 (D_{4h})	2.26			1.56		DIM	269
4.1 (D_{2h})	2.27	2.48		1.58		DIM	269
4.3 (T_d)	2.33			1.60		DIM	269
4.4 (D_{2d})	2.22	2.38		1.63		DIM	269
4. (C_{2h})	2.26	2.71		1.030		DIM	269
5. ($D_{\infty h}$)	3.2	2.07				CNDO	260
5.3 (C_{4v})	2.26			0.30		SCF	177
5. ($D_{\infty h}$)	2.26			0.53		SCF	177
5.2 (D_{3h})	2.26			0.62		SCF	177
5.3 (C_{4v})	2.26			0.60		SCF	262
5. (D_{4h})	2.26			0.50		SCF	262
5. (D_{4h})	2.26			1.20		DV-Xα	272
5.3 (C_{4v})	2.26			1.58		DV-Xα	272
5. ($D_{\infty h}$)	2.45	2.30		0.96		EH	261
5.6 (T_d)	2.25			1.05		DIM	269
5. ($D_{\infty h}$)	2.28			1.20		DIM	269
5. (D_{4h})	2.23			1.22		DIM	269
5.4 (D_{5h})	2.27			1.41		DIM	269
5.3 (C_{4v})	2.26	2.39		1.76		DIM	269
5.2 (D_{3h})	2.47	2.29		1.78		DIM	269
6.3 (O_h)	2.26[c]			1.65		DV-Xα	272
6.3 (O_h)	2.26[c]			0.51		SCF	270
6. ($D_{\infty h}$)	3.2			2.30		CNDO	260
6.3 (O_h)	2.32			2.17		DIM	269
6.4 (D_{3h})	2.31	2.21		2.02		DIM	269
6. (D_{2h})	2.28	2.25		1.74		DIM	269
7.3 (D_{6h})	2.26			1.83		DV-Xα	272
8.3 (O_h)	2.40[c]			0.85		SCF	262
D_{4d} (antiprism)	2.40[c]			0.88		SCF	262
(5,4)	2.26[c]			1.87		DV-Xα	272
13.2 (O_h)	2.26[c]					SCF	271
13.1 (O_h)	2.26[c]			1.13		SCF	271
13.2 (O_h)	2.26[c]			0.633		SCF	263
13.2 (O_h)	2.41			2.19		LSD	191
13.2 (O_h)	2.67			0.78		EH	261
(1,12,6,24,12,24)	2.54			3.03		LSD	191

[a] r_1, r_2, and r_3 are characteristic interatomic distances in the cluster. [b] $(Cu_n)^+$ cluster. [c] Distance not optimized.

based on Anderson's model.[261] Calculations carried out at the same level of accuracy as those performed for Cu_3 have been reported[264-266] for the Cu_4 cluster (see Table VII). Flad et al.[264,265] obtained BE/n values equal to 1.14 and 1.08 eV for the rhombus and T-shape cluster employing the above-mentioned ECP-correlated method. The same order in stability was obtained by another ECP–CI study[266] in which only the 4s electrons were correlated. However, in the last case, the BE/n values are smaller than the previous ones, and the difference in stability between the two forms is further reduced. Moreover, differences should be noted also in the results of the geometry optimization carried out in the two studies. For instance, Flad et al.[264,265] re-

ported for the side length and the shortest diagonal of the Cu_4 rhombus the values 2.31 and 2.47 Å, respectively, while the corresponding results of Jeung et al.[266] are 2.45 and 2.51 Å.

The geometric structure of the higher nuclearity copper cluster (up to Cu_{13}) have been investigated with HF,[177,179,262,263,271] DV-Xα,[272] DF,[191] DIM,[269] and Anderson's Hamiltonian methods.[261] The corresponding results are reported in Table VII.

Only in one HF study were several conformations[262,263] for the Cu_5 cluster investigated, leading to the conclusion that stability decreases in the following order: trigonal bipyramid, square pyramid, linear, and centered square planar form. The results agree with the experimental evidence obtained from the analysis of the ESR spectra of Cu_5 in matrix:[254] The ground state of Cu_5 is a Jahn–Teller distorted trigonal bipyramid. Moreover, the HF results do not contradict the DF–Xα results of Post et al.[272] but are in complete disagreement with the EH-type calculations[260,261] which predicted that the linear form is the most stable one. Among the semiempirical calculations, only those performed according to the DIM method by Richtsmeier et al.[269] reached conclusions similar to those obtained from more rigorous methods. One should note that the DIM investigation of the most stable conformations for Cu_5[269] is much more complete than in the above HF studies since it includes the optimization of the Cu–Cu nearest-neighbor distance for each assumed basic structure. This may show that even for a relatively small TM aggregate like Cu_5, a nearly complete geometry optimization in the framework of the HF theory requires a discouragingly large computational work. The same considerations are valid for the Cu_6 cluster for which only the DIM geometry optimization is available:[269] The octahedron is found to be more stable than the trigonal prism and the planar rectangular form.

The fact that the geometry optimization is an essential step in studying the basic properties of the clusters may be proved by the quite surprising result obtained by the HF–Slater method:[272] when the Cu–Cu distance is fixed to the bulk value, the Cu_5 cluster with the three dimensional structure (D_{3h}) (5.2) is found to be the most stable one, while Cu_7 prefers the centered-hexagonal structure (7.3) instead of the more compact pentagonal bipyramid (7.1). This result does not match with the expectation that three-dimensional structures are more and more preferred as the cluster size increases, as it is confirmed in the case of alkali metal clusters for which accurate geometry optimization are available.

Cu_{13} is the largest transition-metal cluster for which a comparison between results obtained with different theoretical methods is possible.

First, let us consider the work done in order to find the most stable conformation. The study of Demuynck et al.[271] represents the largest HF all electron calculation of a TM cluster up to now available. It has been carried out with a basis of about 250 contracted Gaussian functions, a dimension probably close to the upper limit for such a theoretical approach. The results showed that the icosahedron (I_h) (13.1) is the most stable form in comparison with the cubo-octahedron (O_h) (13.2) and the bicapped double-decker sandwich (D_{5h}) form (see ref 271).

The determination of the ground state of the different forms of Cu_{13} is complicated by the existence of states of different spin multiplicity. Indeed, while the ground state of the icosahedron $^6A_g(h_g^5)$ can be assumed with large confidence, for the two other forms both high spin, $^6A_{1g}$ and $^6A_1$, and low spin states, $^2T_{2g}$ and $^2A_1$, for O_h and D_{5h}, respectively, are possible. The states of the D_{5h} cluster are very close in energy to the corresponding states of the cubo-octahedral form (0.16 and 0.22 eV, for high and low spin states, respectively). Simple arguments suggest that the correction of the HF total energies due to the correlation effects should favor the low spin states. However, on this basis it is difficult to decide the relative stability of the O_h and D_{5h} forms. More likely it is that, even considering possible correlation corrections, the two latter geometries are less stable than the icosahedral structure.

In order to stress how difficult it is to perform HF calculations at this level of accuracy, it is worthwhile mentioning that the above study has been carried out assuming a Cu–Cu bond distance fixed to the bulk value and adopting a basis of contracted Gaussian of 5s, 3p, 1d type which corresponds to a double ζ representation only for the 4s orbitals. A quite large BSSE is certainly associated with the basis set decreasing the accuracy of the computed binding energies. The HF calculations with slightly better basis (not free from BSSE) yielded the BE/n equal to 1.13 eV for the Cu_{13} cluster in I_h symmetry.

The same icosahedral cluster was investigated[191] in the framework of the DF theory using both the simple exchange Xα potential and the exchange-correlation potential of Hedin–Lundquist.[273] The cluster wave function is expanded in an accurate basis of numerical orbitals. For the selected cubo-octahedral structure (no other forms have been examined) the Xα geometry optimization gave a Cu–Cu bond distance equal to 2.41 Å (a value considerably larger than the bulk one assumed in the HF calculations) and a stability of 2.19 eV/atom (a value twice larger than the HF one). The latter quantity was found equal to 2.39 eV/atom when computed with the Hedin–Lundquist potential for a fixed Cu–Cu distance of 2.38 Å. The two potentials adopted gave the same ground state $^2T_{2g}$, in agreement with the HF result, when corrected for the estimated correlation energy. Xα–SW calculations have been carried out for Cu_8 and Cu_{13} clusters assumed in cubic and cubo-octahedral geometry.[236]

The properties of the copper clusters, such as the DOS diagram and the derived values of the ionization energies, represent a benchmark for the comparison between the results obtained from HF or Xα–SW methods. In this context, the paper of Demuynck et al.[271] reported a detailed analysis and a quite strong criticism of the Xα–SW findings,[236] essentially based on the following considerations. (i) The HF d energy levels are well separated from the s-type levels in Cu_8, and only a small overlap between the top of the d band and the bottom of the s band occurs in Cu_{13}. This shows the necessity to analyze a cluster of much larger nuclearity in order to find a complete overlap between the two bands. It must be recalled that the Xα–SW method finds a complete overlap already in very small clusters. (ii) The qualitative features of the spectrum of the HF one-electron energies do not change notice-

ably when the relaxation of the orbitals of the ionic species is considered. The relaxation is larger for d than for s electrons and decreases in a regular way as the cluster size increases. In the case of Cu_8 cluster values as low as 0.27 and 1.90 eV are computed for s and d electrons, respectively. These values are expected to be even lower for Cu_{13} and, in any case, too low in order to produce a d-band–s-band overlap. (iii) It was pointed out[271] that the Xα–SW eigenvalues differ from the true ionization energy by a self-interaction term of the ionized MO. The correction computed by using HF MO's gave the values 10.6 and 6.5 eV for d- and s-type MO's, respectively. Therefore, it was concluded[271] that neglecting the self-repulsion correction artificially reduces the d electron IP values, with respect to the corresponding values of the s electrons.

The listed considerations allowed the statement that the electronic and geometrical structure of the Cu_{13} cluster is far from being similar to the situation occurring in the bulk copper metal.

A reply to the above criticisms was made by Messmer et al.[274] who pointed out that the relaxation energy accompanying the d-electron ionization is artificially small when computed in the HF approximation, forcing the hole to be completely delocalized over several atomic centers, due to symmetry restrictions. If the localization of the d hole is allowed (which implies that the wave function of the ionic species has a symmetry-broken character) the resulting relaxation energy becomes much larger. This is equivalent to a lowering of the total energy of the ionic species and, consequently to a decrease of the d ionization energy values which now overlap with the corresponding values of the s electrons for which the relaxation effect is much smaller. These arguments were supported by Xα–SW results obtained from the Cu_4 square planar cluster.[274] The results are in agreement with those of the HF calculations on Cu_2[275] and confirm the findings of Newton[235] in the case of the Ni_4 cluster. In conclusion, the above calculations show that the d and s ionization energies may be clearly degenerate also in the case of very small metal clusters. However, this conclusion is clearly against the assumption commonly accepted in several Xα–SW calculations that the similarity between the DOS diagrams of a cluster and the bulk metal is an indication of convergence of the cluster properties to the bulk properties. On the contrary, this similarity seems to have little significance, since it is hard to believe that the electronic structure of a cluster of very few metal atoms is similar to that of the bulk metal.

The largest cluster studied with the quantum mechanical methods is Cu_{79},[191] the structure of which includes up to five coordination shells around a central metal atom, containing 12, 6, 24, 12, and 24 atoms, respectively. A nearest-neighbor Cu–Cu distance of 2.54 Å was assumed and the binding energy/atom resulted equal to 3.03 eV, when computed according to the DF formalism using a simple Xα potential (α = 0.70). On the basis of the BE/n values obtained with the same computational procedure for Cu_2, Cu_4, and Cu_{13}, Delley et al.[191] were able to show that the binding energy per atom of the copper clusters can be reproduced by a simple linear relationship of BE/n vs. $n^{-1/3}$, and that the extrapolated BE/n value for the bulk metal (4.1 eV) is 17% larger than the experimental value but reproduces the computed value for the bulk copper in a very satisfactory way. The $n^{-1/3}$ parameter is proportional to the surface-to-volume ratio if a fixed atomic volume is associated with all the atoms of the cluster. Therefore the $n^{-1/3}$ relationship may well represent the cluster-size dependence of some physical quantities, since the dependence is essentially due to surface effects.

When the same $n^{-1/3}$ relation is applied to the available BE/n data obtained from EH-type or HF methods, it appears that these two methods are unable to give a correct bulk-extrapolated value of the binding energy. In particular the HF results give a linear BE/n vs. $n^{-1/3}$ relationship which is characterized by a positive but very small slope. The slope associated with the EH data has a wrong sign.

In their DF study, Delley et al.[191] carried out a DOS analysis for the three inner shells (19 atoms) and for the other atoms belonging to the outermost shells, separately. The band associated with these latter atoms is sharper and shifted to lower binding energy values with respect to the band characteristic for the "bulk atoms" of the clusters. Even for them, the DOS profile cannot be assumed as completely equivalent to that of a bulk metals. These observations, which are clearly related to surface effects or to the presence of "exposed atoms", show that the cluster possesses some very particular feature and, in particular, that the DOS profile of low nuclearity clusters (in which almost all the atoms are surface atoms) cannot seriously be taken as an indication of convergence to the bulk characteristics.

C. Second and Third Row Transition-Metal Clusters

The electronic structure of the 4d and 5d transition-metal clusters has been mostly investigated by employing semiempirical methods (EHT, DIM, or CNDO)[269,277-281] and the Xα–SW method[236,282-289] while very few examples making use of the HF–SCF approach[290,291] have been reported. Finally, attempts to compute cluster wave functions in the framework of many-electron methods (CI or DF) are almost completely lacking.[292] The reason for this unsatisfactory situation is due to the fact that 4d and 5d elements are much more difficult to treat than the first transition metals, both because of the large number of electrons and because of severe complications arising from the large relativistic effects that are characteristic for atoms with a high nuclear charge.

All these difficulties prevented the theorists from investigating the specific nature of the metal–metal bond in second and third transition clusters in a detailed manner, as the following discussion will show.

Little work has been done on the first 4d and 5d elements with the exception of Xα–SW calculations carried out for relatively small Zr,[288] Nb,[284,285] Mo,[286-287] and W[285] clusters.

The Xα–SW potential energy curve for the Zr_4 cluster in a tetrahedral arrangement and closed shell configuration is found[288] to be repulsive for every Zr–Zr distance. This is a quite surprising result if we consider that the homologous Ti_4 tetrahedral cluster has been found to be stable both on the basis of semiempirical[215] and ECP–CI[220] calculations. However, it should be noted that a Zr–Zr distance equals to 3.23 Å (corre-

sponding to the nearest-neighbor distance in the hcp bulk metal) and the Xα–SW interaction energy is only very slightly repulsive. The Zr_4 cluster in a spin state different from the considered closed shell may very likely have some stability.

An Xα–SW study[289,285] on the dependence of some physical quantities upon the cluster size has been carried out for the series Nb_2, Nb_4 (tetrahedron), Nb_6 (octahedron), and Nb_9 (bcc unit cell).

The clusters have been investigated by using a fixed metal–metal distance equal to 2.97 Å. The DOS curves (properly energetically scaled with respect to the Fermi level) of the different clusters appear to be very similar, while the cluster size influences the d band width to a larger extent. No data on the stability of the Nb clusters have been reported, and all these results parallel those obtained by many other Xα–SW calculations.

The analysis of the effect of the α parameter on the position and shape of the DOS diagram revealed that a large value ($\alpha = 1$) stabilizes the d-type levels (for which the exchange energy is large) much more than the s-type ones, and all the levels are shifted to a lower energy value with respect to those computed with $\alpha = 0.7038$.[293] As a consequence, also the degree of overlap of the d and s bands depends upon the value chosen for the α parameter.

Similar calculations have been carried out for the series of octahedral clusters of Mo, W, and Ta,[284] too, and the conclusions about the DOS profiles and the width of the valence band are similar to those reported above. Molybdenum systems in a pseudolinear metallic chain composed by discrete Mo_3 (D_{3h}) units have been considered by Le Beuze et al.[286] in an Xα–SW study which was carried out according to the computational scheme of overlapping atomic spheres. The series of clusters includes Mo_3 (equilateral triangle), Mo_6, and Mo_{12} in trigonal prismatic arrangements. The trigonal antiprism (D_{3d}) conformation of Mo_6 has also been considered.

The geometry of the clusters has been taken from the experimental X-ray structure of $Tl_2Mo_6S_6$[294] and corresponds to a Mo–Mo intralayer and interlayer distance equal to 2.66 and 2.73 Å, respectively. The bond within a Mo_3 triangular basic unit can be described in terms of a double bond, σ in plane and π out of plane, plus a weak bond of σ type for each molybdenum pair.

Whatever the stacking mode is (D_{3h} or D_{3d}), the out-of-plane interaction between different Mo_3 subunits is dominated by orbitals that have an overlap much larger than the σ orbitals which are mainly localized in the Mo_3 planes.

BE/n values have been reported for the Mo_3 (D_{3h}) and Mo_6 (D_{3h} and D_{3d}) clusters only and are equal to 4.69, 6.08, and 6.53 eV, respectively. This shows that the interlayer interaction plays an important role in the growth of linear chains; its value has been estimated to be about 4.0–5.0 eV. The D_{3d} structure of Mo_6 is more stable than the D_{3h} one, but simple considerations based on orbitals correlation diagrams show that the Mo_6 in the octahedral arrangement should be even more stable. The latter Mo_6 species and the related $PbMo_6S_6$ cluster have been also investigated in a previous paper[287] by using an Xα–SW computational approach including relativistic effects. These corrections were found to be of little importance at least as far as the evaluation of the ionization energies of the core levels is concerned; the latter are almost coincident in nonrelativistic and relativistic calculations.

It was found that the valence bandwidth does not linearly increase with the number of the Mo_3 subunits and tends to a limit not yet reached by the largest Mo_{12} cluster. This size-dependent effect has been related to the fact that the "exposed" Mo_3 subunits and subunits inside the chain undergo different bonding interactions.

The electronic characters of the $(Mo_3)_n$ clusters may be modeled in a very simple way when we assume that each Mo_3 cluster plays the role of a hypothetic "pseudoatom" in a linear metallic chain. According to this model, the electronic characteristics of the quasi-one-dimensional conductor have been obtained by extrapolating the results to the case of a $(Mo_3)_\infty$ system.

EHT calculations have been reported for a variety of clusters of 4d and 5d elements,[248-250] mainly with the aim to model the metal surface and its local interactions with chemisorbates. As in the case of Ni_{13}, the use of semiempirical approaches for studying the electronic structure of metal clusters has been strongly criticized because of poor agreement between their results and those obtained with the Xα–SW method for clusters of similar nuclearity.[236] In particular, it was pointed out that the EHT net charge on the cental metal atom in W_9 and W_{13} (as well as in Ni_9 and Ni_3) has a sign opposite to the Xα–SW one. Moreover, the DOS curves obtained by the two computational approaches are found to have little similarity.

The dependence of the EHT results upon the choice of the set of atomic parameters which enter the effective Hamiltonian matrix elements is well documented by the work of Bartel et al.[283] In the case of Pt_6 and Ir_6 octahedral clusters, a good coincidence exists between the EHT and Xα–SW DOS curves only in the case that the ionization energies for 5d and 5s orbitals used in the EHT calculation have not been obtained from experimental values but from the theoretical one-electron energies of the atomic HF–Slater calculations. Both the Xα–SW and EHT DOS curves and the valence bandwidths for the Ir_6 and Pt_6 clusters appear to be quite different from those obtained from band-structure calculations.[295] This was interpreted[283] as an indication of nonconvergence to the bulk properties.

A systematic investigation of the platinum cluster growing process has been undertaken by Bigot and Minot[281] by means of a modified EHT method which includes an "ad hoc" correction of the diagonal elements of the EHT hamiltonian in order to obtain the nearest-neighbor Pt–Pt distance in Pt_{13} (I_h) in close agreement with the observed bulk value. The effect of the inclusion of spin–orbit interaction in the EHT effective Hamiltonian has been also investigated. A series of about 200 clusters up to Pt_{20} has been analyzed and the main conclusions can be summarized as follows: The BE/n quantity approximately obeys a linear relationship as a function of the mean number of nearest neighbors for platinum atoms. On the contrary, the energy for the process $Pt_{n-1} + Pt \rightarrow Pt_n$ (which is an important parameter for the cluster growing process) shows quite wide oscillations as n increases. In addition, no simple and systematic rules have been discovered for predicting the most stable structure of the Pt_n cluster on the basis of the known structure of the Pt_{n-1}

cluster because important geometrical rearrangements always accompany each step of the cluster growth. On the other hand, the most stable Pt clusters with a given nuclearity very often qualitatively have the same forms as the theoretically predicted stable clusters of alkali metals.[48,75]

In early Xα–SW calculations[236] carried out on Pd_{13} and Pt_{13} clusters, a cubo-octahedral arrangement (13.2) was assumed, with a metal–metal distance equal to 2.74 and 2.77 Å, respectively. The aim of this pioneering Xα–SW work was to investigate the magnetic properties of 13-atom clusters, their charge distribution and DOS profiles. Typical surface effects were noted on the net atomic charge: the central metal atom carries a quite large negative charge (–0.748 and –0.935 in Pd and Pt clusters, respectively) which is balanced by a positive charge delocalized all over the other surface atoms. Unlike the Ni_{13} cluster, Pd_{13} and Pt_{13} were not found to be paramagnetic.

ECP calculations using a model Hamiltonian that includes the major direct and indirect relativistic effects[33,350] have been carried out on the Pd_4 and Pt_4 species.[290] As far as we know, this is the only example in which a geometry optimization and the analysis of different electronic states has been attempted for clusters of the second and third transition series.

The geometry was assumed to be tetrahedral, and the HF wave function was determined in the D_{2d} subgroup, while a contracted Gaussian basis of 3s, 1p, 2d type for Pd and Pt atoms was adopted. As is known, the ground states are $^1S(1d^{10})$ and $^3D(5d^96s^1)$, respectively. Therefore, if one assumes that the metal–metal bond is dominated by the s–s interaction, one has to conclude that in the case of platinum the formation of the cluster is much easier than in the case of palladium which needs to be excited to the $4d^95s^1$ state. This situation is documented in a detailed way in the paper by Miyoshi et al.,[290] who considered the following states (D_{2d} notation): $^1A_1$, $^3B_2$, $^3A_1$, $^7A_1$, and $^7B_2$ which correlate with the dissociation limits $4(d^{10})$ (that is four d^{10} atoms), $3(d^{10})(d^9s^1)$, $2(d^{10})2(d^9s^1)$, $3(d^9s^1)(d^{10})$, and $4(d^9s)$, respectively. In other words, these different states correlate with dissociation limits in which one or more metal atoms have been promoted into an excited state (d^9s^1 for Pd and d^{10} for Pt). In the case of Pd_4, only the $^7B_2$, $^3B_2$, and $^3A_1$ states exhibit a minimum in their potential curve, and all lie above the singlet-state $^1A_2$ which shows a repulsive curve for every Pd–Pd distance. This means that the HF method predicts the Pd_4 cluster to be an unstable species. However, some important conclusions can be drawn. The formation of Pd_4 in the $^7B_2$ state (which is the lowest state characterized by an attractive potential curve) requires the "preparation" of four Pd atoms in the d^9s^1 excited configuration: the cluster is not bound with respect to the ground-state atoms because the BE/n quantity is smaller than the atomic promotion energy.

Qualitative considerations about the intraatomic correlation energy seem to suggest that the lowest bound state of Pd_4 is $^3B_2$, arising from $3(d^{10})d^9s^1$, that is a state in which only one atom needs to be promoted to an excited state. However, even considering these partial correlation corrections, the $^3B_2$ state is not expected to be bound with respect to the ground-state atoms. The importance of the atomic promotion energy for the stability of the metal clusters can be further confirmed. The Pt_4 cluster in the $^7B_2$ state, which correlates with the ground-state atoms, in a stable cluster.[290] For both Pd_4 and Pt_4 the computed metal–metal distance for the lowest energy bound states (3.06 and 2.97 Å, respectively) are larger than the bulk values (2.75 and 2.77 Å, respectively). This is in contrast to the common expectation that the nearest-neighbor distance increases with the cluster size and the shortcoming can be due both to limitations of the ECP approach and to the lack of d–d and d–s correlation corrections.

Other ECP calculations on Pd and Pt clusters have been reported[291-292] in the framework of the cluster approach to the chemisorption theory. In ref 292, in which the ECP–SCF wavefunction was improved by means of MRD–CI calculations, it was pointed out that the stability of Pd_2, Pd_3, and Pd_4 (all considered as closed-shell systems) is as low as 0.2–0.3 eV and is entirely due to correlation effects.

The silver clusters are the only clusters of second row transition metals investigated with numerous experimental techniques.[296-302] The obvious similarity between silver and copper atoms also results from the experimental investigation in the sense that for both Ag and Cu the trimer has been fully characterized by EPR,[254,297] Raman,[300] or UV–vis spectroscopy.[296] Spectroscopic data are also available for silver clusters as large as Ag_{10}.[298,299,301,302]

The EPR spectrum of the trimer Ag_3 was interpreted[297] as due to a molecule that has the unpaired electron localized mainly on the terminal atoms (88%). This would indicate a linear $D_{\infty h}$, ($^2\Sigma_u^+$) or a distorted (C_{2v}) form the equilateral triangle. The observed symmetry of the g tensor is in favor of a C_{2v} ($^2B_2$) bent molecule, in contrast to the evidence derived from the Raman spectrum,[300] which suggests a linear configuration. CNDO calculations[279] predicted the linear form of Ag_3 to be much more stable than the triangular one while other nonempirical theoretical investigations reached the opposite conclusions. According to the results of ECP–CI study of Basch,[304] Ag_3 is a bent molecule with a $^2B_2$ ground state. Recent ECP calculations including correlation corrections[264] showed that $^2B_2$ is the correct ground state and that a strict similarity exists between geometric shapes and stability of the clusters Cu_3 and Ag_3 (see Table VI). The obtuse triangle is slightly more stable than the acute one (BE/n = 2.27 and 2.19 eV, respectively), while an intermediate stability (BE/n = 2.23 eV) characterizes the linear form ($^2\Sigma_u^+$).[269] Also the vertical and adiabatic ionization potentials for the two clusters Cu_3 and Ag_3 are very similar; the largest computed difference is as small as 0.16 eV for the $^2B_2$ state (3.1). The theoretical estimate of D_e for Ag_3 agrees well with the experimental value 2.54 ± 0.13 eV.[305]

The study of Flad et al.[264] was extended also to the Ag_4 clusters in rhombic (4.1) and T-shaped form (4.5). The computed values of BE/n are 3.81 and 3.73 eV, which closely reproduce the difference in stability between the corresponding forms of the Cu_4 cluster (cf. Table VI).

The results of the DIM calculations of Richtsmeier et al.[269] are in agreement with the previously reported nonempirical calculations for the most stable conformations of Ag_3 and Ag_4. The BE/n values of the tri-

angular forms (3.1), (3.2), and (3.3) predict nearly equal stability, while the square arrangement (4.2) is almost degenerate with the rhombic one (4.1).

For the Ag_5 cluster, the DIM method[269] predicts the regular D_{3h} trigonal bipyramid (5.2) to be more stable than the square pyramid (5.3) and the planar D_{5h} (5.4) form. This finding agrees with the experimental EPR result for the Ag_5 cluster,[299] which, however, undergoes a Jahn–Teller distortion. Finally, according to the DIM method[269] among the six different structures investigated for Ag_6, the octahedral one is supposed to be most stable.

An $X\alpha$–SW study of the Ag_5 cluster and of its ionic species Ag_5^{n+} (n = 2, 4)[303] has recently been reported. Ground-state electronic properties, excitation energies, ionization potentials, and isotopic and anisotropic as well as the hyperfine EPR tensor have been computed for the neutral and charged species. The theoretically determined quantity in general agrees with the available experimental data. The blue shift of the excitation energies computed for Ag_5^0 ($^2E'$), Ag_5^{2+} ($^2A_1$), and Ag_5^{4+} ($^2A_2''$) parallel the stabilization of all the one-electron energy levels as the positive charge increases. The latter, in addition, drastically influences the computed EPR parameters.

VI. General Conclusions

The electronic structure of small clusters built from group Ia (1), IIa (2), IIIa (3), and IVa (4) atoms can be investigated with appropriately elaborate quantum chemical methods, which give general insight into the regularities of cluster properties. The reason for the generally increasing stability of clusters with the cluster size is well understood as due to the growing average coordination number.

It is a well-known fact that finite arrangements of atoms can be more closely packed than infinite lattices (compare the stability of the steps in pentagonal crystal growth). The high compactness of a cluster can partly compensate the unfavorable influence of an inevitable large proportion of surface atoms on cluster stability. It is natural to assume that a cluster will try to approach a spherical form and that the electronic cloud will have a shape similar to that in "perturbed giant atom". The framework of atomic nuclei should exhibit as many condensed tetrahedral substructures as possible (Boerdijk's principle).

Degeneracies and near degeneracies of the one-electron functions (MO's and NO's), characteristic for the electronic structure together with the number of available valence electrons, substantially influence the optimal cluster geometry.

The symmetries and near symmetries of the electron cloud are naturally significantly influenced by the positions of atomic nuclei in the cluster. Consequently, the nonaccidental degeneracies of relevant one-electron functions for a cluster are determined by a point group that describes the symmetry of the atomic framework. The irreducible representations of a point group can usually cause only at most threefold degeneracies (a well-known exception is the icosahedron group I_h with H irreducible representations).

The fivefold degeneracies analogous to those of d AO's usually split into twofold and threefold degeneracies due to the atomic nuclei which necessarily disturb the ideal spherical symmetry of a "superatom" model of a cluster. The analogy between the role of atomic nuclei in a small cluster and that of ligands in the field theory of inorganic complex compounds is very instructive.

It is possible, of course, to argue that the actual position of nuclei is of less importance for clusters with larger nuclearity. However, the properties of the interesting class of clusters with a nuclearity smaller than 25 depends necessarily strongly on the detailed cluster geometry.

The deviations of the cluster geometry from the expectations deduced from the principle of maximal possible compactness can be interpreted as due to the general properties of the relevant wave functions (to MO degeneracies and Jahn–Teller and pseudo-Jahn–Teller effects, as well as to related phenomena). The consideration of the number of available valence electrons in a cluster can also explain the difference in the geometries and stabilities of clusters built from atoms that belong to different columns of the periodic table of elements.

The interpretation of the character of the AO basis set is also very useful to reach an understanding of chemical bonds in simple clusters. Nevertheless, even if it is not absolutely necessary to include d-type AO's into the calculations of the electronic structure of a cluster, the computational difficulties can start to be prohibitive for medium-size clusters. Therefore, it is advisable to try to develop semiquantitative methods which make it possible to extrapolate some rules for medium-size clusters. These rules should be obtained from the investigation of small clusters by means of elaborate (e.g., ab initio) quantum chemical methods. Such extrapolation methods can either have the form of simple quantum mechanical (e.g., semiempirical) methods or can be of classical type (e.g., various additive schemes). Such methods are highly desirable and useful if they are based on the knowledge achieved with an appropriate use of quantum mechanical studies on small clusters.

Very characteristic and somewhat simple are the electronic structures of the clusters at geometries that represent the true minima on the ground-state energy hypersurface for the given nuclearity: the excited states of these clusters are quite well separated from the energy of the ground state. The opposite is true for unstable geometrical structures which often exhibit a biradicaloid character. This property of the relatively most stable clusters devoid of biradicaloid character is also very advantageous from the methodological point of view. The electronic structure of stable clusters with closed electronic shells can be satisfactorily studied also with quantum mechanical methods in which the description of a few open electron shells is not easy. This is perhaps the true reason why ab initio Hartree–Fock-type methods give results qualitatively very similar to those obtained with one-electron density type procedures, at least for group Ia (1) and IIa (2) clusters.

Of course, the less stable cluster geometries very often exhibiting biradicaloid character are not without interest, since these clusters can have the shapes of some sections of the crystal lattices in which the corresponding metal crystallizes. This circumstance present a dangerous dilemma for the modeling of the chemi-

sorption sites and the centers of catalytic activity because an improper selection of models can lead to a false predictions of surface reactivity. On the other hand, it is not excluded that such unstable cluster forms can be of some importance as intermediates during the cluster growth process.

The general state of knowledge for clusters built from nontransition-metal atoms can be characterized as highly promising. On the contrary, the investigation of the probably more important transition-metal clusters is in a much less satisfactory state from the point of view of the fundamental research on the nature of interactions responsible for their stability. For example, the ab initio quantum chemical methods using a nonlocal potential are hardly able to predict the proper stability of most transition-metal diatomics. The excited states of transition-metal clusters, which are of importance for a full understanding of the chemical bonds in clusters, are completely unexplored.

Up to now, it seems that only the Xα–SW and DF methods (see appendix VII.B) can be applied to transition-metal clusters of any interesting size. However, these methods do not allow for a simpler and clear interpretation of the TM cluster stabilities as HF and CI methods do for simpler clusters. The Xα–SW calculations claim a remarkable similarity between relatively small clusters and TM bulk for the density of states (DOS) dependence and the mean value of the magnetic moment/atom. The dangers involved in drawing conclusions from the "DOS" for finite clusters have been mentioned already in the Introduction.

Furthermore, the results of Xα–SW calculations contradict the results of semiempirical methods. Also, the spin distribution obtained from the Xα–SW approach is extremely inhomogeneous. In conclusion, the very interesting and challenging results of the Xα–SW methods badly need an independent confirmation employing other methods.

In principle, semiempirical methods (EHT, CNDO) can be used to study TM clusters, but they hardly give parallel results to the HF or Hartree–Slater methods.

Evidently, further efforts in the interesting field of the quantum mechanical investigation of small- and medium-size clusters are necessary and desirable to achieve a better understanding of the fundamental properties of these challenging and intriguing species.

Acknowledgments. This work was supported by the Deutsche Forschungsgemeinschaft, Sonderforschungsbereich 6 "Structure and Dynamics of Interfaces", and by the Italian CNR. We express our gratitude to Prof. V. Bonačić-Koutecký for fruitful collaboration in the course of research on clusters and discussions during work on this contribution. In addition we thank our collaborators H.-O. Beckmann, I. Boustani, G.-H. Jeung, G. Pacchioni, W. Pewestorf, and D. Plavšić. P.F. would like to dedicate this contribution to Prof. Lamberto Malatesta (University of Milan, Italy) as sign of scientific and personal appreciation.

VII. Appendixes

The most important theoretical notions needed in the main part of this review article should be mentioned in a short and lucid form in the Appendixes without any claim as far as completeness or systematization are concerned.

A. Hartree–Fock and Configuration Interaction Methods

"Ab initio" methods of quantum chemistry are characterized by the effort to obtain information on the properties of a molecular system from an approximate wave function (chosen among all functions of a given class) which minimizes the expectation value of the "exact" Hamiltonian. The "exact" Hamiltonian usually considered neglects all the relativistic effects, which certainly may have a nonnegligible influence on the results of the theory if heavier atoms (like transition-metal atoms) are involved. It is needless to say that the use of the variational principle, too, which is valid for the energy, does not necessarily yield optimal information about other properties of the system. These limitations always ought to be kept in mind when "ab initio" results are discussed.

Various methods differ in the assumptions about the form of the many-electron function. The methods mostly used start from the concept of a "configuration" which can be written either as a superposition of Slater determinants with fixed spatial parts of the one-electron functions or as the antisymmetrical product of the fixed spatial parts of one-electron functions multiplied by an appropriate spin factor.

In the Born-Oppenheimer approximation a N–electron wave function ψ_i can be written as a linear combination of Slater determinants D_K (configuration interaction method, CI)

$$\psi_i = \sum_K C_{iK} D_K \qquad \text{(A1.1)}$$

A Slater determinant D_K is built for a given selection (configuration) K from the space V of the one-electron (spin–orbit) functions $\phi_j\alpha$ and $\phi_k\beta$. If both $\phi_j\alpha$ and $\phi_j\beta$ are included in the configuration K we name the orbital ϕ_j spin paired, otherwise it is unpaired. ψ_i is necessarily an eigenfunction of the spin operators $\hat{S}^2$ and $\hat{S}_z$. An individual D_K is always an eigenfunction of the operator $\hat{S}_z$, but it is eigenfunction of $\hat{S}^2$, only if the unpaired spatial one-electron functions are muliplied by the same spin function (e.g., $\phi_i\alpha$, $\phi_j\alpha$).

The functional which should be minimized is then

$$\bar{H}_i = \langle\psi_i|\hat{H}|\psi_i\rangle = \sum_{K,K'} C_{iK}C_{iK'}\langle D_K|\hat{H}|D_{K'}\rangle \qquad \text{(A1.2)}$$

with

$$\hat{H} = \sum_{j=1}^{N} \hat{h}_1(j) + \sum_{j<k} r_{jk}^{-1} \qquad \text{(A1.3)}$$

The value of $\bar{H}_i$ does not depend on any linear transformation in the space V if the summation in (A1.1) goes over all possible choices of K. In other words the selection of the basis in the space V is irrelevant if the configuration interaction is complete. If the sum in (A1.1) is truncated, the result of the CI procedure can depend crucially on the choice of ϕ_j's.

Suitable one-electron functions used in construction of the Slater determinants in (A1.1) are the eigenfunctions of the Hartree–Fock operator which for molecular systems are named molecular orbitals (MO). These one-electron functions are advantageous for two reasons: the ϕ's are orthogonal, and very often they yield an acceptable description of the state in a single configuration approximation. Indeed, if chemical bonds

are strong enough, usually one of the configurations in the expansion (A1.1) for the ground state has a dominant weight $|C_{iK}|^2$ in comparison with all other configurations. This is not always the case for excited states and for some systems where the spin pairing is not well developed (biradicaloid compounds).

According to Roothan[305] the Hartree–Fock operator $\hat{F}$ assigned to the Hamiltonian $\hat{H}$ (cf., e.g., (A1.3)) has the form

$$\hat{F}(1) = \hat{h}_1(1) + \hat{G}(1) + \hat{M}(1) \qquad \text{(A1.4)}$$

where

$$\hat{G} = \sum_{j=1}^{N} N_j(\hat{J}_j - \hat{K}_j/2) \qquad \text{(A1.5)}$$

$$\hat{M} = [(\hat{P}_v + \hat{P}_{os}/2)\hat{K}_{os} + \hat{K}_{os}(\hat{P}_v + \hat{P}_{os}/2)]/2 \qquad \text{(A1.6)}$$

with

$$\hat{K}_{os} = \sum_{j \in os} \hat{K}_j \qquad \text{(A1.7)}$$

N_j is the occupation number of the orbital ϕ_j. J_j and K_j are the Coulomb and exchange operators, respectively, defined in terms of orbitals ϕ_j. $\hat{P}_c$, $\hat{P}_{os}$, and $\hat{P}_v$ are the projection operators on the space of closed-shell, open-shell, and virtual orbitals, respectively.

An orbital belongs to a closed shell if it, as well as all other orbitals degenerate with it (which have the same eigenvalue of the operator $\hat{F}$), are doubly occupied. If this condition is not fulfilled for an orbital selected in K, it belongs to an open shell. The unoccupied orbitals which are not degenerate with any occupied orbitals are named virtual orbitals. The summation in (A1.7) goes over the open shell orbitals.

It is necessary to notice that for an open-shell system the definition of the operator $\hat{F}$ of (A1.4) has the advantage that the associated equations have the simple form

$$\hat{F}\phi_j = \epsilon_j\phi_j \qquad \text{(A1.8)}$$

However the definition (A1.4) is not unique. Another possibility is[305] to define different operators $\hat{F}_c$ and $\hat{F}_{os}$ which separately act on the MO's that belong to the subspace C and OS (ϕ_k^c and ϕ_k^{os})

$$\hat{F}_c\phi_k^c = \eta_k^c\phi_k^c \qquad \text{(A1.9)}$$

$$\hat{F}_{os}\phi_k^{os} = \eta_k^{o}\phi_k^{os}$$

$$\begin{aligned} \hat{F}_c(1) &= \hat{h}_1(1) + \hat{G}(1) + \hat{M}_c(1) \\ \hat{F}_{os}(1) &= \hat{h}_1(1) + \hat{G}(1) + \hat{M}_{os}(1) \end{aligned} \qquad \text{(A1.10)}$$

where

$$\hat{M}_c = (\hat{P}_{os}\hat{K}_{os} + \hat{K}_{os}\hat{P}_{os})/2$$

and

$$\hat{M}_{os} = [(\hat{P}_c - \hat{P}_v - \hat{P}_{os})\hat{K}_{os} + \hat{K}_{os}(\hat{P}_c - \hat{P}_v - \hat{P}_{os})]/2 = \hat{P}_c\hat{K}_{os} + \hat{K}_{os}\hat{P}_c - \hat{K}_o \qquad \text{(A1.11)}$$

are coupling operators between the closed shell and the open shell and guarantee that the orbitals ϕ_k^c and ϕ_k^{os} of (A1.9) are mutually orthogonal.

The eigenfunctions and eigenvalues of the operators $\hat{F}$, $\hat{F}_c$, and $\hat{F}_{os}$ are not identical. If no open shells are present, the coupling operators $\hat{M}$, $\hat{M}_c$, and $\hat{M}_{os}$ disappear and the Hartree–Fock equation take the classical form[306]

$$\hat{F}(1) = \hat{h}_1(1) + \hat{G}(1) \qquad \text{(A1.12)}$$

The complications in the HF approximation caused by the existence of open shells can be avoided if the MO spatial parts combined with the spin up and the MO spatial parts combined with the spin down are considered independently. This unrestricted Hartree–Fock (UHF) procedure has many practical advantages and it also takes into account correlation effects to a certain degree. On the other hand, a single determinant, used in this UHF method,[307] of the form

$$D_{K_\alpha K_\beta} = (N!)^{1/2}\hat{\mathcal{A}} \prod_{j=1}^{N_\alpha} \phi_j^\alpha(j)\alpha(j) \prod_{k=1}^{N_\beta} \phi_k^\beta(k)\beta(k) \qquad \text{(A1.13)}$$

is not an eigenfunction of the spin operator $\hat{S}^2$.

Different Hartree–Fock operators are used for electrons with different spin orientations in the UHF equations:

$$\hat{F}_\alpha\phi_j^\alpha = \epsilon_j^\alpha\phi_j^\alpha \qquad \hat{F}_\beta\phi_j^\beta = \epsilon_j^\beta\phi_j^\beta \qquad \text{(A1.14)}$$

where

$$\begin{aligned} \hat{F}_\alpha &= \hat{h}_1(1) + \hat{J}_U - \hat{K}_\alpha \\ \hat{F}_\beta &= \hat{h}_1(1) + \hat{J}_U - \hat{K}_\beta \end{aligned} \qquad \text{(A1.15)}$$

with

$$\hat{J}_U = \sum_{j=1}^{N_\alpha} \hat{J}_{j\alpha} + \sum_{j=1}^{N_\alpha} \hat{J}_{j\beta} \qquad \hat{K}_\alpha = \sum_{j=1}^{N_\alpha} \hat{K}_{j\alpha}$$

$$\hat{K}_\beta = \sum_{j=1}^{N_\beta} \hat{K}_{j\beta} \qquad \text{(A1.16)}$$

where $\hat{J}_{j\alpha}$, $\hat{K}_{j\alpha}$ and $\hat{J}_{j\beta}$, $\hat{K}_{j\beta}$ are Coulomb and exchange integrals defined in terms of the orbitals ϕ_j^α and ϕ_j^β, respectively. Notice that ϕ_i^α and ϕ_i^β are orthogonal only due to the orthogonality of spin functions.

The expectation value for a many electron wavefunction of an arbitrary one-electron operator

$$\hat{A} = \sum_{j=1}^{N} \hat{a}(j) \qquad \text{(A1.17)}$$

can be written as

$$\langle\psi|\hat{A}|\psi\rangle = \sum_{j,k}\langle\phi_j|\hat{a}|\phi_k\rangle\langle\psi|\hat{E}_k^j|\psi\rangle = \sum_{j,k}\langle\phi_j|\hat{a}|\phi_k\rangle\langle\psi|\hat{X}_j^+\hat{X}_k|\psi\rangle \qquad \text{(A1.18)}$$

where $\hat{X}_j^+$ and $\hat{X}_j$ are creation and annihilation operators for the one electron function ϕ_j and

$$\hat{E}_k^j = \hat{X}_j^+\hat{X}_k \qquad \text{(A1.19)}$$

The diagonalization of the matrix

$$(\langle\psi|\hat{X}_j^+\hat{X}_k|\psi\rangle) \qquad \text{(A1.20)}$$

yields the natural orbitals (NO) f_j as eigenfunctions and natural orbital occupation numbers n_j (NOON) as eigenvalues.[308] The expectation value of $\hat{A}$ takes a simple and instructive form

$$\langle\psi|\hat{A}|\psi\rangle = \sum_j n_j\langle f_j|\hat{a}|f_j\rangle \qquad \text{(A1.21)}$$

In "normal" molecular systems with an even number of electrons the values of NOON's do not appreciably differ from 2 or 0. It two electrons, say k and j are not well paired, the independent contributions $\langle f_k|\hat{a}|f_k\rangle$ and

$\langle f_j|\hat{a}|f_j\rangle$ with similar weights $n_j \sim 1$ and $n_k \sim 1$ manifest the independent behavior of the two electrons j and k. The situation typical for biradicaloid systems occur. In the framework of the one-electron description a perfect biradicaloid can be defined as a system with degenerate highest occupied and lowest unoccupied MO's (HOMO and LUMO).

A principal difficulty arising when HF eigenfunctions are used for molecular systems of biradicaloid nature is that a single determinant does not usually represent any helpful description of the electronic structure. Because the complete CI procedure is not feasible in any case of practical importance, the quality of a truncated CI depends on the basis of one-electron functions used.

The natural orbitals as a one-electron basis (naturally) do not suffer from the same drawback as the HF MO's, but the NO's can be formed only by means of a time-consuming iterative procedure starting from a chosen set of one-electron functions.

Another possibility is to determine a set of one-electron functions which minimize the expectation value of $\hat{H}$ for a trial function ψ_{tr} which is already assumed to be a lineear combination of some configurations K'

$$\psi_{tr} = \sum_{K'} C_{K'}{}^{tr} D_{K'} \qquad \text{(A1.22)}$$

The optimization of

$$\langle \psi_{tr}|\hat{H}|\psi_{tr}\rangle = \sum_{K',L'} C_{K'}{}^{tr} C_{L'}{}^{tr} \langle D_{K'}|\hat{H}|D_{L'}\rangle \qquad \text{(A1.23)}$$

with respect to the one-electron function ϕ_k and the coefficients $C_{K'}{}^{tr}$ yields the multiconfiguration SCF (MCSCF)[309] molecular orbitals. If the configurations K' exhaust all possibilities of excitations for a given subspace of ϕ_k' (so-called active space), the procedure, which evidently has some important advantages, is named complete active space SCF (CAS–SCF)[310] method.

Naturally, the equations of the MCSCF eigenproblems are much more complicated than the usual SCF equations. Nevertheless, a large progress has been recently achieved in the development and application of MCSCF methods.

In the multireference diexcited configuration interaction method (MRD-CI),[311,312] a few configurations are considered as the leading (or main) configurations. The configurations resulting from single and double excitations from all these main configurations which according to an accepted criterion can contribute to the energy lowering are included together with the main configurations in the final secular CI problem. The problem of a reasonable choice of the one-electron functions used for the construction of the configurations of course still remains in this method. On the other hand, in many cases the choice of these MO's is less important if the number of main configurations M and the number of the additional selected singly and doubly excited configuration are large enough.

The selection of the additional configurations in the MRD–CI method is practically carried out according to the following recipe: The lowest root (E_0) of a secular determinant built with M main configurations is determined. The single and doubly excited configurations are added one by one to the M main configurations and the corresponding secular problem of the order M + 1 is solved. If the difference between the lowest root for this secular problem of the order $M + 1$ and E_0 is larger than a given threshold T, then the added configuration is considered in the final secular problem.

An extrapolation procedure from the energy which is obtained with a selection threshold T to the threshold $T \rightarrow 0$ is used in the MRD–CI method.[311,312] This extrapolation seems to work quite well, but it is important to realize that the limit $T \rightarrow 0$ does not give an energy value valid for the whole CI space but only for the CI space generated by all the singly and doubly excited configurations with respect to the main configurations.

The general capabilities as well as the principal drawbacks of the MRD–CI method are evident. It is nevertheless encouraging that, for example, the MRD–CI procedure, which uses triplet SCF MO's as one-electron functions, often gives result similar to those of a MRD–CI treatment in which the configurations are constructed with the help of singlet MO's. This proves that the results of such a CI approach do not depend dramatically upon the particular chosen set of one-electron basis functions, provided that a careful selection of the M reference configurations is made.

A very unpleasant property of all the configuration interaction methods which include in the CI expansion only configurations that are doubly excited with respect to a single reference configuration (SD–CI) is the so-called "CI size-consistency" error.[313,314] The omitted higher excitations represent larger and larger neglects of correlation energy as the systems studied include an increasing number of electrons.

The MRD–CI procedure considers a few main configurations from the start, so that one can hope that for a good choice of main configurations the size-consistency error can be less important. However, it is necessary to realize that it cannot be completely eliminated for larger systems.

An estimate of the correction ΔE_Q for the full CI energy may be obtained with the formula of Davidson.[315]

$$\Delta E_Q = (1 - C_0{}^2)\Delta E_D \qquad \text{(A1.24)}$$

where ΔE_D is the correlation energy due to the double excitations and C_0 is the coefficient of the main configuration in the SD–CI. A few modified forms of the estimate (A1.24), as well as a generalization for the case that many reference configurations are used in the CI method, have been published.

In the case of a very stable closed-shell system which is usually qualitatively well described by a single HF configuration only, a really good calculation of the correlation energy is very difficult. This correlation energy results from an extremely large number of small contributions from the many configurations which together form an appreciable sum.

Very often hundreds of thousands of configurations must be considered. Therefore, the usual methods of diagonalization of the CI matrix are not well applicable. The direct configuration interaction methods[316,317] and perturbative Møller–Plesset[318] schemes are nowadays commonly used. Obviously the Møller–Plesset procedure does not yield an upper limit of the energy of the investigated systems.

Let us mention other methods, too, which do not start from the concept of molecular orbitals but explicitly consider two-electron covalent pairing at the outset. A

natural complement to the molecular orbital theories has historically been the valence bond (VB) method. A new very powerful version of this approach which does not yield wrong dissociation limits, as the HF and related theories do, is the generalized valence bond (GVB) method.[319,320] This method has been used in some studies on smaller clusters (see Table II). The electron-pair theories[321] represent another important group of quantum chemical methods. The correlated electron pair theory (CEPA)[322,323] has been also applied in the treatment of smaller clusters yielding interesting results (see Tables I and V).

A satisfactory choice of the one-electron functions is the prerequisite of any successful treatment of the electronic structure. In the current use the functions used for the definition of the space of one-electron are the atomic-orbital-like functions (e.g., ref 56 and 324–326). Gaussian functions localized at the atomic positions exhibit some computational advantages in comparison with the Slater-type AO's (STO's), in spite of their sometimes qualitatively wrong behavior at the atomic nucleus. Linear combinations of a few Gaussian functions can then be used to mimic the properties of the STO's. If a fixed linear combination of Gaussians (contracted Gaussians) is used to describe each atomic orbital, one names the basis minimal in contrast to the split AO basis set, where the number of contracted Gaussian function is larger than the number of atomic orbitals needed. The exponential coefficients in the Gaussians determine the spatial size of the electronic clouds and are of a large importance for the interatomic interaction in the studied compounds. An improper choice of these exponents can conceal very important features of bonds in clusters, where quite often linear combinations of the basis functions located on the same atoms (hybridization, polarization) are of the greatest importance for the proper description of the electronic and geometric structure of a cluster.

The notion of a polarization function is of course based on a convention. Usually p-type Gaussians are not considered polarization functions for Li and Be, in spite of the fact that the p atomic orbitals are vacant in the Li and Be atoms. For instance, in this review we used the name polarization functions for basis functions of any type different from the occupied AO's in a free atom.

Ab initio calculations of higher quality suffer from a seemingly difficult interpretation of their results. This disadvantage is in reality not of an essential nature. In reality a clear and lucid interpretation and rationalization of the ab initio results is only a little more laborious than in the case of simplified methods but possible.

Two properties of the one-electron functions built from the localized basis functions can lead to difficulties when the ab initio methods are applied to the problems of cluster structure:

The LCAO-type (linear combination of atomic orbitals) procedure can lead to overcompleteness if the basis functions localized at different centers overlap enough, and the number of AO's is large. This approximate linear dependence of the molecular orbitals can be of course avoided, if the superfluous MO's are eliminated, but the whole phenomenon is a big computational nuisance. Another unpleasant technical feature of LCAO methods using relatively limited AO basis set is the basis set superposition error (BSSE). The basis functions localized at neighboring centers can be used to describe the electron density in the neighborhood of an atom better than the basis functions localized only at the atoms can do alone.

This effect can lead to spurious minima on the Hartree–Fock potential curves and can predict nonexisting bonds to be present. HF basis set superposition error and the CI size-consistency error[313,314] can lead to wrong predictions concerning the stability of weakly bonded composite systems, if these two sources of relatively small errors are not carefully eliminated.

B. Density Functional Theory

In this appendix a brief review of the quantum mechanical methods based on the density functional (DF) theory is presented. Such methods, originally developed and applied in the field of solid-state theory, recently became very popular also in the field of molecular quantum chemistry.

1. The Density Functional Method

The DF theory was developed by Hohenberg, Kohn, and Sham[327,328] and several of its theoretical aspects, computational strategies, and applications to a variety of problems of interest in solid-state physics, cluster science, chemisorption theory, and molecular quantum chemistry have been lately reviewed.[329,330,332] In the DF model, all the properties of an electronic system are expressed in terms of the electron density $\rho(\bar{r})$ which, in principle, can be obtained from the exact N-electron wave function ψ (1,2....N), according to the following basic defintion:

$$\rho(\bar{r}) = N \int |\psi|^2 \, d\bar{r}_2 \, d\bar{r}_3 \ldots d\bar{r}_N \qquad \text{(A2.1)}$$

As has been proved by Hohenberg and Kohn,[327] $\rho(\bar{r})$ fully determines the potential that the electrons are subjected to. A wrong density gives an energy value higher than that associated with the exact $\rho(\bar{r})$. Therefore, the stationary principle for the energy can be reformulated in terms of electron density, instead of in terms of the wave function, as it is usually done in the context of the HF "orbital" theory.

If the "external potential" (associated with the electron–nucleus intraction) is symbolically represented by $V(\bar{r})$, the total energy functional assumes the form

$$E(\rho) = F(\rho) + \int \rho(\bar{r}) V(\bar{r}) \, d\bar{r} \qquad \text{(A2.2)}$$

where $F(\rho)$, a functional independent from $V(\bar{r})$, obeys the following definition:

$$F(\rho) = \frac{1}{2} \int \frac{\rho(\bar{r}) \, \rho(\bar{r}')}{|\bar{r} - \bar{r}'|} \, d\bar{r} \, d\bar{r}' + T_o(\rho) + E_{xc}(\rho) \qquad \text{(A2.3)}$$

The first term (A2.3) is the classical electrostatic interaction, $T_o(\rho)$ is the kinetic energy of N noninteracting electrons and $E_{xc}(\rho)$ includes the exchange functional $K(\rho)$ and all the many-body terms of the interacting electron system. $E_{xc}(\rho)$ is usually referred to as the exchange-correlation functional. Since several problems are met while working directly with (A2.2) or (A2.3), the minimization of the energy functional is better carried

out introducing the Kohn–Sham orbitals (KSO) obeying the definition

$$\rho(\bar{r}) = \sum_{k=1}^{N} |\phi_k|^2 \qquad \text{(A2.4)}$$

The KSO's ϕ_k can be variationally determined by solving N one-electron equations of the form

$$\hat{F}_{KS}\phi_K = \epsilon_K^{KS}\phi_K \qquad \text{(A2.5)}$$

where the $\hat{F}_{KS}$ operator is defined by

$$\hat{F}_{KS} = -\nabla^2/2 + V(\bar{r}) + \int \frac{\rho(\bar{r}')\,d\bar{r}'}{|\bar{r} - \bar{r}'|} + \frac{\partial E_{xc}(\rho)}{\partial\rho} \qquad \text{(A2.6)}$$

The KSO's have a physical meaning only in the sense that they sum up to the exact density (eq A2.4). Nevertheless, they are important "working functions" in the global process of minimization of the energy functional.

The "orbital" form of (A2.5) is reminiscent of the corresponding equation of the HF method (see appendix A), but the KSO's are different from the one-electron functions $\{\phi_k^{HF}\}$ occurring in the definition of the single-determinant HF wave function.

In particular,

$$\rho^{HF} = \sum_K |\phi_K^{HF}|^2$$

is the electron density computed according to the one-electron picture, while $\rho(\bar{r})$ defined in eq (A2.1) results from considering all the possible many-electron contribution and is related to the (exact) natural orbitals $\{f_j\}$ (see appendix A)

$$\rho(\bar{r}) = \sum_j n_j|f_j|^2 \qquad \text{(A1.21')}$$

(A2.5) can be solved to self-consistency (with the help of (A2.3), which leads, in principle, to the exact solution for $\rho(\bar{r})$. Unfortunately, this cannot be achieved because the form of the $E_{xc}(\rho)$ functional is unknown. Therefore, in practice one is forced to accept "a priori" assumptions about the functional dependence of the exchange-correlation potential upon the electron density.

As is well-known from HF theory, all computational difficulties connected with the exchange operator are related to its nonlocal character. Enormous simplifications are expected if a suitable local density approximation (LD) may be devised. This is what has been actually proposed for both the exchange and correlation terms included in the $E_{xc}(\rho)$ functional. This is known as the local density approximation of the DF theory. Its extension to the spin-polarized case in which different densities for spin up (ρ_+) and spin down (ρ_-) are defined ($\rho = \rho_+ + \rho_-$) is known as local spin density (LSD) approximation. The equation

$$E_{xc}(\rho) = \int \epsilon_{xc}(\rho)\rho(\bar{r})\,d\bar{r} \qquad \text{(A2.7)}$$

can be easily worked out if for instance $\epsilon_{xc}(\rho)$ (a local functional) is assumed to be the exchange and correlation energy per particle for the homogeneous electron gas.

Moreover, in the special case in which the correlation contributions are neglected, $\epsilon_{xc}(\rho)$ assumes the simple form

$$\epsilon_x(\rho) = -3\left|\frac{3}{8}\rho(\bar{r})\right|^{1/3} \qquad \text{(A2.8)}$$

and the corresponding exchange operator has the form

$$\frac{\partial\epsilon_x}{\partial\rho} = -4\left|\frac{3}{8\pi}\rho(\bar{r})\right|^{1/3} \qquad \text{(A2.9)}$$

Note that (A2.8) and A2.9) implicitly contain the definition of the Xα potential

$$\epsilon_{x\alpha} = \alpha\rho(\bar{r})^{1/3} \qquad \text{(A2.10)}$$

the form of which has been obtained also by Slater in the framework of the statistical exchange method.[331] The computational methods based on the Xα approximation will be considered in next section.

More elaborate forms of the $\epsilon_{xc}(\rho)$ functional entering the (A2.7) have been worked out, both in the framework of the LD (or LSD) approximation and in a nonlocal approximation based on the gradient expansion of the functional in terms of ρ, $\nabla\rho$, $\nabla^2\rho$, etc.[332,333]

Due to the limitations connected with the assumption that $\epsilon_{xc}(\rho)$ can be obtained from the homogeneous gas theory, the LD or LSD computational schemes are not free from errors, especially in the case that the physical quantities of interest must be computed as the difference between the total energy values of states characterized by large variations in $\rho(\bar{r})$. A detailed analysis of the shortcomings accompanying the applications of the LSD theory has appeared recently.[334]

Several LD or LSD computational schemes violate the simple principle that an electron cannot interact with itself. This requires that the self-interaction correction (SIC) should be taken into account.[29,335-336]

However, in practice, this is seldom done, especially in the case of large systems, mainly because of the additional computational difficulties.

Recently, a new computational scheme has been proposed[337] in which the single determinant wave function is computed according to the HF method (an exact exchange potential method) while the LSD approximation is adopted to estimate the correlation energy only, according to

$$E_c(\rho^{HF}) = \int \rho^{HF}(\bar{r})\epsilon_c(\rho_+^{HF},\rho_-^{HF})\,dr$$

The approach is based on the observation that the correlation treatment does not significantly alter the "starting" HF densities, which, as a consequence, can be used directly for the evaluation of the correlation energy.

2. The Hartree–Fock–Slater (Xα) Method

The form of an exchange potential based on a statistical treatment was

$$V_x(\bar{r}) = -6\left|\frac{3}{8}\rho(r)\right|^{1/3}$$

which is exactly $^3/_2$ times larger than the corresponding potential derived from the homogeneous electron gas theory (eq A2.9). A correction parameter α applied to V_x, leads to the definition of very popular expression of the Xα potential

$$V_{x\alpha} = -6\alpha\left|\frac{3}{8}\rho(\bar{r})\right|^{1/3} \qquad \text{(A2.11)}$$

Comparing (A2.11) and (A2.9) one obtains $\alpha = 0.67$. However, in practice, α is used as an adjustable pa-

rameter with value ranging from 0.78 for light atoms to 0.69 for heavy atoms. The "best" value for each atom can be obtained in such a way that the Xα one-electron energies fit the corresponding HF total atomic energies.[293]

It should be noted that the original formulation of the Slater's[331,338] method was developed within the framework of the single-determinant theory in order to obtain a "good approximation" to the HF method. Evidently, the HF–Slater (HFS) Xα method can be considered as a special case of local density approximation applied to the exchange potential only and neglecting all the correlation effects. These considerations are of some importance especially because it is not uncommon to find authors who claim the numerical results obtained with HFS–Xα calculations to be better than those provided by the HF method. Since both procedures are based on the one-electron picture and the Xα method is an approximation to the HF method the numerical success of the former cannot prove the theoretical inadequacy of the latter.

One of the most popular methods based on the Xα approximation is the so-called scattered wave (Xα–SW) method[339] in which the potential is spherically averaged within spheres centered around each atom, and it is assumed to be constant in the intersphere regions (muffin-tin potential). In this case, the solution of the Schrödinger equation in each molecular region is enormously simplified. Correspondingly, the computation time required by the Xα–SW method is much smaller than that required by the HF method. Moreover, since the Xα–SW computing time does not dramatically increase with the number of electrons, the method does not necessarily force the adoption of effective core potentials in the case of heavy atoms. This allows the computation of the wave function at an "all-electron" level from which all the quantities connected with the electron (and spin) density at the nuclei can be derived.

The major shortcoming of the Xα–SW method is due to the muffin-tin approximation which neglects the angular dependence of the potential in the vicinities of the atomic centers. Moreover, general "a priori" rules cannot be established for the determination of the radii of the various spheres into which the molecular space is partitioned. The dimensions of such tangent spheres can be determined by minimizing the intersphere volume. On the other hand, it is not unusual to base the choice of the volume of the spheres on empirical values of the atomic or ionic radius.

With the aim to overcome the difficulties connected with the muffin-tin approximation a variety of computational procedures have been developed. One of the most widely applied, especially in the case of large metal clusters, is the discrete variational Xα (DV–Xα) method.[340-342] The single-determinant wave function is built in a (usually very flexible) basis of Slater-type or numerical orbitals and the energy secular equation is determined in a discrete set of sampling points. The cumbersome evaluation of the many-center two-electron integrals in the basis of atomic functions is avoided by computing the electrostatic repulsion and the exchange terms with the aid of an electron density which is approximated by an expansion of multicenter overlapping multipoles.

As for the description of other relevant theoretical procedures based on the simple Xα or exchange-correlation LSD potential the reader may refer to the book of Dahl and Avery.[343]

In the field of metal clusters, the rapidly growing interest in the DF methods is motivated also by the fact that they can be successfully applied to systems of large dimensions for which HF–CI (and even simple HF) calculations cannot be carried out because of the tremendous computational effort required.

However, the present status of the DF theory in its various approximations cannot be considered completely satisfactory. The overcoming of the difficulties connected with the local approximations and the general use of the self interaction correction would certainly improve the reliability of the DF methods in the near future.

C. Effective Core Potential (Pseudopotential) Methods

In order to reduce the computational difficulties that rapidly grow as the number of the electrons increases, it has been suggested a long time ago[344] to study the wave function of the valence electrons only, by means of a procedure in which the potential of the core electrons is replaced by a simple suitable operator.

The use of an effective core potential (ECP) is physically justifiable considering that the valence electrons are the only ones mainly responsible for the energies involved in the formation of the chemical bond and for the shape of the energy hypersurface associated with intramolecular motions.

A variety of computation techniques have been developed in the framework of the ECP theory, and they are now routinely adopted in different fields of the quantum chemical studies. However, before presenting the main features of the ECP methods, it is worthwhile noting that two main difficulties accompany the basic assumptions on which such methods are based. The first is due to the fact that the core electrons are treated in a rigid way, that is, that the spherical core-electron density is assumed to be perfectly transferable from the atomic to the molecular case in which polarization effects can occur. The second and perhaps most striking difficulty is that the definition of a fixed core, and correspondingly of an active valence subspace, is sometimes ambiguous. This may be the case when the core–valence interactions are very important due to the similar radial extension of the core and valence orbitals. For instance, for the transition metals, the use of the ns and np shells as valence orbitals, together with the nd, (n + 1)s, and (n + 1)p shells, certainly would correspond to a much more realistic (and effective) description of the valence.

Therefore, one of the main features of the ECP methods should allow a flexible definition of the core and valence subsets of electrons; it should depend on the particular characteristics of the system under study and the physical quantities to be evaluated. In general, however, this is not done, mainly because the determination of the effective core operators (and the suitable valence basis sets) requires tedious numerical work. Most of the existing tabulations of the ECP operators are relative to a "standard" chemical definition of valence, and the associated valence basis sets are usually

available for ground-state atoms only.

The starting point for the derivation of the expressions of an ECP operator is to define a valence Hamiltonian of the form

$$\hat{F}_v = \hat{h} + \sum_c (2\hat{J}_c - \hat{K}_c) + \sum_{i<j}{}^{v} \frac{1}{r_{ij}} \qquad \text{(A3.1)}$$

where $\hat{h}$ is the one-electron (kinetic and nuclear attraction) operator and $\hat{J}_c$ and $\hat{K}_c$ are operators representing the Coulomb and exchange interaction with the fixed core-electron density.

The variational collapse of the valence states is avoided by means of the projector

$$\hat{P} = \sum_c |\phi_c\rangle\langle\phi_c| \qquad \text{(A3.2)}$$

where $|\phi_c\rangle$ are atomic HF solutions for the core states.

The eigenequation of the simplest projected valence Hamiltonian is

$$(1 - \hat{P})\hat{F}_v(1 - \hat{P})\chi_v = \epsilon_v(1 - \hat{P})\chi_v \qquad \text{(A3.3)}$$

where χ_v is a "pseudoorbital".

(A3.3) may be rewritten in the form

$$(\hat{F} + \hat{W}^{GPK})\chi_v = \epsilon_v\chi_v \qquad \text{(A3.4)}$$

where,

$$\hat{W}^{GPK} = -\hat{P}\hat{F}_v - \hat{F}_v\hat{P} + \hat{P}\hat{F}_v\hat{P} + \epsilon_v\hat{P} \qquad \text{(A3.5)}$$

and it is known as the generalized Phillips–Kleinman operator.[345,346]

Collecting all the terms depending on the definition of the core orbitals and the associated density, one obtains

$$\left(\hat{h} + \hat{U}_c + \sum_{i<j}{}^{v} \frac{1}{r_{ij}}\right)\chi_v = \epsilon_v\chi_v \qquad \text{(A3.6)}$$

where

$$\hat{U}_c = \sum_c (2\hat{J}_c - \hat{K}_c) + W^{GPK} \qquad \text{(A3.7)}$$

The above procedure leading to the definition of $\hat{U}_c$ is strictly valid for the case of one valence electron only. A similar treatment, however, can be developed in an approximate way also for many-valence-electron atoms.

Two different approaches have been proposed in order to specify the pseudoorbitals and, corresponding, the actual form of the effective core potential.

The first approach[347-350] requires that the orbitals χ_v solutions of the (A3.4) reproduce the shape of the true valence atomic orbitals as closely as possible, for every electron–nucleus distance. In this case, due to the orthogonality conditions, the pseudoorbitals must present radial nodes in the core region. The variational collapse is avoided by means of a "level-shifting" operator of the form

$$\hat{P}_c = \sum_c |\phi_c\rangle B_c \langle\phi_c| \qquad \text{(A3.8)}$$

which is similar to that originally proposed by Phillips and Kleinman.[344b] The Coulomb and exchange core operators appearing in (A3.6) may be approximated by a local operator of the form

$$\sum_c (2\hat{J}_c - \hat{K}_c) \approx \sum_i A_i' r^{n_i} e^{-\alpha_i r^2} \qquad \text{(A3.9)}$$

The various constants B_c, A_i, n_i, and α_i of (A3.8) and (A3.9) are treated as adjustable parameters, and their best values are obtained by minimizing the error

$$\sum_v \sum_i |\phi_v^{HF}(r) - \chi_v(r)|^2_{r=r_i} \qquad \text{(A3.10)}$$

where ϕ_v^{HF} are the HF solutions for the valence states coimputed with a reference atomic basis.

In the above procedure, the nonlocal core-valence exchange operator is approximated by the local operator (A3.9). This assumption is not considered valid in other ECP methods[351-353] in which the angular momentum dependence of the ECP operators is properly taken into account by means of a projected operator of the form

$$U_c = \sum_{l=0}^{\infty} \sum_{m=-l}^{l} U_{cl}(r)|lm\rangle\langle lm| \qquad \text{(A3.11)}$$

where

$$\sum_{l=0}^{\infty} \sum_{m=-l}^{l} |lm\rangle\langle lm| = 1 \qquad \text{(A3.12)}$$

due to the closure property of the projection operator. In practice the sum (A3.12) is truncated at a maximum value $l = L$, depending on the characteristics of the valence basis of the considered atom.

In this scheme, the pseudoorbitals are obtained by imposing the following additonal conditions: they have no radial nodes and must be characterized by a minimum spatial ondulation. Moreover the χ_v functions should reproduce the corresponding ϕ_v^{HF} orbitals in the valence region as well as possible. According to these prescriptions, the pseudoorbitals are obtained as a suitable mixture of the core and valence (ϕ_c^{HF}, ϕ_v^{HF}) "exact" HF orbitals. Since the set of the χ_v functions is known, the radial dependence of the $U_{cl}(r)$ (eq A3.11) can be obtained in an "exact" way, in a numerical form. For reasons of computation convenience, the numerical form of $U_{cl}(r)$ is then fitted by a Gaussian expansion similar to that of (A3.9).

All the mentioned ECP procedures are well suited for applications in the framework of the HF theory. Corresponding ECP theoretical schemes have been proposed also in connection with Xα LD or LSD theories.[34-35,354-355] For instance, one very recent development[34-35] of the ECP method within the framework of the LSD theory makes use of an effective core operator of the form

$$V_c = -\frac{Z_c}{r} + \int \frac{\rho_c(\bar{r}')\,d\bar{r}'}{|\bar{r} - \bar{r}'|} + \epsilon_{xc}(\rho_{c+}, \rho_{c-}), \qquad \text{(A3.13)}$$

where $\rho_c = \rho_{c+} + \rho_{c-}$ is the core-electron density summed over the spin components. It should be noted that, according to the LSD philosophy, (A3.13) also includes the core-valence correlation effects in a natural way, if a suitable ϵ_{xc} functional is adopted.

As mentioned at the beginning of this appendix, one of the major problems connected with the ECP methods (and in general with every method based on the frozen-core approximation) is the neglect of the core-valence correlation and polarization. On the contrary, these effects are taken into account in the "all-electron" methods.

Two ways of overcoming this definiency of the ECP theories have been proposed. The first[357] is based on a second-order perturbation treatment of the core-valence correlation and polarization problem, leading to a correction of the valence electron energy defined in

terms of (*i*) the core polarizability (taken from experiment), (ii) the electric fields created by the static and transition valence densities, and (iii) the valence excitation energies. According the suggestion of ref 357, the corrections can be introduced only after a CI treatment of the valence electrons. On the contrary, a second approach to the problem[358] directly takes into account the core-valence polarization contributions by means of an additional one-electron operator of the form

$$V_{\mathrm{pol}}{}^{c} = -\alpha_c f_c/2$$

$$f_c = \sum_i r_{ic}{}^{-3}\, \bar{r}_{ic}\, |1 - \exp(-\delta_c r_{ic}{}^{2})| - \sum_{c' \neq c} r_{c,c'}{}^{-3}\, \bar{r}_{cc'} \qquad \text{(A3.14)}$$

where c,c' label the core electrons and i the valence electrons, respectively. The parameters entering the (A3.14) are thus determined to reproduce the experimental valence excitation energies and ionization potentials. In this respect, such corrections assume the form of semiempirical corrections, a character which is absent in the formulation of the ref 357.

A typical field of application of the ECP methods is certainly that of molecular or cluster systems containing heavy atoms. It is well-known that in this case the relativistic effects can play a crucial role, for instance, in stabilizing the metal–metal bond. Therefore it seems very natural that the ECP methods should be developed for every atom in order to include the major parts of the relativistic contributions at least.

Recent works in this direction[30,31] led to the formulation of relativistic ECP (RECP) methods which, from a computational point of view, are only little more complicated than the nonrelativistic version. The improvement in the predictive capability of the ECP method consequent to the inclusion of the relativistic effects can be well documented considering for instance that the dissociation energy of Au_2 computed with a RECP method[30] amounts to 2.27 eV, in good agreement with the experimental value 2.31 eV.[359] The corresponding nonrelativistic estimate of D_e is about 1 eV lower. The improvement of the computed dissociation energy obtained with the RECP method is certainly well comparable in magnitude with that expected from the correlation treatment. It is easy to conclude that computational schemes based on association of RECP procedures with valence-electron correlation methods should be more and more widely adopted in quantum chemical studies of heavy atom systems.

References

(1) Johnson, K. H. In "The New World of Quantum Chemistry"; Pullman, B., Parr, R., Eds.; D. Reidel: Dordrecht, 1976.
(2) Baetzold, R. C. *Adv. Catal.* **1976**, *25*, 1.
(3) Ozin, G. A. *Catal. Rev. Sci. Eng.* **1977**, *16*, 191.
(4) Ozin, G. A. *Faraday Symp. Chem. Soc.* **1980**, *14*, 7.
(5) Kunz, A. B. In "Theory of Chemisorption"; Smith, J. R., Ed.; Springer-Verlag: Berlin, 1980.
(6) Davis, S. C.; Klabunde, K. J. *Chem. Rev.* **1982**, *82*, 153.
(7) Baetzold, R. C.; Hamilton, J. F. *Prog. Solid State Chem.* **1983**, *15*, 1.
(8) Ozin, G. A.; Mitchell, S. A. *Angew. Chem.* **1983**, *95*, 706.
(9) Buttet, J.; Borel, J. P. *Helv. Phys. Acta* **1983**, *56*, 541.
(10) Friedel, J. *Helv. Phys. Acta* **1983**, *56*, 507.
(11) Jortner, J. *Ber. Bunsenges. Phys. Chem.* **1984**, *88*, 188.
(12) Recknagel, E. *Ber. Bunsenges. Phys. Chem.* **1984**, *88*, 201.
(13) Recknagel, E. *At. Phys.* **1984**, *9*, 153.
(14) Messmer, R. P. *Surf. Sci.* **1981**, *106*, 225.
(15) Wood, D. M. *Phys. Rev. Lett.* **1981**, *46*, 749.
(16) Kappes, M. M.; Schär, M.; Radi, P.; Schumacher, E. *J. Chem. Phys.*, in press.
(17) (a) Knight, W. D.; Clemenger, K.; De Heer, W. A.; Saunders, W. A.; Chou, M. Y.; Cohen, M. L. *Phys. Rev. Lett.* **1984**, *52*, 2141. (b) Mc Adon, M. H.; Goddard, W. A., III. *Phys. Rev. Lett.* **1985**, *55*, 2563. Mc Adon, M. H.; Goddard, W. A., III. *J. Non-Cryst. Solids* **1985**, *75*, 149.
(18) Ekardt, W. *Phys. Rev. Lett.* **1984**, *52*, 1925.
(19) Ekardt, W. *Phys. Rev. B* **1984**, *29*, 1558.
(20) Ekardt, W. *Surf. Sci.* **1985**, *152/153*, 180.
(21) Slater, J. C. *Adv. Quantum Chem.* **1972**, *6*, 1.
(22) Johnson, K. H. *Adv. Quantum Chem.* **1973**, *7*, 143.
(23) Gunnarson, O.; Harris, J.; Jones, R. O. *Phys. Rev. B* **1977**, *15*, 3027.
(24) Echt, O.; Sattler, K.; Recknagel, E. *Phys. Rev. Lett.* **1981**, *47*, 1121.
(25) Kappes, M. M.; Kunz, R. W.; Schumacher, E. *Chem. Phys. Lett.* **1982**, *91*, 413.
(26) Döhnert, D.; Koutecký, J. *J. Am. Chem. Soc.* **1980**, *102*, 1789.
(27) (a) Hoare, M. R. *Adv. Chem. Phys.* **1979**, *40*, 49. (b) Hoare, M. R.; Pal, P. *Adv. Phys.* **1971**, *20*, 161.
(28) Bachelet, G. B.; Hamann, D. R.; Schlüter, M. *Phys. Rev. B* **1982**, *26*, 4199.
(29) Perdew, J. P.; Zunger, A. *Phys. Rev. B* **1981**, *23*, 5048.
(30) Pitzer, K. S. *Int. J. Quantum Chem.* **1984**, *25*, 131.
(31) Kahn, L. R. *Int. J. Quantum Chem.* **1984**, *25*, 149.
(32) Durand, Ph.; Barthelat, J. C. *Theor. Chim. Acta* **1975**, *38*, 283.
(33) Sakai, Y. *J. Chem. Phys.* **1981**, *75*, 1303. Sakai, Y.; Huzinaga, S. *J. Chem. Phys.* **1982**, *76*, 2537, 2552.
(34) Andzelm, J.; Radzio, E.; Salahub, D. R. *J. Chem. Phys.* **1985**, *83*, 4573.
(35) Andzelm, J.; Radzio, E.; Barandiadrán, Z.; Seijo, L. *J. Chem. Phys.* **1985**, *83*, 4565.
(36) Hermann, K.; Bagus, P. S. *Phys. Rev. B* **1978**, *17*, 4082.
(37) Fantucci, P.; Balzarini, P. *J. Mol. Catal.* **1978**, *4*, 337.
(38) Beckmann, H.-O.; Koutecký, J.; Botschwina, P.; Meyer, W. *Chem. Phys. Lett.* **1979**, *67*, 119.
(39) Beckmann, H.-O.; Koutecký, J.; Bonačič-Koutecký, V. *J. Chem. Phys.* **1980**, *73*, 5182.
(40) Rao, B. K.; Jena, P. *Phys. Rev. B* **1985**, *32*, 2058.
(41) Ray, A. K.; Fry, J. L.; Myles, C. W. *J. Phys. B* **1985**, *18*, 381.
(42) Pacchioni, G.; Beckmann, H.-O.; Koutecký, J. *Chem. Phys. Lett.* **1982**, *87*, 151.
(43) Flad, J.; Igel, G.; Dolg, M.; Stoll, H.; Preuss, H. *Chem. Phys.* **1975**, *75*, 331.
(44) Flad, J.; Stoll, H.; Preuss, H. *J. Chem. Phys.* **1979**, *71*, 3042.
(45) Fripiat, J. G.; Chow, K. T.; Boudart, M.; Diamond, J. B.; Johnson, K. H. *J. Mol. Catal.* **1975**, *1*, 59.
(46) Car, R.; Martins, J. L. *Surf. Sci.* **1981**, *106*, 280.
(47) Martins, J. L.; Buttet, J.; Car, R. *Phys. Rev. Lett.* **1984**, *53*, 655.
(48) Martins, J. L.; Buttet, J.; Car, R. *Phys. Rev. B* **1985**, *31*, 1804.
(49) Martins, J. L.; Car, R.; Buttet, J. *J. Chem. Phys.* **1983**, *78*, 5646.
(50) Martins, J. L.; Buttet, J.; Car, E. *Ber. Bunsenges. Phys. Chem.* **1984**, *88*, 239.
(51) Skála, L. *Phys. Status Solidi B* **1981**, *107*, 351.
(52) Companion, A. L.; Stieble, D. J.; Starshak, A. J. *J. Chem. Phys.* **1968**, *49*, 3637.
(53) Pickup, B. T.; Byer, W.; Brown, S. *Mol Phys.* **1972**, *23*, 1189.
(54) Companion, A. L. *Chem. Phys. Lett.* **1978**, *56*, 500.
(55) Richtsmeier, S. C.; Dixon, D. A.; Gole, J. L. *J. Phys. Chem.* **1982**, *86*, 3942.
(56) Poirier, R.; Kari, R.; Csizmadia, I. G. "Handbook of Gaussian Basis Sets"; Elsevier: Amsterdam, 1985.
(57) Beckmann, H.-O.; Koutecký, J. *Surf. Sci.* **1980**, *120*, 127.
(58) Fantucci, P.; Koutecký, J.; Pacchioni, G. *J. Chem. Phys.* **1984**, *80*, 325.
(59) Pacchioni, G.; Koutecký, J. *J. Chem. Phys.* **1984**, *81*, 3588.
(60) Jahn, H. A.; Teller, E. *Proc. R. Soc. London, A* **1937**, *161*, 220.
(61) Öpik, V.; Pryce, M. H. L. *Proc. R. Soc. London, A* **1957**, *238*, 425.
(62) Bersuker, I. B. "The Jahn–Teller Effects and Vibronic Interactions in Modern Chemistry"; Plenum: New York, 1984.
(63) Kendrick, J.; Hillier, I. H. *Mol. Phys.* **1977**, *33*, 635.
(64) Gerber, W. H.; Schumacher, E. *J. Chem. Phys.* **1978**, *69*, 1692.
(65) Polák, R.; Vojtík, J.; Schneider, F. *Chem. Phys. Lett.* **1978**, *53*, 117.
(66) Kress, J. W.; Carberry, J. J.; Kuczynski, G. C. *Mol. Phys.* **1978**, *36*, 717.
(67) Martins, J. L.; Car, R. *Helv. Phys. Acta* **1981**, *54*, 262.
(68) Gole, J. L.; Childs, R. H.; Dixon, D. A.; Eades, R. A. *J. Chem. Phys.* **1980**, *72*, 6368.
(69) Beckmann, H.-O. *Chem. Phys. Lett.* **1982**, *93*, 240.
(70) Martin, R. L.; Davidson, E. R. *Mol. Phys.* **1978**, *35*, 1713.
(71) Dietz, E. R. *Phys. Rev. A* **1981**, *23*, 751.
(72) Davies, D. W.; Del Conde, G. *Faraday Discuss. Chem. Soc.* **1973**, *55*, 369.
(73) Davies, D. W.; Del Conde, G. *Chem. Phys.* **1976**, *12*, 45.

(74) Koutecký, J.; Pacchioni, G. *Ber. Bunsenges. Phys. Chem.* **1984**, *88*, 233.
(75) Koutecký, J.; Boustani, I.; Pewestorf, W.; Fantucci, P.; Bonačič-Koutecký, V., to be published.
(76) Plavšič, D.; Koutecký, J.; Pacchioni, G.; Bonačič-Koutecký, V. *J. Phys. Chem.* **1983**, *87*, 1096.
(77) Fantucci, P.; Banačič-Koutecký, V.; Koutecký, J. *J. Comput. Chem.* **1985**, *6*, 462.
(78) Pacchioni, G.; Plavšič, D.; Koutecký, J. *Ber. Bunsenges. Phys. Chem.* **1983**, *87*, 503. (a) Pacchioni, G.; Koutecký, J. *Ber. Bunsenges. Phys. Chem.* **1984**, 88, 242.
(79) Koutecký, J.; Plavšič, D.; Döhnert, D. *Croat. Chim. Acta* **1983**, *56*, 451.
(80) Rao, B. K.; Jena, P. *Phys. Rev. B* **1984**, *30*, 7293.
(81) Skála, L. *Phys. Status Solidi B* **1982**, *110*, 299.
(82) Skála, L. *Phys. Status Solidi B* **1982**, *109*, 733.
(83) Marshall, R. F.; Blint, R. J.; Kunz, A. B. *Solid State Commun.* **1976**, *18*, 731.
(84) Marshall, R. F.; Blint, R. J.; Kunz, A. B. *Phys. Rev. B* **1976**, *13*, 333.
(85) Herman, K.; Schumacher, E.; Wöste, L. *J. Chem. Phys.* **1978**, *68*, 2327.
(86) Schumacher, E.; Kappes, M. M.; Marti, K.; Radi, P.; Schär, M.; Schmidthalter, B. *Ber. Bunsenges. Phys. Chem.* **1984**, *88*, 220.
(87) Peterson, K. I.; Dao, P. D.; Farley, R. W.; Castleman, A. W., Jr. *J. Chem. Phys.* **1984**, *80*, 1780.
(88) Saunders, W. A.; Clemenger, K.; De Heer, W. A.; Knight, W. D. *Phys. Rev. B* **1985**, *32*, 1366.
(89) Kappes, M. M.; Kunz, R. W.; Schumacher, E. *Chem. Phys. Lett.* **1982**, *91*, 413.
(90) Kimoto, K.; Nishida, I. *J. Phys. Soc. Jpn.* **1977**, *42*, 2071.
(91) Kimoto, K.; Nishida, I.; Takaikashi; Kato, H. *Jpn. J. Appl. Phys.* **1980**, *19*, 1821.
(92) Thompson, G. A.; Lindsay, D. M. *J. Chem. Phys.* **1981**, *74*, 959.
(93) Lindsay, D. M.; Thompson, G. A. *J. Chem. Phys.* **1982**, *77*, 1114.
(94) Garland, D. A.; Lindsay, D. M. *J. Chem. Phys.* **1983**, *78*, 2813.
(95) Thompson, G. A.; Tischler, F.; Lindsay, D. M. *J. Chem. Phys.* **1983**, *78*, 5946.
(96) Wu, C. H. *J. Chem. Phys.* **1975**, *65*, 3181.
(97) Wu, C. H. *J. Phys. Chem.* **1983**, *87*, 1534.
(98) Knight, W. D.; Clemenger, K.; De Heer, W. A.; Saunders, W. A. *Phys. Rev. B* **1985**, *31*, 2539.
(99) Delacretaz, G.; Fayet, P.; Wöste, L. *Ber. Bunsenges. Phys. Chem.* **1984**, *88*, 284.
(100) Froben, F. W.; Schulze, W. *Ber. Bunsenges. Phys. Chem.* **1984**, *88*, 312.
(101) Welker, T.; Martin, T. P. *J. Chem. Phys.* **1979**, *70*, 5683.
(102) Bauschlicher, C. W., Jr.; Partridge, H. *J. Chem. Phys.* **1984**, *80*, 334.
(103) Bagus, P. S.; Schaefer, H. F., III; Basuchlicher, C. W., Jr. *J. Chem. Phys.* **1983**, *78*, 1390.
(104) Bauschlicher, C. W., Jr.; Liskow, D. H.; Bender, C. F.; Schaefer, H. F., III *J. Chem. Phys.* **1975**, *62*, 4815.
(105) Bauschlicher, C. W., Jr.; Bender, C. F.; Schaefer, H. F., III. *Chem. Phys.* **1976**, *15*, 227.
(106) Bauschlicher, C. W., Jr. *Chem. Phys. Lett.* **1985**, *117*, 33.
(107) Bagus, P. S.; Nelin, C. J.; Bauschlicher, C. W., Jr. *Surf. Sci.* **1985**, *156*, 615.
(108) Bauschlicher, C. W., Jr.; Petterson, L. G. M. *J. Chem. Phys.* **1986**, *84*, 2226.
(109) Whiteside, R. A.; Krishnan, T.; Pople, J. A.; Krogh-Jespersen, M.; Raguê-Schleyer, P.; Wenke, G. *J. Comput. Chem.* **1980**, *1*, 307.
(110) Brewington, R. B.; Bender, C. F.; Schaefer, H. F., III *J. Chem. Phys.* **1976**, 64, 905.
(111) Dykstra, C. E.; Schaefer, H. F., III; Meyer, W. *J. Chem. Phys.* **1976**, *65*, 5141.
(112) Bauschlicher, C. W., Jr.; Bagus, P. S.; Cox, B. N. *J. Chem. Phys.* **1982**, *77*, 4032.
(113) Stoll, H.; Flad, J.; Golka, E.; Krüger, Th. *Surf. Sci.* **1981**, *106*, 251.
(114) Kato, H.; Hirao, K.; Teramae, H. *Chem. Phys.* **1984**, *86*, 361.
(115) Pacchioni, G.; Koutecký, J. *J. Chem. Phys.* **1982**, *77*, 5850.
(116) Jordan, K. D.; Simons, J. *J. Chem. Phys.* **1980**, *72*, 2889.
(117) Chiles, R. A.; Dykstra, C. E.; Jordan, K. D. *J. Chem. Phys.* **1981**, *75*, 1044.
(118) Pacchioni, G.; Koutecký, J. *Chem. Phys.* **1982**, *71*, 181.
(119) Liu, B.; McLean, A. D. *J. Chem. Phys.* **1980**, *72*, 3418.
(120) Daudey, J. P.; Novaro, O.; Kołos, W.; Berrondo, M. *J. Chem. Phys.* **1979**, *71*, 4297.
(121) Garcia-Prieto, J.; Novaro, O. *J. Chem. Phys.* **1979**, *71*, 3137.
(122) Jordan, K. D.; Simons, J. *J. Chem. Phys.* **1977**, *67*, 4027.
(123) Koutecký, J.; Pacchioni, G.; Jeung, G.-H.; Hass, E.-C. *Surf. Sci.* **1985**, *156*, 650.
(124) Pacchioni, G.; Pewestorf, W.; Koutecký, J. *Chem. Phys.* **1984**, *83*, 201.
(125) Butkus, A. M.; Fink, W. H. *J. Chem. Phys.* **1980**, *73*, 2884.
(126) Diercksen, G. H. F.; Gruner, N. E.; Oddershede, J.; Sabin, J. B. *Chem. Phys. Lett.* **1985**, *117*, 29.
(127) Fink, W. H. *J. Chem. Phys.* **1978**, *69*, 3325.
(128) Grev, R. S.; Schaefer, H. F., III. *Chem. Phys. Lett.* **1985**, *119*, 111.
(129) Jones, R. O. *J. Chem. Phys.* **1985**, *82*, 5078.
(130) Kraemer, W. H.; Buenker, R. J.; Yoshimine, M. *J. Mol. Spectrosc.* **1984**, *107*, 191.
(131) Kunz, L.; Skála, L.; Bílek, L. *Phys. Status Solidi B* **1983**, *173*, 118.
(132) Martin, T. P.; Schaber, H. *Z. Phys. B: Condens. Matter Quanta* **1979**, *35*, 61.
(133) Martin, T. P.; Schaber, H. *J. Chem. Phys.*, in press.
(134) Liskov, D. H.; Bender, C. F.; Schaefer, H. F., III. *J. Chem. Phys.* **1972**, *56*, 5075.
(135) Pacchioni, G. *Mol. Phys.* **1983**, *49*, 727.
(136) Pacchioni, G. *Chem. Phys. Lett.* **1984**, *107*, 70.
(137) Pacchioni, G. *Theor. Chim. Acta* **1983**, *62*, 461.
(138) Perić-Radić, J.; Romelt, J.; Peyerimhoff, S. D.; Buenker, R. J. *Chem. Phys. Lett.* **1977**, *30*, 344.
(139) Quinn, C. M.; Schwartz, M. E. *J. Chem. Phys.* **1981**, *74*, 5181.
(140) Salahub, D. R.; Messmer, R. P. *Phys. Rev. B* **1977**, *16*, 2526.
(141) Schwartz, M. E.; Quinn, C. M. *Surf. Sci.* **1984**, *105*, 258.
(142) Whiteside, R. A.; Krishnan, R.; Defrees, D. J.; Pople, J. A.; Raguê-Schleyer, P. *Chem. Phys. Lett.* **1981**, *78*, 538.
(143) Whiteside, R. A.; Krishnan, R.; Frisch, M.; Pople, J. A.; Schleyer, P. v. R. *Chem. Phys. Lett.* **1981**, *80*, 547.
(144) Pacchioni, G.; Koutecký, J. *J. Chem. Phys.* **1986**, *84*, 3301.
(145) Weltner, W., Jr.; McLead, D., Jr. *J. Chem. Phys.* **1966**, *45*, 3096.
(146) Graham, W. R. M.; Dismuke, K. I.; Weltner, W., Jr. *Astrophys. J.* **1976**, *204*, 301.
(147) Krätschmer, W.; Sorg, N.; Hoffmann, D. R. *Surf. Sci.* **1985**, *156*, 814.
(148) Honig, R. E. *J. Chem. Phys.* **1954**, *22*, 1610.
(149) Bloomfield, L. A.; Freeman, R. R.; Brown, W. L. *Phys. Rev. Lett.* **1985**, *20*, 2240.
(150) Kingcade, J. E., Jr.; Chondary, U. V.; Gingerich, K. A. *Inorg. Chem.* **1979**, *11*, 3094.
(151) Gingerich, K. A.; Shim, I., Gupta, S. K.; Kingcade, J. E., Jr. *Surf. Sci.* **1985**, *156*, 495.
(152) Kant, A.; Strauss, B. H. *J. Chem. Phys.* **1966**, *45*, 82.
(153) Weltner, W., Jr.; Van Zee, R. J. *Annu. Rev. Phys. Chem.* **1984**, *35*, 291.
(154) Cooper, W. H.; Clarke, G. A.; Hare, C. R. *J. Phys. Chem* **1972**, *76*, 2268.
(155) Das, C. P. *Chem. Phys. Lett.* **1982**, *86*, 482.
(156) Busby, R.; Klotzbucher, W.; Ozin, G. A. *J. Am. Chem. Soc.* **1976**, *98*, 4013.
(157) Wood, C.; Doran, M.; Hillier, I. H. *Faraday Symp.* **1980**, *14*, 159
(158) Wolf, A.; Schmidtke, H.-H. *Int. J. Quantum Chem.* 1980, *43*, 1187.
(159) Walch, S. P.; Bauschlicher, C. W., Jr. *Chem. Phys. Lett.* **1983**, *94*, 290.
(160) Walch, S. P.; Bauschlicher, C. W., Jr. *J. Chem. Phys.* **1983**, *79*, 3590.
(161) Fursova, V. D.; Klyagina, A. P.; Levin, A. A.; Gutsev, G. L. *Chem. Phys. Lett.* **1985**, *116*, 317.
(162) Harris, J.; Jones, R. O. *J. Chem. Phys.* **1979**, *70*, 830.
(163) Knight, L. B., Jr.; Van Zee, R.; Weltner, W., Jr. *Chem. Phys. Lett.* **1983**, *94*, 296.
(164) (a) Verhaegen, G.; Smoes, S.; Drowart, J. *J. Chem. Phys.* **1964**, *40*, 239. (b) DiLella, D. P.; Limm, W.; Lipson, R. H.; Moskovits, M.; Taylor, K. V. *J. Chem. Phys.* **1982**, *77*, 5263. Moskovits, M.; DiLella, D. P.; Limm W. *J. Chem. Phys.* **1984**, *80*, 626.
(165) Elfremov, Y. M.; Samoilova, A. N.; Kozhukovsky, V. B.; Gurvich, L. V. *J. Mol. Spectrosc.* **1978**, *73*, 430.
(166) Bondybey, V. E.; English, J. H. *Chem. Phys. Lett.* **1983**, *94*, 443.
(167) Michalopoulos, D. L.; Geusic, M. E.; Hansen, S. G.; Powers, D. E.; Samlley, R. E. *J. Chem. Phys.* **1982**, *86*, 3914.
(168) Riley, S. J.; Parks, E. K.; Pobo, L. G.; Wexler, S. *Ber. Bunsenges. Phys. Chem.* **1984**, *88*, 287.
(169) Kant, A.; Strauss, B. H. *J. Chem. Phys.* **1966**, *45*, 822.
(170) McLean, A. D.; Liu, B. *Chem. Phys. Lett.* **1983**, *101*, 144.
(171) Goodgame, M. M..; Goddard, W. A., III; *J. Phys. Chem.* **1981**, *85*, 215.
(172) (a) Goodgame, M. M.; Goddard, W. A., III *Phys. Rev. Lett.* **1982**, *48*, 35. (b) Goodgame, M. M.; Goddard, W. A., III. *Phys. Rev. Lett.* **1985**, *54*, 661.
(173) Walch, S. P.; Bauschlicher, C. W., Jr.; Roos, B. O.; Nelin, C. J. *Chem. Phys. Lett.* **1983**, *103*, 175.
(174) Das, G. P.; Joffé, R. L. *Chem. Phys. Lett.* **1984**, *109*, 206.
(175) Baykara, N. A.; McMaster, B. N.; Salahub, D. R. *Mol. Phys.* **1984**, *52*, 891.
(176) Witko, M.; Beckmann, H.-O. *Mol. Phys.* **1982**, *47*, 945.
(177) Tatewaki, H.; Miyoshi, E.; Nakamura, T. *J. Chem. Phys.* **1982**, *76*, 5073.

(178) Bauschlicher, C. W., Jr.; Walch, S. P.; Siegbahn, P. E. M. *J. Chem. Phys.* **1982**, *76*, 6015.
(179) Miyoshi, E.; Tatewaki, H.; Nakamura, T. *J. Chem. Phys.* **1983**, *78*, 815.
(180) Martin, R. L. *J. Chem. Phys.* **1983**, *78*, 5840.
(181) Bauschlicher, C. W., Jr.; Walch, S. P.; Siegbahn, P. E. M. *J. Chem. Phys.* **1983**, *78*, 3347.
(182) Shim, I.; Gingerich, K. A. *J. Chem. Phys.* **1983**, *79*, 2903.
(183) Bauschlicher, C. W., Jr. *Chem. Phys. Lett.* **1983**, *97*, 204.
(184) Werner, H.-J.; Martin, R. L. *Chem. Phys. Lett.* **1985**, *113*, 451.
(185) Scharf, P.; Brode, S.; Ahlrichs, R. *Chem. Phys. Lett.* **1985**, *113*, 447.
(186) Raghavachari, K.; Sunil, K. K.; Jordan, K. D. *J. Chem. Phys.* **1985**, *83*, 4633.
(187) Huber, K. P.; Herzberg, G. "Molecular Spectra and Molecular Structure"; Van Nostrand: Princeton, 1979.
(188) Pelissier, M. *J. Chem. Phys.* **1981**, *75*, 775.
(189) Pelissier, M. *J. Chem. Phys.* **1983**, *79*, 2099.
(190) Cowan, R. D.; Griffin, D. C. *J. Opt. Soc. Am.* **1976**, *66*, 1010.
(191) Delley, B.; Ellis, D. E.; Freeman, A. J.; Baerends, E. J.; Post, D. *Phys. Rev. B* **1983**, *27*, 2132.
(192) Painter, G. S.; Averill, F. W. *Phys. Rev. B* **1983**, *28*, 5536.
(193) Cossé, C.; Fonassier, M.; Mejean, T.; Tranquille, M.; DiLella, D. P.; Moskovits, M. *J. Chem. Phys.* **1980**, *73*, 6076.
(194) (a) Moskovits, M.; DiLella, D. P. In "Metal Bonding and Interactions in High-Temerpature Systems"; Gole, J. L., Smalley, W. C., Eds.; American Chemical Society: Washington, DC, 1982; Am. Chem. Soc. Sym. Ser. No. 179. (b) Kant, K.; Lin, S.-S. *J. Chem. Phys.* **1969**, *51*, 1644. (c) Gingerich, K. A. *J. Cryst. Growth* **1971**, *9*, 31.
(195) Walch, S. P.; Bauschlicher, C. W., Jr., quoted in ref 153.
(196) Langridge-Smith, P. R. R.; Morse, M. D.; Hansen, G. P.; Smalley, R. E.; Merer, A. J. *J. Chem. Phys.* **1984**, *80*, 593.
(197) Salahub, D. R.; Baykara, N. A. *Surf. Sci.* **1985**, *156*, 605.
(198) Van Zee, R. J.; Baumann, O. A.; Weltner, W., Jr. *J. Chem. Phys.* **1981**, *74*, 6977.
(199) Baumann, C. A.; Van Zee, R. J.; Bhat, S. V.; Weltner, W., Jr. *J. Chem. Phys.* **1983**, *78*, 190.
(200) Nesbet, K. *Phys. Rev. A* **1964**, *135*, 460.
(201) Shim, I.; Gingerich, K. A. *J. Chem. Phys.* **1982**, *77*, 2490.
(202) (a) Rohling, E. A.; Cox, D. M.; Kaldor, A.; Johnson, K. H. *J. Chem. Phys.* **1984**, *81*, 3846. (b) Montano, P. A.; Shenoy, G. K. *Solid State Commun.* **1980**, *35*, 53. (c) Purdum, H.; Montano, P. A.; Shenoy, G. K.; Morrison, T. *Phys. Rev. B* **1982**, *25*, 4412. (d) Moskovits, M.; DiLella, D. P. *J. Chem. Phys.* **1980**, *73*, 4917.
(203) Shim, I.; Gingerich, K. A. *J. Chem. Phys.* **1983**, *78*, 5693.
(204) See ref 205 and references therein.
(205) Basch, H.; Newton, M. D.; Moskovits, J. w. *J. Chem. Phys.* **1980**, *73*, 4492.
(206) (a) Shim, I.; Dahl, J. P.; Johansen, H. *Int. J. Quantum Chem.* **1979**, *15*, 311. (b) Melius, C. F.; Moskovitz, J. W.; Mortola, A. P. Baillie, M. B.; Ratner, M. A. *Surf. Sci.* **1976**, *59*, 279. (c) Noell, J. O.; Newton, M. D.; Hay, P. J.; Martin, R. L.; Bobrowicz, F. W. *J. Chem. Phys.* **1980**, *73*, 2360. (d) Upton, T. H.; Goddard, W. A., III. *J. Am. Chem. Soc.* **1978**, *100*, 5659.
(207) Morse, M. D.; Hansen, G. P.; Langridge-Smith, P. R. R.; Zheng, L.-S.; Geusic, M. E.; Michalopoulos, D. A.; Smalley, R. E. *J. Chem. Phys.* **1984**, *80*, 5400.
(208) Basch, H. *Faraday Symp. Chem. Soc.* **1980**, *14*, 149.
(209) Basch, H.; Cohen, D.; Topiol, S. *Isr. J. Chem.* **1980**, *19*, 233.
(210) Ziegler, T.; Snijders, J. G.; Baerends, E. J. *J. Chem. Phys.* **1981**, *74*, 1271. Martins, J. L.; Anderson, W. *Phys. Rev. A* **1983**, *28*, 3637. Stoll, M.; Fuentealba, P.; Dolg, M.; Flad, J.; von Szentpaly, L.; Preuss, H. *J. Chem. Phys.* **1983**, *79*, 5532.
(211) Lee, Y. S.; Ermler, W. C.; Pitzer, K. S.; McLean, A. D. *J. Chem. Phys.* **1979**, *70*, 288. Lee, Y. S.; Ermler, W. C.; Pitzer, K. S. *J. Chem. Phys.* **1979**, *70*, 293.
(212) Knight, L. B., Jr.; Woddward, R. W.; Van Zee, R. J.; Weltner, W., Jr. *J. Chem. Phys.* **1983**, *79*, 5820.
(213) Moskovits, M.; DiLella, D. P.; Limm, W. *J. Chem. Phys.* **1984**, *80*, 626.
(214) Longuet-Higgins, H. C.; Stone, A. J. *Mol. Phys.* **1962**, *5*, 417.
(215) Anderson, B. *J. Chem. Phys.* **1976**, *64*, 4046.
(216) Wise, M. B.; Jacobson, D. B.; Freiser, B. S. *J. Am. Chem. Soc.* **1985**, *107*, 1590.
(217) Salahub, D. R. In "Impact of Cluster Physics in Material Science and Techonology"; Davenas, J., Ed.; The Hague: Nijhoff, 1983.
(218) Whitten, L. J.; Pakkanen, T. A. *Phys. Rev. B* **1980**, *21*, 4357.
(219) Whitten, L. J. *Phys. Rev. B* **1981**, *24*, 1810.
(220) Cremaschi, P.; Whitten, L. J. *Chem. Phys. Lett.* **1984**, *111*, 215.
(221) Salahub, D. R.; Messmer, R. P. *Surf. Sci.* **1981**, *106*, 415.
(222) Slater, J. C.; Johnson, K. H. *Phys. Rev. B* **1972**, *5*, 831.
(223) Rohlfing, E. A.; Cox, D. M.; Kaldor, A. *Chem. Phys. Lett.* **1983**, *99*, 161.
(224) Yang, C. Y.; Johnson, K. H.; Salahub, D. R.; Kaspar, J. *Phys. Rev. B* **1981**, *24*, 5673.
(225) Callaway, J.; Wong, C. S. *Phys. Rev. B* **1977**, *16*, 2095.
(226) Wong, C. S.; Callaway, J. *Phys. Rev. B* **1977**, *15*, 298.
(227) Danan, H.; Herr, A.; Meyer, A. J. P. *J. Appl. Phys.* **1968**, *39*, 669.
(228) Lee, K.: Callaway, J.; Dhar, S. *Phys. Rev. B* **1984**, *30*, 1724.
(229) Lee, K.; Callaway, J.; Kwong, K.; Tang, R. Ziegler, A. *Phys. Rev. B* **1985**, *31*, 1796.
(230) Anderson, A. B. *J. Chem. Phys.* **1977**, *66*, 5108.
(231) (a) Renner, R. *Z. Phys.* **1934**, *92*, 172. (b) Sponer, H.; Teller, E. *Rev. Mod. Phys.* **1941**, *13*, 75.
(232) Blyholder, G. *Surf. Sci.* **1974**, *42*, 249.
(233) Moskovits, M.; Hulse, J. E. *J. Chem. Phys.* **1977**, *66*, 3938.
(234) Moskovits, M.; DiLella, D. P. *J. Chem. Phys.* **1980**, *72*, 2267.
(235) Newton, M. D. *Chem. Phys. Lett.* **1982**, *90*, 291.
(236) Messmer, R. P.; Knudson, S. K.; Johnson, K. H.; Diamond, J. B.; Yang, C. Y. *Phys. Rev. B* **1976**, *13*, 1396.
(237) Rosch, N.; Menzel, D. *Chem. Phys.* **1976**, *13*, 243.
(238) Messmer, R. P.; Tucker, C. W., Jr.; Johnson, K. H. *Chem. Phys. Lett.* **1975**, *36*, 423.
(239) Adachi, H.; Tsukada, M.; Satoko, C. *J. Phys. Soc. Jpn.* **1978**, *45*, 875.
(240) Hoogewijs, R.; Dalmai, G.; Vennik, J. *Phys. Status Solidi A* **1980**, *59*, 461.
(241) Hoogewijs, R.; Dalmai, G.; Vennik, J. "Growth and Properties of Metal Clusters"; Bourdon, J., Ed.; Elsevier: Amsterdam, 1980.
(242) Jones, R. O.; Jennings, P. J.; Painter, G. S. *Surf. Sci.* **1975**, *53*, 409.
(243) Carter, J. L.; Sinfelt, J. H. *J. Catal.* **1968**, *10*, 134.
(244) Janak, J. F.; Moruzzi, V. L.; Williams, R. R. *Phys. Rev. B* **1975**, *12*, 1257.
(245) Salahub, D. R.; Raatz, F. *Int. J. Quantum Chem.* **1984**, *18*, 173.
(246) Callaway, J.; Wang, C. S. *Phys. Rev. B* **1973**, *7*, 1096.
(247) Baetzold, R. C. *J. Catal.* **1973**, *29*, 129.
(248) Anders, L. W.; Hansen, R. S.; Bartell, L. S. *J. Chem. Phys.* **1973**, *59*, 5277.
(249) Baetzold, R. C.; Mack, R. E. *J. Chem. Phys.* **1975**, *62*, 1513.
(250) Anderson, B.; Hoffmann, R. *J. Chem. Phys.* **1974**, *61*, 4545.
(251) Kaspar, J.; Salahub, D. R. *Phys. Rev. Lett.* **1981**, *47*, 54.
(252) Wang, C. S.; Callaway, J. *Phys. Rev. B* **1977**, *15*, 298.
(253) Howard, J. A.; Preston, K. F.; Sutcliffe, R.; Mile, B. *J. Phys. Chem.* **1983**, *87*, 536.
(254) Howard, J. A.; Sutcliffe, R.; Tse, J. S. *Chem. Phys. Lett.* **1983**, *94*, 561.
(255) Hilpert, K.; Gingerich, K. A. *Ber. Bunsenges. Phys. Chem.* **1980**, *84*, 739.
(256) DiLella, D. P.; Raylor, K. V.; Moskovits, M. *J. Phys. Chem.* **1983**, *87*, 524.
(257) Morse, M. D.; Hopkins, J. B.; Langridge-Smith, P. R. R. Smalley, R. E. *J. Chem. Phys.* **1983**, *79*, 5316.
(258) Ozin, G. A.; Mitchell, S. A.; McIntosh, D. F.; Mattar, S. M.; Garcia-Prieto, J. *J. Phys. Chem.* **1983**, *87*, 4651.
(259) Powers, D. E.; Hansen, S. G.; Geusic, M. E.; Michalopoulos, D. L.; Smalley, R. E. *J. Chem. Phys.* **1983**, *78*, 2866.
(260) Baetzold, R. C. *J. Phys. Chem.* **1976**, *80*, 1504.
(261) Anderson, A. B. *J. Chem. Phys.* **1978**, *68*, 1744.
(262) Bachman, C.; Bemuynck, J.; Veilard, A. *Faraday Symp. R. Soc.* **1980**, *14*, 170.
(263) Bachman, C.; Demuynck, L.; Veillard, A. "Growth and Properties of Metal Clusters"; Bourdon, J., Ed.; Elsevier: Amsterdam, 1980.
(264) Flad, J.; Igel-Mann, G.; Preuss, H.; Stoll, H. *Chem. Phys.* **1984**, *90*, 257.
(265) Flad, J.; Igel, G.; Preuss, H.; Stoll, H. *Ber. Bunsenges. Phys. Chem.* **1984**, *88*, 241.
(266) Jeung, G.-H.; Pelissier, M.; Barthelat, J. C. *Chem. Phys. Lett.* **1983**, *97*, 369.
(267) Novaro, O.; Garcia-Prieto, J. *Kinam* **1982**, *4*, 421.
(268) del Conde, G.; Bagus, P. S.; Novaro, O. *Phys. Rev. B* **1982**, *25*, 7843. del Conde, G.; Garcia-Prieto, J.; Novaro, O. *Mol. Phys.* **1981**, *44*, 477.
(269) Richtsmeier, S. C.; Gole, J. L.; Dixon, D. A. *Proc. Natl. Acad. Sci. U.S.A.* **1980**, *77*, 5611.
(270) Miyoshi, E.; Tatewaki, H.; Nakamura, T. *Int. J. Quantum Chem.* **1983**, *23*, 1201.
(271) Demuynck, J.; Rohmer, M.; Strich, A.; Veillard, A. *J. Chem. Phys.* **1981**, *75*, 3443.
(272) Post, D.; Baerends, E. J. *Surf. Sci.* **1982**, *116*, 177.
(273) Hedin, L.; Lundquist, B. I. *J. Phys. Chem.* **1971**, *4*, 2064.
(274) Messmer, R. P.; Caves, T. C.; Kao, C. M. *Chem. Phys. Lett.* **1982**, *90*, 296.
(275) Cox, P. A.; Benard, M.; Veillard, A. *Chem. Phys. Lett.* **1982**, *87*, 159.
(276) Moruzzi, V. L.; Janak, J. F.; Williams, A. R. "Calculated Properties of Metals"; Pergamon: New York, 1978.
(277) Baetzold, R. C. *J. Chem. Phys.* **1978**, *68*, 555.
(278) Baetzold, R. C.; Mason, M. G.; Hamilton, J. F. *J. Chem. Phys.* **1980**, *72*, 366.

(279) Baetzold, R. C. *J. Chem. Phys.* **1971**, *55*, 4363.
(280) Baetzold, R. C. *J. Solid State Chem.* **1973**, *6*, 352.
(281) Bigot, B.; Minot, C. *J. Am. Chem. Soc.* **1984**, *106*, 6601.
(282) Messmer, R. P.; Salahub, D. R.; Johnson, K. H.; Yang, C. Y. *Chem. Phys. Lett.* **1977**, *51*, 84.
(283) Bartel, H.-G.; Scholz, G.; Neumann, R.; Schmidt, W. *Phys. Status Solidi B* **1984**, *123*, 641.
(284) Seifert, G.; Rosan, E. M.; Müller, H. *Phys. Status Solidi B* **1978**, *89*, 553.
(285) Seifert, G.; Rosan, E. M.; Müller, H.; Ziesche, P. *Phys. Status Solidi B* **1978**, *89*, K175.
(286) Le Beuze, L.; Lamandé, P.; Lissillour, R.; Chermette, H. *Phys. Rev. B* **1985**, *31*, 5094.
(287) Le Beuze, L.; Makhyoun, M. A.; Lissillour, R.; Chermette, H. *J. Chem. Phys.* **1982**, *76*, 6060.
(288) Bahuzmuz, A. A.; Woo, C. H. AECL Report 1984, 7798.
(289) Ozin, G. A.; Mattar, S. M.; McIntosh, D. F. *J. Am. Chem. Soc.* **1984**, *106*, 7765.
(290) Miyoshi, E.; Sakai, Y.; Mori, S. *Chem. Phys. Lett.* **1985**, *113*, 457.
(291) Gavezzotti, A.; Tantardini, G. F.; Simonetta, M. *Chem. Phys.* **1984**, *84*, 453.
(292) Pacchioni, G.; Koutecký, J. *Surf. Sci.* **1985**, *154*, 126.
(293) Swartz, K. H. *Phys. Rev. B* **1971**, *5*, 2466.
(294) Chevrel, R.; Sayent, M. "Topic in Current Physics"; Fischer, O., Maple, M. B., Eds.; Springer: New York, 1981; Vol. 32, and references therein.
(295) Nemosh Kalenko, V. V.; Antonov, Vl. N.; Antonov, V. N. *Phys. Status Solidi B* **1980**, *99*, 471.
(296) Ozin, G. A.; Huber, H.; Mitchell, S. A. *Inorg. Chem.* **1979**, *18*, 2932.
(297) Howard, J. A.; Preston, K. F.; Mile, B. *J. Am. Chem. Soc.* **1981**, *103*, 6226.
(298) Schulze, W.; Frank, F.; Charlé, K.-P.; Tesche, B. *Ber. Bunsenges. Phys. Chem.* **1984**, *88*, 263.
(299) Howard, J. A.; Sutcliffe, R.; Mile, B. *J. Phys. Chem.* **1983**, *87*, 2268.
(300) Schulze, W.; Becker, H.-U.; Minkwitz, R.; Manzel, K. *Chem. Phys. Lett.* **1978**, *55*, 59.
(301) Schulze, W.; Becker, H.-U., Abe, H. *Chem. Phys.* **1978**, *35*, 177.
(302) Schulze, W.; Abe, H. *Faraday Symp. Chem. Soc.* **1980**, *14*, 87.
(303) Ozin, G. A.; Huber, H. *Inorg. Chem.* **1978**, *17*, 155.
(304) Basch, H. *J. Am. Chem. Soc.* **1981**, *103*, 4657.
(305) Roothaan, C. C. *Rev. Mod. Phys.* **1960**, *32*, 179.
(306) Roothaan, C. C. *Rev. Mod. Phys.* **1951**, *23*, 69.
(307) Pople, J. A.; Nesbet, R. K. *J. Chem. Phys.* **1954**, *22*, 571.
(308) Löwdin, P. O. *Phys. Rev.* **1955**, *97*, 1974.
(309) Das, G.; Wahl, A. C. *J. Chem. Phys.* **1966**, *44*, 87.
(310) Roos, B. O.; Taylor, P. R.; Siegbahn, P. E. M. *Chem. Phys.* **1980**, *48*, 157.
(311) Buenker, R. J.; Peyerimhoff, S. D. *Theor. Chim. Acta* **1974**, *35*, 33. Buenker, R. J.; Peyerimhoff, S. D.; Butscher, W. *Mol. Phys.* **1978**, *35*, 771.
(312) Buenker, R. J. "Proceedings of the Workshop on Quantum Chemistry and Molecular Physics"; Burton, P. G., Ed.; Woollongong: Australia, 1980. Buenker, R. J. "Studies in Physical and Theoretical Chemistry"; Elsevier: Amsterdam, 1982; Vol. 21. Buenker, R. J.; Phillip, R. A. THEOCHEM **1985**, *123*, 291.
(313) Pople, J. A. In "Energy, Structure and Reactivity"; Smith, D. W.; McRae, W. B., Eds.; Wiley: New York, 1973; p 51.
(314) Kelly, H. P. *Phys. Rev.* **1963**, *131*, 684.
(315) Langhoff, S. R.; Davidson, E. R. *Int. J. Quantum Chem.* **1974**, *8*, 61.
(316) Roos, B. *Chem. Phys. Lett.* **1972**, *15*, 153.
(317) Roos, B. O.; Siegbahn, P. M. In "Methods of Electronic Structure Theory"; Schaefer, H. F., III, Ed.; Plenum: New York, 1977; p 277.
(318) Møller, C.; Plesset, M. S. *Phys. Rev.* **1934**, *64*, 618.
(319) Goddard, W. A., III. *Phys. Chem.* **1967**, *157*, 81.
(320) Brobrowicz, F. W.; Goddard, W. A., III. In "Methods of Electronic Structure Theory"; Schaefer, H. F., III, Ed.; Plenum: New York, 1977; p 79.
(321) Kutzelnigg, W. In "Methods of Electronic Structure Theory"; Schaefer, H. F., III, Ed.; Plenum: New York, 1977; p 129.
(322) Meyer, W. *Int. J. Quantum Chem. Symp.* **1971**, *5*, 341.
(323) Meyer, W. *J. Chem. Phys.* **1973**, *58*, 1017.
(324) Boys, S. F. *Proc. R. Soc. London, A* **1950**, *200*, 542.
(325) Newton, M. D.; Lathan, W. A.; Hehre, W. J.; Pople, J. A. *J. Chem. Phys.* **1970**, *52*, 4064.
(326) Dunning, T. H. *J. Chem. Phys.* **1970**, *53*, 2823.
(327) Hohenberg, P.; Kohn, W. *Phys. Rev. B* **1964**, *136*, 864.
(328) Kohn, W.; Sham, C. J. *Phys. Rev. B* **1965**, *140*, 1133.
(329) Kohn, W.; Vashika, P. In "Theory of Inhomogeneous Electron-Gas"; Lundquist, S., March, N. H., Eds.; Plenum: New York, 1983.
(330) Rajagopal, A. K. *Adv. Chem. Phys.* **1980**, *41*, 59.
(331) Slater, J. C. "Quantum Theory of Molecules and Solids"; McGraw-Hill: New York; Vol. 4. See also ref 21.
(332) Parr, R. G. *Annu. Rev. Phys. Chem.* **1983**, *34*, 631.
(333) See the contributions of Gunnarson, O.; Jones, R. O.; Fritsche, L.; Gollisch, H., in ref 343.
(334) Gunnarson, O.; Jones, R. O. *Phys. Rev. B* **1985**, *31*, 7588.
(335) Lindgren, L. *Int. J. Quantum Chem. Symp.* **1971**, *5*, 411.
(336) (a) Perdew, J. P. *Chem. Phys. Lett.* **1979**, *64*, 127. (b) Wang, S.-W.; *J. Chem. Phys.* **1985**, *82*, 4633.
(337) See the contribution of Sevin, A.; Stoll, H.; Preuss, H., in ref 343.
(338) Slater, J. C. *Phys. Rev. B* **1951**, *81*, 385; *82*, 538.
(339) Johnson, K. H. *Annu. Rev. Phys. Chem.* **1975**, *26*, 39. See also ref. 22.
(340) Baerends, E. J.; Ros, P. *Int. J. Quantum Chem. Suppl.* **1978**, *12*, 169.
(341) Baerends, E. J.; Ellis, D. E.; Ros, P. *Chem. Phys.* **1973**, *2*, 41. Baerends, E. J.; Ros, P. *Chem. Phys.* **1973**, *2*, 52.
(342) Delley, B.; Ellis, D. E. *J. Chem. Phys.* **1982**, *76*, 1949.
(343) "Local Density Approximations in Quantum Chemistry and Solid State Physics"; Dahl, J. P.; Avery, J., Eds.; Plenum: New York; 1984.
(344) (a) Fock, V.; Vesselow, M.; Petraschen, M. *Zh. Eksp. Theor. Fiz.* **1940**, *10*, 723. (b) Phillips, J. C.; Kleinmann, L. *Phys. Rev.* **1959**, *116*, 287.
(345) Weeks, J. D.; Rice, A. *J. Chem. Phys.* **1968**, *49*, 2741.
(346) Weeks, J. D.; Hazi, A.; Rice, S. A. *Adv. Chem. Phys.* **1969**, *16*, 283.
(347) Huzinaga, S.; Klobukowski, M.; Sakai, Y. *J. Chem. Phys.* **1984**, *88*, 4880. Klobukowski, M. *J. Comput. Chem.* **1983**, *4*, 350. See also ref 33.
(348) Gropen, O.; Wahlgren, V.; Pettersen, L. *Chem. Phys.* **1982**, *66*, 49.
(349) A recent development of the ECP method of ref 33 has been proposed by Andzelm, J. et al. (see ref 35).
(350) Coffey, P.; Ewing, C. W.; van Wazer, J. R. *J. Am. Chem. Soc.* **1975**, *97*, 1656. Ewing, C. S.; Van Wazer, J. R. *J. Chem. Phys.* **1975**, *63*, 4035.
(351) Barthelat, J. C.; Durand, P.; Serafini, A. *Mol. Phys.* **1977**, *33*, 159; Barthelat, J. C.; Durand, Ph. *Gazz. Chim. Ital.* **1978**, *108*, 225. Pellisier, M.; Durand, Ph. *Theor. Chim. Acta* **1980**, *55*, 43. Barthelat, J. C.; Pellisier, M.; Durand, Ph. *Phys. Rev. A* **1980**, *21*, 1773. See also ref 32.
(352) Kahn, L. R.; Baybutt, P.; Truhlar, D. G. *J. Chem. Phys.* **1976**, *65*, 3826 and references therein. Hay, P. J.; Wadt, W. R.; Kahn, L. R. *J. Chem. Phys.* **1978**, *68*, 3059.
(353) Christiansen, P. A.; Lee, Y. S.; Pitzer, K. S. *J. Chem. Phys.* **1979**, *71*, 4445. Hay, P. J.; Wadt, W. R. *J. Chem. Phys.* **1985**, *82*, 299, 270; Wadt, W. R.; Hay, P. J. *J. Chem. Phys.* **1985**, *82*, 284.
(354) Snijders, J. G.; Baerends, E. J. *Mol. Phys.* **1979**, *33*, 1651.
(355) Bachelet, G. B.; Hammann, D. R.; Schülten, M. *Phys. Rev. B* **1982**, 26, 4199 and references therein. Ramson, S. H.; Messmer, R. P. *Chem. Phys. Lett.* **1983**, *98*, 72.
(356) Katsuki, S.; Takata, H. *Int. J. Quantum Chem.* **1980**, *18*, 25. Katsuki, S.; Inokuchi, M. *J. Phys. Soc. Jpn.* **1982**, *51*, 3652.
(357) (a) Jeung, G.-H.; Malrieu, J. P.; Daudey, J. P. *J. Chem. Phys.* **1982**, *77*, 3571. (b) Jeung, G.-H.; Barthelat, J. C. *J. Chem. Phys.* **1983**, *78*, 2097.
(358) Fuentealba, P.; Preuss, H.; Stoll, H.; von Szentpály, L. *Chem. Phys. Lett.* **1982**, *89*, 418. Stoll, H.; Fuentealba, P.; Dolg, M.; Flad, J.; von Szentpály, L.; Preuss, H. *J. Chem. Phys.* **1983**, *78*, 5532.
(359) Kordis, J.; Gingerich, K. H.; Seyse, R. J. *J. Chem. Phys.* **1974**, *61*, 5114.
(360) In this paper the periodic group notation given in parentheses is in accord with recent actions by IUPAC and ACS nomenclature committees. A and B notation is eliminated because of wide confusion. Groups IA and IIA become groups 1 and 2. The d-transition elements comprise groups 3 through 12, and the p-block elements comprise groups 13 through 18. (Note that the former Roman number designation is preserved in the last digit of the new numbering: e.g., III → 3 and 13.)